An incremental variational approach and computational homogenization for composites with evolving damage

Ghita Ben-El-Barguia

SORBONNE UNIVERSITY

DOCTORAL THESIS

Presented by

Ghita BEN-EL-BARGUIA

A thesis submitted in fulfillment of the requirements
for the degree of Doctor of Philosophy

—

An incremental variational approach and computational homogenization for composites with evolving damage

M. Renaud MASSON	CEA Cadarache	Rapporteur
M. Julien YVONNET	Université Gustave Eiffel	Rapporteur
M. Noël LAHELLEC	Aix-Marseille Université	Examinateur
Mme Carole NADOT-MARTIN	Université Poitiers	Présidente
M. Corrado MAURINI	Sorbonne Université	Examinateur
Mme Hélène WELEMANE	Université Toulouse	Examinatrice
Mme Sophie DARTOIS	Sorbonne Université	Co-Encadrante
M. Djimédo KONDO	Sorbonne Université	Directeur de thèse

Institut Jean Le Rond ∂'Alembert - Équipe M.I.S.E.S.

"The only thing greater than the power of the mind is the courage of the heart."

A Beautiful Mind

Institut Jean Le Rond ∂'Alembert | Sorbonne University

An incremental variational approach and computational homogenization for composites with evolving damage

This work is part of the large framework of nonlinear mechanics and focuses on modeling the mechanical response of elasto-damageable composite materials when loaded. The occurrence and/or growth of microcracks induces stress softening response which can lead to macroscopic failure. Although significant progress has been achieved in recent years in the field of damage modeling and of the resulting fracture phenomena, taking into account this damage in homogenization approaches still remains a largely open issue in solid mechanics. In this study, we establish an upscaling procedure for elasto-damageable composites derived from the Effective Internal Variable principle (EIV model) dedicated so far to elasto(visco)plastic composites. To this end, we consider an isotropic damage law within the framework of Generalized Standard Materials, i.e. using an internal damage variable and two potentials. Following the EIV approach, we propose a simple linearization of the local behavior coupling elasticity and damage, from which a Linear Comparison Composite (LCC) with per-phase homogeneous properties is deduced. The effective behavior is then estimated using a classical linear homogenization scheme (Hashin-Shtrikman). We develop and implement the incremental variational procedure first for a hollow sphere and then for composites consisting of elastic spherical particles in an elasto-damageable matrix. The model predictions for monotonous and cyclic loadings are compared to the results of full-field simulations carried out on a 3D cell by implementing a phase field approach. An evaluation of the method is thus performed at the scale of the composite and that of the constituents.

Acknowledgements

As I reflect upon the culmination of this Ph.D. journey, I find it impossible to express the depth of gratitude and admiration I hold for the countless individuals who have walked beside me on this path. This thesis is not only a testament to my efforts but a tribute to the profound impact of family, friends, mentors, and colleagues.

First and foremost, my heartfelt appreciation extends to my esteemed supervisors, Djimedo Kondo and Sophie Dartois. Your mentorship has been the guiding force of this academic journey. Djimedo, your profound expertise in our field and your unrelenting pursuit of excellence have been a constant source of motivation for me. Sophie, your dedication to fostering a nurturing academic environment and unwavering support have been the bedrock upon which I've built my research. Beyond supervisors, you've been mentors, friends, and role models. Thank you for your availability (for work, coffee, and whatnot), thank you for your patience, thank you for everything!

I would like to extend my gratitude to the distinguished members of the jury. To the diligent rapporteurs, I am very appreciative of the time and meticulous effort you devoted to thoroughly reading and evaluating my thesis. To the president, who presided over the day of the defense I express my gratitude for your role in overseeing and facilitating the proceedings. To the members of the jury, I extend my sincere thanks for your time, your engagement, and the stimulating exchange of ideas during the evaluation process. Your constructive feedback and valuable comments have added a layer of depth and perspective to this thesis that I greatly appreciate.

To my parents, whose careers in science ignited the spark of curiosity and instilled a love for knowledge within me, I offer my deepest gratitude. You both have shown me the limitless horizons of scientific exploration, and your unwavering support has been my constant source of inspiration. Your boundless love, unwavering belief in my potential, and ceaseless encouragement have been the driving forces behind every step I've taken. Your support extended to the countless conversations over the dinner table (when possible) or over the phone, the reassuring words during moments of self-doubt, and the countless sacrifices you made, nothing went unnoticed.

My dear sisters, Meriam and Ibtissam, have been my steadfast companions throughout this often tumultuous journey. Your love, empathy, and patience have been my sanctuary. Through the long nights, the moments of self-doubt, and the countless hours of my endless rants, you have been my unwavering support system. Your ability to lend an empathetic ear and offer thoughtful advice has been a balm to my soul and a guiding light through the darkest of academic storms.
To my witty and ever-teasing brother-in-law (or as he likes to call himself: jerk), Walid, your ability to find humor in the most serious of situations has been a true gift and somehow managed to bring me a smile. While some might consider your teasing a form of distraction, I've come to realize that it was a much-needed break from the intensity of academic

life. You reminded me that it's okay to take a step back and laugh at myself, even when the research seemed daunting.
And to my most beloved nieces Noor, Nada, and nephew Noah, though you may be too young to understand the complexities of the research within these pages, your presence in my life has given me a profound sense of purpose. You embody the spirit of curiosity and wonder, and your unwavering enthusiasm for life continually reminds me of the importance of embracing curiosity and learning at every age. You inspire me more than you can imagine. Your innocence and the promise of your future remind me of the importance of the work we do, not only for ourselves but for generations to come.

To my second family, my childhood friends – Zineb, Yasmine, Randa, Aya, Alae, Youssef, Amine, and Ilyass – you have been the constant light in my life, offering support not only during my Ph.D. journey but throughout every phase of life's adventure. The memories we've created together are woven into the very fabric of my existence, and I am forever grateful for all of you. But most of all, you've kept me sane, in your own weird fascinating way (mugs, notes, food, drives, late-night talks, games, ... accidents ...), but it worked. It is often said that friends are the family we choose, and I couldn't have chosen a better group of individuals to be my second family. Your friendship has been a source of warmth, inspiration, and strength that I will carry with me throughout my life.

Jussieu, the place where I've spent countless hours pursuing knowledge and forming deep connections, holds a special place in my heart. Patricia, Zakia, Sirine and Mihaja, thanks to you, when I think of what was, happy moments come first. I am so thankful and grateful for walking alongside of you throughout this journey. To Patricia, who had to endure me for almost 7 years now, thank you for our deep conversations, our aimless walks, our coffee breaks, our crazy potential career alternatives, thank you for being you! To ∂'Alembert, my 2nd home these past 3.5 years, alongside Cecilia, Yutao, Sagar, Adrien, Mandeep, Cecile, Nicolas, Gabriel, Amine, Lyes, Samy, Camilla, Priscilla, and others, you have all made this journey not only survivable but genuinely enjoyable through the countless coffee breaks, late-night apéros (shhhh), and the music of our laughter echoing through the corridors. I wish you all the very best in your endeavors. Simona, the mother of the lab, the chocolate provider, the problem solver, the listener … thank you for everything you've done and that you still do for us!! Also, as a foreign student, always confused about the administrative world, I'd like to thank Catherine for your kindness and patience, Olivier for your cheering and constant help, and Sandrine for our discussions and all the meditation material you've shared with me throughout the years.

To all the professors, colleagues, and friends who have contributed to my academic and personal growth, I extend my sincere gratitude. Your insightful discussions, shared experiences, and intellectual exchange have enriched me beyond measure. As I move forward into the next chapter, I do so with the invaluable lessons, deep friendships, and unwavering inspiration that all of you have provided.

Contents

List of Figures

General introduction

Composite materials with a brittle matrix such as « Ceramics Matrix Composites » (CMC), rocks, and concrete materials are generally considered for various thermostructural applications relevant to different industrial fields such as aeronautics, civil engineering, mechanical engineering, shipbuilding industry, etc. The major reason for such various industrial applications is the capability of these materials to have satisfactory rigidity and to sustain high levels of loadings. However, a possible major limitation of brittle matrix composites is their susceptibility to failure following progressive and complex damage phenomena due to microcracking in the matrix or to a decohesion of the interface between the matrix and the reinforcement. For this class of quasi-brittle heterogeneous materials, characterized by a significant degradation of mechanical properties, microcracks, and microvoids growth are indeed recognized to be the main deformation mechanisms. The approaches used for their modeling range from pure phenomenological procedures to micro-mechanical-based ones, the latter being restricted to the determination of the effective elastic properties of the materials. Naturally, the solution to overcome or limit the quasi-brittle failure process requires a better understanding of the effects provided by the incorporation of particles or fiber reinforcements. For instance, analysis of damage in CMCs has been, since the nineties, the subject of several studies both from experimental characterization (see for instance [5], [70], [49], to cite very few of these early studies) and theoretical modeling. Concerning the damage modeling in brittle composites, the approaches have been mainly of pure macroscopic character, using Continuum Damage Mechanics (CDM) tools. Mention can be made of the studies by [24], [85] and some attempts of micromechanical modeling through Transformation Field Analysis (TFA) [63], etc. which, despite their great interest can hardly capture in detail the coupled elasto-damage interaction between reinforcement deformation and damage phenomena in the matrix.

Powerful methods to obtain the effective response of heterogeneous materials, as well as their local response for each constituent, are provided by advanced numerical homogenization techniques which deliver full-field computations. These techniques rely on the well-known finite element method (FEM) or on Fast Fourier Transform approaches [136, 103]. However, although parallelization methods are available, numerical simulations of composite structure responses based on those numerical homogenization methods [38] are still very time-consuming. In order to circumvent this high numerical cost and to facilitate structural computations, mean-field homogenization methods are generally considered, since they allow to obtain reasonable semi-analytical estimates. In particular, these methods, also known

as upscaling methods, help to better understand the nonlinear mechanical response of composites in relation to their microstructure.
However, since the seminal work of Ponte-Castañeda [118], significant progress has been also achieved in the nonlinear homogenization of composites whose nonlinear constituents behaviors are described by means of a single potential.
In the context of viscoelastic and/or elasto(visco)plastic composites where the coupling between elasticity and dissipative phenomena is of paramount importance, Lahellec and Suquet [75], based on [94] (see also [109]), have introduced an incremental variational approach dedicated to composites whose constituents' behaviors are described by means of two potentials (a free energy and a dissipation potential), as required for generalized standard materials. The latter, namely known as the EIV, consists of replacing the inelastic strain with an effective internal variable. This approach has been developed and applied to viscoelastic composites by [76, 128], and elasto(visco)plastic composites by several authors among which [2, 83], etc. Mention must also be made of the studies by [20] and [21].
An EIV alternative formulation was proposed by Idiart et al. [60, 61] for linear viscoelastic composites where the Cauchy-Shwarz inequality was used instead of the Legendre transform. Lahellec and Suquet [74] introduced a modified incremental variational principle in a rate form (RVP) to extend the previously mentioned approach to elasto(visco)plastic composites with both isotropic and linear kinematic hardening. An extension to anisotropic behaviors was proposed by the same authors [71].
Although significant advances have been achieved in the above-mentioned domains, taking into account damage phenomena in a fully coupled homogenization approach still remains a largely open and barely explored issue in solid mechanics. The very few works dealing with this topic are recent and at an early stage of development (see for instance [36]). Particular mention has to be made of the thesis by [43] in which the author provides an approach that suitably combines analytical methods with theoretical and numerical homogenization of composites experiencing brittle damage. Full-field numerical models based on Finite Elements Methods as well as Fast Fourier transforms approaches have been used to quantify the composite response at both micro and macro scales and to provide a way to assess mean-field analytical nonlinear models that he proposed by relying on linear-comparison methods. This first attempt of modeling, dedicated to a material involved in the nuclear industry, is in the same vein as our study which aims at developing a homogenization framework for appropriate constitutive laws of heterogeneous materials with elastic damageable constituents. Our concern in this thesis will be primarily to investigate, via a recent nonlinear homogenization approach and a suitable approach to damage, the responses of composites with elasto-damageable constituents. This damage may generally induce an effective response with softening and leads at its ultimate stage (damage localization) to macroscopic brittle fracture phenomena.

The study presented hereafter relies then for its theoretical part on the incremental variational procedure initially introduced by Lahellec and Suquet [75] and developed so far for elasto(visco)plastic composites by themselves or by several other authors. To this end, and

for simplicity we will consider an isotropic damage law within the framework of Generalized Standard Materials, i.e. using two potentials.

Although the incremental variational approach has been already applied to viscoelastic and elasto(visco)plastic composites several difficulties must be faced for this class of composites due to the coupling between elasticity and damage on one hand, and of the resulting softening phenomena on the other hand.

The manuscript is organized into 4 chapters as follows:

- Chapter 1 : *Damage models and a closed-form solution on a hollow sphere*
  We start with a recall of the main physical mechanisms of damage in quasi-brittle materials. Then, we briefly present the basic ingredients of the continuum thermodynamics of irreversible processes, helpful for the formulation of local damage models which will serve for the analysis of the mechanical response of damageable structures. This mainly relies on the framework of Generalized Standard Materials (GSM). The second part of this chapter concerns the presentation of exact solutions for mechanical fields (damage distribution, displacement, and stress fields) in a hollow sphere made up of an elastic damageable material subjected to radial loading. As already pointed out by [17], this structural problem does not fit into the framework of nonlinear homogenization theories of heterogeneous media, but has the advantage of admitting an exact analytical solution that can be compared to various approximate solutions such as the one that will be presented in chapter 2.

- Chapter 2 : *An Effective Internal Variable (EIV) approach for quasi-brittle composites*
  This chapter begins with an overview of nonlinear homogenization methods for composites including the incremental variational approach. The latter, introduced first by [75] allows to handle local constitutive behavior described by means of two potentials, the ones considered for Generalized Standard Materials. Next, we will adapt this framework to the context where elasto-damageable constituents are involved in the composite material. The procedure for such extension will be presented in detail for the case of a scalar damage model, leading to the derivation of the effective damageable behavior of the composite and to the prediction of the local field statistics. For completeness, the chapter ends with a presentation of the numerical implementation of the model based on the solution to the resulting nonlinear system of equations.

- Chapter 3 : *Full-field computations and assessment of the EIV approach with damage*
  This chapter aims at providing an assessment of the proposed model by comparison to full-field simulations. For the robustness of these full-field computations, we rely on variational regularized damage-based models (see [19], [4]), reinterpreted later in

terms of variational gradient damage models (see [88], [112]). The use of such variational numerical framework is briefly discussed in order to argue its interest in evaluating the nonlinear homogenization model formulated in the previous chapter. For these comparisons, the composites considered are constituted of an elasto-damageable matrix reinforced by spherical elastic particles.

- Chapter 4 : *An extension of the EIV model accounting for hardening effects*
  This chapter is devoted to an extension of the EIV model which accounts for a positive hardening accompanying the damage processes. This will require a slight modification of the incremental variational procedure. Evaluation of the hardening effects on the composite response will be done with respect to the comparison to full-field simulations

Finally, the thesis ends with a general conclusion and an indication of some future research directions. Two appendices are added on some complementary details on unilateral effects in isotropic damage modeling and on some further preliminary extensions of the EIV damage model that we carried out.

Chapter 1

Isotropic elastic damage models : thermodynamics-based formulation and a closed-form solution

Contents

This chapter aims first to recall the thermodynamics-based formulation of local damage models. To this end, we begin with a brief summary of the principles of thermodynamics of irreversible processes and of the Generalized Standard Materials (GSM) framework. The standard local isotropic elastic damage laws are recalled, with an emphasis on the partial deactivation of the damage effects under compression-like loadings, the so-called unilateral

contact effects. This is completed by a description of the corresponding variational formulations. In a second part of the chapter, and based on [30], we briefly present the derivation of closed-form solutions for mechanical fields (displacements, stress, damage) in a hollow sphere made up of an elastic damage material and subjected to radial loadings. Although these solutions do not strictly constitute homogenization results, they will be considered for comparison with the theoretical models that will be established in the next chapter.

1.1 Mechanical behavior and damage of quasi-brittle matrix composites

1.2 Thermodynamics-based formulation of local damage laws and corresponding variational expression

We aim here to briefly recall the main ingredients of Continuum thermodynamics and the Generalized Standard Materials (GSM) framework. The reader interested by this subject may refer to [53], [44], [92], [104], [86], etc.
A powerful method for the formulation of constitutive models for various mechanical behaviors is provided by the Generalized Standard Materials (GSM) framework which relies on the continuum Thermodynamics of Irreversible Processes (TIP). We recall here the two principles of TIP, the first one corresponds to a balance of energy exchanged in various forms, and the second one to the positivity of entropy production. For a continuum medium, and under the assumption of small perturbations, the local forms of these two principles read:

- for the first principle
$$\rho\dot{e} = \underline{\underline{\boldsymbol{\sigma}}} : \underline{\underline{\dot{\boldsymbol{\varepsilon}}}} + r - \mathrm{div}(\underline{q}) \tag{1.1}$$
in which e represents the specific internal energy density.

- for the second principle
$$\rho\dot{s} + \frac{1}{T}\mathrm{div}(\underline{q}) - \frac{r}{T} - \frac{\underline{q}.\underline{\nabla} T}{T^2} \geq 0 \tag{1.2}$$
where s denotes the specific entropy.

The latter allows distinguishing between reversible and irreversible processes.
Combining the above local forms of the two principles leads to the so-called Clausius-Duhem inequality which expresses the positivity of the total dissipation :
$$\mathcal{D} = \rho T\dot{s} - \rho\dot{e} + \boldsymbol{\sigma} : \dot{\boldsymbol{\varepsilon}} - \frac{\underline{q}.\underline{\nabla} T}{T} \geq 0 \tag{1.3}$$

An adequate framework of modeling allows to satisfy automatically Clausius-Duhem's inequality lies in the Generalized Standard Materials framework presented in the following subsection.

1.2.1 Constitutive equations for Generalized Standard Materials

We begin with the local state approach which assumes that the mechanical state of a system is described by means of a finite number of state variables $(\boldsymbol{\varepsilon}, T, \alpha)$, α representing the internal variables. Under isothermal conditions and infinitesimal strain hypothesis, the formulation of the constitutive models in the GSM framework requires a thermodynamics potential, generally the Helmholtz free energy $w(\boldsymbol{\varepsilon}, \alpha)$[1], and a dissipation potential $\varphi(\dot{\alpha})$.

The thermodynamics potential provides the reversible forces through the state laws

$$\begin{cases} \boldsymbol{\sigma}^{rev} = \dfrac{\partial w}{\partial \boldsymbol{\varepsilon}}(\boldsymbol{\varepsilon}, \alpha) \\ \mathcal{A}_\alpha^{rev} = \dfrac{\partial w}{\partial \alpha}(\boldsymbol{\varepsilon}, \alpha) \end{cases} \tag{1.4}$$

The intrinsic dissipation, given by $\boldsymbol{\sigma} : \dot{\boldsymbol{\varepsilon}} - \dot{w}$, reads then :

$$\mathcal{D}_1 = \left(\boldsymbol{\sigma} - \frac{\partial w}{\partial \boldsymbol{\varepsilon}}\right) : \dot{\boldsymbol{\varepsilon}} - \frac{\partial w}{\partial \alpha} : \dot{\alpha} \tag{1.5}$$

and must be positive according to the Clausius-Duhem inequality, which becomes:

$$\mathcal{D}_1 = (\boldsymbol{\sigma} - \boldsymbol{\sigma}^{rev}) : \dot{\boldsymbol{\varepsilon}} - \mathcal{A}^{rev} : \dot{\alpha} \tag{1.6}$$

The strain $\dot{\boldsymbol{\varepsilon}}$ being non-dissipative here (the dissipation will be produced by the evolution of the internal variables), it follows that $\boldsymbol{\sigma}^{irr} = \boldsymbol{\sigma} - \boldsymbol{\sigma}^{rev} = 0$. And the irreversible thermodynamic force associated with the set of internal variables α is obtained by $\mathcal{A}^{irr} = -\mathcal{A}^{rev}$ and will be noted $\mathcal{A}_\alpha$:

$$\begin{cases} \boldsymbol{\sigma} = \dfrac{\partial w}{\partial \boldsymbol{\varepsilon}}(\boldsymbol{\varepsilon}, \alpha) \\ \mathcal{A}_\alpha = -\dfrac{\partial w}{\partial \alpha}(\boldsymbol{\varepsilon}, \alpha) \end{cases} \tag{1.7}$$

The intrinsic dissipation takes then the form :

$$\mathcal{D}_1 = \mathcal{A}_\alpha : \dot{\alpha} \tag{1.8}$$

Such result does not provide any information about the evolution of the internal variables which requires the introduction of a dissipation potential that depends on the rates of the internal variables and must be positive scalar-valued and equal to zero for $\dot{\alpha} = 0$.

The complementary laws are given by :

$$\mathcal{A}_\alpha = \frac{\partial \varphi}{\partial \dot{\alpha}}(\dot{\alpha}) \tag{1.9}$$

[1]The dual of w is the partial Legendre-Fenchel transform of the internal energy: w=e-TS

In the case where the potential φ is not differentiable, one should refer to the notion of subdifferential $\partial\varphi$. The constitutive law then takes the form ($\mathcal{A}_\alpha$ is said to belong to the subdifferential of φ at the considered point) :

$$\mathcal{A}_\alpha \in \partial\varphi(\dot{\alpha}) \tag{1.10}$$

In general, the irreversible forces $\boldsymbol{\sigma}^{irr}$ and $\mathcal{A}_\alpha$ belong to the subdifferential of φ at $(\dot{\boldsymbol{\varepsilon}}, \dot{\alpha})$ if for any rate $\boldsymbol{\varepsilon}^*$:

$$\varphi(\dot{\boldsymbol{\varepsilon}}, \dot{\alpha}) - \varphi(\boldsymbol{\varepsilon}^*, \alpha^*) + \boldsymbol{\sigma}^{irr} : (\boldsymbol{\varepsilon}^* - \dot{\boldsymbol{\varepsilon}}) + \mathcal{A}_\alpha(\alpha^* - \dot{\alpha}), \in \partial\varphi(\dot{\alpha}) \leq 0 \tag{1.11}$$

which represents the normality rule.
Equivalently, and coming back to the case where the deformation is not a dissipative variable, the evolution law (1.10) can be obtained by means of the dual potential $\varphi^*(\mathcal{A})$:

$$\dot{\alpha} \in \partial\varphi^*(\mathcal{A}_\alpha) \tag{1.12}$$

$\varphi^*(\mathcal{A}_\alpha) = \sup_{\dot{\alpha}>0} \{\mathcal{A}_\alpha\dot{\alpha} - \varphi(\dot{\alpha})\}$ is the Legendre–Fenchel transform of φ.

For rate-independent models, it is classically shown that:

$$\varphi^*(\mathcal{A}_\alpha) = \begin{cases} 0 & \text{if} \quad f(\mathcal{A}_\alpha) \leq 0 \\ \infty & \text{otherwise} \end{cases} \tag{1.13}$$

which is the indicator function of a convex domain $\mathcal{C}$ defined by :

$$\mathcal{C} = \{\mathcal{A}_\alpha / f(\mathcal{A}_\alpha) \leq 0\} \tag{1.14}$$

$f(\mathcal{A}) \leq 0$ defines the domain of elasticity.

From (1.7) and (1.9), the constitutive equations of the GSM can be summarized as

$$\boldsymbol{\sigma} = \frac{\partial w}{\partial \boldsymbol{\varepsilon}}(\boldsymbol{\varepsilon}, \alpha), \qquad \frac{\partial w}{\partial \alpha}(\boldsymbol{\varepsilon}, \alpha) + \frac{\partial \varphi}{\partial \dot{\alpha}}(\dot{\alpha}) = 0 \tag{1.15}$$

The second equation in (1.15) is known as the Biot equation (see [104], chapter15, or [125])[2] in reference to a series of works conducted by Biot mainly in viscoelasticity and/or thermoelasticity (see for instance [13, 14]).

[2] An interesting study of Biot equation in link with quasi-static stability analysis can be found in [1]

1.2.2 Presentation of variational formulations related to the GSM framework

A class of variational constitutive updates has been proposed by Ortiz and Stainier [109] in the form of rate variational principles (see also Mielke [97] and Reddy [122]). We follow here a recent paper of [15] in order to summarize this principle. To this end, we consider a time increment $[t_n; t_{n+1}]$, for which the mechanical quantities are known at time t_n. It can be shown that the solution at time t_{n+1} of the mechanical problem is that of the following minimization principle (here the dissipation potential is taken in a general form $\varphi(\dot{\boldsymbol{\varepsilon}}, \dot{\alpha})$:

$$(u_{n+1}, \boldsymbol{\varepsilon}_{n+1}, \alpha_{n+1}) \;=\; \underset{(u,\boldsymbol{\varepsilon},\alpha)}{\operatorname{argmin}} \int_{t_n}^{t_{n+1}} \int_\Omega \left(\dot{w}(\boldsymbol{\varepsilon}, \alpha) \;+\; \varphi(\dot{\boldsymbol{\varepsilon}}, \dot{\alpha})\right) d\Omega dt \;-\; \int_{t_n}^{t_{n+1}} \underset{(u,\boldsymbol{\varepsilon})\in\mathcal{K}(E)}{\mathcal{P}_{ext}(\dot{u})} dt \quad (1.16)$$

where :

- $\mathcal{P}_{ext}(\dot{u})$ corresponds to the power of external loads which is assumed here to consist only of fixed body forces f_{n+1} on the time step, so that:

$$\int_{t_n}^{t_{n+1}} \mathcal{P}_{ext} dt \;=\; \int_{t_n}^{t_{n+1}} \int_\Omega f_{n+1}.\dot{u} d\Omega \;=\; \int_\Omega f_{n+1}.\left(u - u_n\right) d\Omega \quad (1.17)$$

- $\mathcal{K}(E)$ is the state of kinematically admissible fields :

$$\mathcal{K}(E) = \left\{ (u, \boldsymbol{\varepsilon}) \;:\; \left| \begin{array}{l} \boldsymbol{\varepsilon} = \nabla^s u \text{ in } \Omega \\ u \;=\; \hat{u}_{n+1} \end{array} \right. \right\} \quad (1.18)$$

  where $\hat{u}_{n+1}$ denotes the imposed displacements at time t_{n+1} on the Dirichlet boundary $\partial\Omega_D$.

This type of formulation can be also found in [102] or [101].

Remark : It is interesting to note that the above minimization principle can be established by combining at the global (structural) level generalized Biot equations and the transposition at global level of the normality rule (1.11). The reader interested in this aspect can refer to [125] or [105]. For an application of Biot equation to damage see for instance [65].

Coming back to the variational principle (1.16), by applying an implicit Euler discretization for the state variables, their rate can be approximated by :

$$\dot{\boldsymbol{\varepsilon}}(t) \;\approx\; \frac{\boldsymbol{\varepsilon} - \boldsymbol{\varepsilon}_n}{\Delta t} \quad ; \quad \dot{\alpha}(t) \;\approx\; \frac{\alpha - \alpha_n}{\Delta t} \quad (1.19)$$

where $\Delta t \;=\; t_{n+1} - t_n$, we can then write :

$$\int_\Omega \int_{t_n}^{t_{n+1}} \;=\; \varphi(\dot{\boldsymbol{\varepsilon}}, \dot{\alpha}) d\Omega \, dt \;\approx\; \int_\Omega \Delta t \varphi \left(\frac{\boldsymbol{\varepsilon} - \boldsymbol{\varepsilon}_n}{\Delta t}, \frac{\alpha - \alpha_n}{\Delta t} \right) d\Omega \quad (1.20)$$

The minimum principle in (1.16) can thus be rewritten as :

$$\begin{aligned}(u_{n+1},\boldsymbol{\varepsilon}_{n+1},\alpha_{n+1}) \;=& \underset{(u,\boldsymbol{\varepsilon},\alpha)}{\operatorname{argmin}} \int_\Omega \left(w(\boldsymbol{\varepsilon},\alpha)-w(\boldsymbol{\varepsilon}_n,\alpha_n)\right) d\Omega \\ &+ \int_\Omega \Delta t\,\varphi\left(\frac{\boldsymbol{\varepsilon}-\boldsymbol{\varepsilon}_n}{\Delta t},\frac{\alpha-\alpha_n}{\Delta t}\right) d\Omega \;-\; \int_{\substack{\Omega \\ (u,\boldsymbol{\varepsilon})\in\mathcal{K}(E)}} f_{n+1}\,.\,(u-u_n)\,d\Omega\end{aligned} \tag{1.21}$$

Putting aside the constant terms $w(\boldsymbol{\varepsilon}_n,\alpha_n)$ and u_n, (1.21) becomes :

$$(u_{n+1},\boldsymbol{\varepsilon}_{n+1},\alpha_{n+1}) \;=\; \underset{(u,\boldsymbol{\varepsilon},\alpha)}{\operatorname{argmin}} \int_{\substack{\Omega \\ (u,\boldsymbol{\varepsilon})\in\mathcal{K}(E)}} J(\boldsymbol{\varepsilon},\alpha) \;-\; \int_\Omega f_{n+1}\,.\,u\,d\Omega \tag{1.22}$$

where the incremental pseudo-potential $J(\boldsymbol{\varepsilon},\alpha)$ takes the following form for the rate-dependant materials :

$$J(\boldsymbol{\varepsilon},\alpha) \;=\; w(\boldsymbol{\varepsilon},\alpha) \;+\; \Delta t\varphi\left(\frac{\boldsymbol{\varepsilon}-\boldsymbol{\varepsilon}_n}{\Delta t},\frac{\alpha-\alpha_n}{\Delta t}\right) \tag{1.23}$$

and for rate-independent materials:

$$J(\boldsymbol{\varepsilon},\alpha) \;=\; w(\boldsymbol{\varepsilon},\alpha) \;+\; \varphi\left(\boldsymbol{\varepsilon}-\boldsymbol{\varepsilon}_n,\alpha-\alpha_n\right) \tag{1.24}$$

Note that this incremental variational principle will be considered in chapter 2 in a context of rate-independent behaviors in which the deformation $\boldsymbol{\varepsilon}$ will not be a dissipative variable, and will therefore not be present in the dissipation potential φ.
Finally, it must be emphasized that the incremental pseudo-potential is a convex function of $(\boldsymbol{\varepsilon},\alpha)$, making the minimization problem (1.22) a convex optimization problem.
For completeness, note that this type of incremental variational formulation has been already considered by [80].
Finally, from a more fundamental point of view, it is important to emphasize the great interest in energetics formulation of evolution problems in rate-independent systems as described by [98].

1.3 Local damage constitutive laws with unilateral effects

Some generalities

Under various loading conditions, the main mechanisms of deformation of many engineering materials involve degradation phenomena due to nucleation and growth of defects such as microvoids and microcracks. In the case of quasi-brittle materials, such deterioration phenomena take their origin in microcracking whose propagation induces irreversible processes and coalescence can lead to fracture occurrence. The year 1958 marked the beginning of the development of damage mechanics. In that year, Kachanov introduced the idea of the deterioration of the material through a scalar variable in continuum mechanics framework, called continuum damage mechanics (CDM). This early development has been consolidated in the eighties by thermodynamics-based studies following the newly introduced framework of

Generalized Standard Materials [53] and which guarantees to the models, thus built, to conform with Clausius-Duhem inequality. Among several contributions, mention can be made of [87, 79]. It is remarkable that some variational principles have been proposed at this early stage of the development of CDM (see again [87] but also [51]).

Continuum damage mechanics models were then progressively enriched: one of the research axes was to improve the description of the state of degradation of the material by considering second-order tensors or higher-order tensors as an internal variable (Chaboche [22], Chaboche et al. [24]) in order to account for induced anisotropy related to microcracks orientation (see for instance [32] or the paper by [52] or [27] in connection with the need to properly account for unilateral effects in presence of damage-induced anisotropy.
In what follows, and for simplicity, the damage which represents the state of degradation within the microstructure (micro-defects, microcracks, etc.) in the material will be represented by a positive scalar variable d, the main reason being the novelty of the topic of consideration of damage in the context of nonlinear homogenization (see chapter 2). Moreover, although the damage takes its origin from a complex irreversible evolution occurring at the microstructural scale (micro-cracking, micro-voids...), its main characteristics at the macroscopic level result in a variety of physical properties (elasticity for instance, induced softening, etc.) which need to be taken into account, even in a simplified manner in a first attempt of homogenization. In this context, the elastic behavior of the damaged material will be described by means of the stiffness tensor $\mathbb{C}(d)$ which depends on d.
Finally, before ending this section mention has to be made of different attempts to construct brittle damage models from an upscaling procedure, that is to derive the damage model from a micromechanical analysis of an elastic medium weakened by a system of multiple microcracks. For this purpose, one can refer to monographs [62], [66] or [30] to mention a few, or the paper by [121]. The main observation is that advances made in this domain are quite limited to the determination of the effective properties by using different linear homogenization schemes (dilute scheme, Hashin-shtrikman bounds, Ponte-Castañeda and Willis bounds), the evolution laws being considered in a phenomenological manner (see for instance or the paper by [111].

A standard isotropic elastic damage model formulation [87]

As already indicated, the GSM-based approach provides a suitable modeling framework allowing to automatically comply with the Clausius-Duhem inequality. In this framework, the first step consists of a suitable choice of state variables. Owing to arguments already recalled, these are chosen here as the infinitesimal strain tensor $(\boldsymbol{\varepsilon}, d)$ and a scalar d as the internal damage variable. The latter may represent a first-order approximation of the microcracks density parameter (see for instance [66] or [132] for analysis and discussion of this point) quantifying the damage evolution. The nonlinear behavior of this class of materials requires two potentials depending on the state variables.

The first potential corresponds to the free energy $w(\boldsymbol{\varepsilon}, d)$ taking the form

$$w(\boldsymbol{\varepsilon}, d) \;=\; \frac{1}{2}\,\boldsymbol{\varepsilon} : \mathbb{C}(d) : \boldsymbol{\varepsilon} \tag{1.25}$$

From the analysis performed in subsection 1.2.1, it readily follows that the Cauchy stress tensor $\boldsymbol{\sigma}$ and the irreversible force $\mathcal{Y}$ associated to the damage d reads :

$$\begin{cases} \boldsymbol{\sigma} \;=\; \dfrac{\partial w}{\partial \boldsymbol{\varepsilon}}(\boldsymbol{\varepsilon}, d) \\ \mathcal{Y} \;=\; -\dfrac{\partial w}{\partial d}(\boldsymbol{\varepsilon}, d) \end{cases} \tag{1.26}$$

while the intrinsic dissipation takes the form

$$\mathcal{D}_1 \;=\; \mathcal{Y}\dot{d} \tag{1.27}$$

For the complementary law, a simple choice of the dissipation potential, positive scalar-valued, convex with $\dot{d}$ and null at $\dot{d} = 0$ is :

$$\varphi(\dot{d}) \;=\; \mathcal{Y}_c(d)\,\dot{d} \tag{1.28}$$

where $\mathcal{Y}_c(d)$ is a characteristic of the elasto-damageable material which a priori may be obtained from experimental data.
With this dissipation potential in hand, and since it is not differentiable, one should refer to the notion of subdifferential $\partial\varphi$. The complementary law reads then :

$$\mathcal{Y} \;\in\; \partial\varphi(\dot{d}) \tag{1.29}$$

The irreversible force $\mathcal{Y}$ is said to belong to the subdifferential of φ at the considered point.

Alternatively, the dual potential of φ, defined by

$$\begin{aligned} \varphi^*(\mathcal{Y}) \;&=\; \sup_{\dot{d}>0} \left\{ \mathcal{Y}\dot{d} \;-\; \varphi(\dot{d}) \right\} \;=\; \sup_{\dot{d}>0} \left\{ \left(\mathcal{Y} - \mathcal{Y}_c(d)\right) \dot{d} \right\} \\ &= \begin{cases} 0 & \text{if} \quad f(\mathcal{Y}) = \mathcal{Y} - \mathcal{Y}_c(d) \leq 0 \\ \infty & \text{otherwise} \end{cases} \end{aligned} \tag{1.30}$$

takes the form of an indicator function of a convex domain $\mathcal{C}$ which is defined by

$$\mathcal{C} \;=\; \{\mathcal{Y} / f(\mathcal{Y}) \leq 0\} \tag{1.31}$$

This damage criterion reads

$$f(\mathcal{Y}) \;=\; -\frac{1}{2}\boldsymbol{\varepsilon} : \mathbb{C}'(d) : \boldsymbol{\varepsilon} \;-\; \mathcal{Y}_c(d) \leq 0 \tag{1.32}$$

Remark: we will refer during the thesis to some particular forms of $\mathcal{Y}_c(d)$ - the case of constant value, and that of linear or affine functions of d. In the later cases, the damaged material will be considered to experience some induced "hardening"-like effects will be investigated. With the help of φ^* and corresponding damage criterion, the normality rule, $\dot{\alpha} \in \partial\varphi^*(\mathcal{Y})$, which provides the irreversible damage evolution law, reads :

$$\dot{d} = \lambda \frac{\partial f}{\partial \mathcal{Y}} \tag{1.33}$$

The Lagrange multiplier λ is determined by the complementarity Karush-Kuhn-Tucker conditions

$$\begin{cases} \lambda \geq 0 \quad , \quad f(\mathcal{Y}) \leq 0 \quad , \quad \lambda . f(\sigma(x)) \;=\; 0 \\ \text{for } f(\mathcal{Y}) = 0 \quad , \quad \lambda \dot{f}(\mathcal{Y}) = 0 \quad \Leftarrow \text{ Consistency conditions} \end{cases} \tag{1.34}$$

This allows classically to build the rate formulation of the damage model by means of a symmetric multi-branch tangent operator and paves the way for specific numerical implementations.

Note that the general form of the isotropic elasticity stiffness tensor of the damaged material, based on a scalar variable d takes the form

$$\mathbb{C}(d) \;=\; 3k(d)\mathbb{J} + 2\mu(d)\mathbb{K} \tag{1.35}$$

where $\mathbb{J} = \frac{1}{3}\mathbb{1} \otimes \mathbb{1}$ and $\mathbb{K} = \mathbb{I} - \mathbb{J}$ are the two isotropic projectors of fourth-order tensors with the symmetries of a stiffness tensor. $\mathbb{I}$ is the symmetric fourth-order identity tensor. $k(d)$ is the bulk modulus of the damaged material, while $\mu(d)$ represents its shear modulus. In the recent literature, a common choice of simplification consists in

$$\mathbb{C}(d) = g(d)\mathbb{C}_s \;= g(d)(3k_s\mathbb{J} + 2\mu_s\mathbb{K}) \tag{1.36}$$

$\mathbb{C}_s$ being the stiffness of the isotropic sound material, and $g(d)$ a degradation function.

On unilateral effect

Modeling elasticity coupled with unilateral damage introduce difficulties that are widely recognized in several recent publications including those devoted to the modeling of gradient damage models [4, 77, 96, 113]. This concern is still debated in terms of different energy decompositions (see for instance [107] for a comparative analysis and a proposal of a new decomposition concerning anisotropic case).

We focus here on the context of bimodular elastic behaviors (then with the distinction of two domains in strain space). Clearly enough, we exclude the case of more than two domains of separation of strain space. In such context, and for isotropic behaviors, the formulation generally attributed to [4, 77] (see also [113]) can be rigorously established as a special case by following a constructive method initially introduced by [133] and developed by [56] based on the argument that the elastic energy must be continuously differentiable while a jump in the elastic stiffness (or compliance) tensor is allowed. This approach, which is summarized in Appendix[A], has been followed in the context of damage-induced anisotropy by several authors among which [32] [131], [129], [130] and [28] to cite few. Mention can also be made of some micromechanically motivated formulations for damage of initially anisotropic materials [47, 48]. Focusing specifically on isotropic materials, the corresponding three-dimensional formulation using a scalar damage variable can be found in [64], and in [28] in which microcracks closure-induced anisotropy has been also discussed.

Since in the present study, we will only use the formulation commonly attributed to Amor et al. [4], the development allowing us to retrieve it by following Curnier et al. [56] is summarized in Appendix[A]

The main result is the following expression of the free energy $w(\boldsymbol{\varepsilon}, d)$ in presence of damage and unilateral effects :

$$w(\boldsymbol{\varepsilon}, d) = \begin{cases} \frac{1}{2}k(d)\left(\mathrm{tr}\left(\boldsymbol{\varepsilon}\right)\right)^2 + \mu(d)\boldsymbol{\varepsilon}^d : \boldsymbol{\varepsilon}^d \quad \text{si} \quad \mathrm{tr}\left(\boldsymbol{\varepsilon}\right) \geq 0 \\ \\ \frac{1}{2}k_s\left(\mathrm{tr}\left(\boldsymbol{\varepsilon}\right)\right)^2 + \mu(d)\boldsymbol{\varepsilon}^d : \boldsymbol{\varepsilon}^d \quad \text{si} \quad \mathrm{tr}\left(\boldsymbol{\varepsilon}\right) \leq 0 \end{cases} \tag{1.37}$$

In summary, the isotropic elastic damage behavior in the presence of unilateral damage, as retained for the present study, will require in addition to the bulk and shear moduli of the sound material, two degradation functions, namely the one linked to $k(d)$ and to $\mu(d)$, which are the same that would be needed for the model without account for the unilateral effect.

1.4 Closed-form solutions on a hollow sphere made up with an elastic-damage material

1.4.1 Context and motivation

As previously mentioned, this thesis aims at determining the effective behavior of elasto-damageable composite (including porous) materials, as well as the local fields in their constituents. The main theoretical nonlinear homogenization approach that will be established for that is the purpose of the second chapter which will be based on the incremental variational procedure introduced by Lahellec and Suquet [75].

Considering the relative novelty of this research topic, it is desirable to have reference benchmark results that can be used for validation purpose of theoretical mean-field models and their predictions in terms of the local fields statistics, and even of some numerical approximations. This idea is not new and can be found in several studies which followed the Composite Sphere Assemblage (CSA) approach as initially proposed by Hashin [55]. It is well known that the effective response of this class of microstructures can be suitably approximated by solving the composite sphere (a spherical inclusion embedded in a concentric spherical matrix). For instance, for nonlinear viscoelastic or elasto(visco)plastic composites, this has been done in the recent study by [124]. Remarkably, these authors succeeded to establish exact solutions for the macroscopic behaviors of such composite spheres under isotropic loading (macroscopic stress or dilatation, swelling of the inclusion phase). For this specific problem, the authors have shown that the radial distribution of the shear stress constitutes the driving force of relaxation phenomena identified for the composite phenomena. For completeness, it is also worth noticing that the authors also reported full-field simulation results on matrix-inclusion representative volume elements

The objectives that we follow in this section are in the same vein, even less ambitious. Indeed, taking advantage of the study by [30], (see also [31]), we aim at presenting exact solutions for mechanical fields in a hollow sphere made up of an elastic damageable matrix and subjected to a radial loading on its external boundary. The solutions will be described for three different degradation functions of the matrix, the first being inspired from results based on available homogenization results of a microcracked matrix (the so-called Ponte-Castañeda and Willis bound, and the Mori-Tanaka scheme), and the last one being a commonly used degradation function in literature. Again, it must be recalled that our goal is to establish simple exact results which will serve as a reference for the assessment of the nonlinear homogenization model of quasi-brittle composites which will be developed in the next chapter.

1.4.2 Field equations of the elasto-damage hollow sphere problem

Let us begin with a description of the mechanical problem related to the hollow sphere under external radial loading. The cavity of inner radius a_0 represents the pore space, the outer part $r \in [a_0, b]$ represents the solid phase, with b the outer radius. The volume fraction $f = \left(\frac{a_0}{b}\right)^3$ corresponds to the initial porosity. The specific isotropic damage model considered for the following structural analysis is defined by a constant bulk modulus k and a shear modulus $\mu(d)$ which depends on a scalar damage variable d:

$$\mathbb{C}(d) = 3k\mathbb{J} + 2\mu(d)\mathbb{K}, \tag{1.38}$$

$\mu(d)$ being the unique degradation function considered in this section. Clearly, it is considered that damage affects only the shear elastic modulus. From a physical point of view, this may correspond to the case of closed microcracks for which it has been established that the bulk modulus remains at the value k of the sound material.

The boundary conditions read :

$$\begin{aligned} r = a_0 &: \boldsymbol{\sigma}_{rr} = 0 \\ r = b &: \boldsymbol{\sigma}_{rr} = T \end{aligned} \tag{1.39}$$

Considering the geometrical symmetry of the structure and the isotropic loading considered, the displacement field is radial and reads: $U = U(r)e_r$. The assumption of small perturbations being adopted throughout all of the study, the deformation tensor is:

$$\boldsymbol{\varepsilon} = \frac{\partial U}{\partial r}\, e_r \otimes e_r + \frac{U}{r}\, e_\theta \otimes e_\theta + \frac{U}{r}\, e_\phi \otimes e_\phi \tag{1.40}$$

By assuming monotonous loadings (a continuous increase of radial displacement applied at the outer boundary), the constitutive relations in the damage regime is $\boldsymbol{\sigma} = \mathbb{C}(d) : \boldsymbol{\varepsilon}$. Taking into account (1.40), the components of the stress tensor as a function of the displacement $U(r)$ in the damaged regime read :

$$\boldsymbol{\sigma}_{rr} = \left(k - \frac{2}{3}\mu(d)\right)\left(\frac{\partial U}{\partial r} + 2\frac{U}{r}\right) + 2\mu(d)\frac{\partial U}{\partial r} \tag{1.41}$$

$$\boldsymbol{\sigma}_{\theta\theta} = \left(k - \frac{2}{3}\mu(d)\right)\left(\frac{\partial U}{\partial r} + 2\frac{U}{r}\right) + 2\mu(d)\frac{U}{r} \tag{1.42}$$

Putting this one in the equilibrium equation $\mathrm{div}(\boldsymbol{\sigma}) = 0$, leads to the extended and coupled Lamé-Navier partial differential equation, obtained for the two unknown fields $U(r)$ and $d(r)$:

$$\left(k + \frac{4}{3}\mu(d)\right)\frac{\partial}{\partial r}\left(\frac{\partial U}{\partial r} + 2\frac{U}{r}\right) + \frac{4}{3}\frac{\partial \mu(d)}{\partial d}\frac{\partial d}{\partial r}\left(\frac{\partial U}{\partial r} - \frac{U}{r}\right) = 0 \tag{1.43}$$

The remaining equation that has to be considered is the damage criterion (1.32) expressed in terms of the deformation tensor. At the saturation of the criterion, by reporting (1.40) in (1.32), one has the following differential equation :

$$-\frac{2}{3}\frac{\partial \mu}{\partial d}\left(\frac{\partial U}{\partial r} - \frac{U}{r}\right)^2 = Y_c \tag{1.44}$$

In the elastic damage regime, (1.44) together with (1.43) constitute the system of partial differential equations to be solved in order to determine both the displacement field $U(r)$ and the damage field $d(r)$.

- **The linear elastic regime**

  As long as this criterion is not reached, all the hollow sphere remains in the linear

elastic regime. In this case, the classical displacement field solution is valid

$$U(r) = Ar + \frac{B}{r^2} \tag{1.45}$$

with the constants A and B expressed as

$$A = \frac{T}{3k}\frac{b^3}{b^3 - {a_0}^3} = \frac{T}{3k}\frac{1}{1-f} \qquad ; \qquad B = \frac{T}{4\mu_s}\frac{a_0^3\, b^3}{b^3 - {a_0}^3} = \frac{T}{4\mu_s}\frac{a_0^3}{1-f} \tag{1.46}$$

in which T represents the radial stress at the external boundary $r = b$ and f the initial porosity as defined before.

By reporting the latter into (1.44), it is readily seen that the damage will first start at the location $r = a_0$ and that the resulting stress at the first yield limit $T = T_{el}$ (instant where the linear elastic regime ends and the damage begins) reads :

$$T_{el} = \frac{4\mu_0}{3}\left(\frac{{a_0}^3}{b^3} - 1\right)\zeta \qquad \text{where} \qquad \zeta = \epsilon\sqrt{-\frac{3Y_c}{2\mu_s'}} \qquad \text{and} \qquad \mu_s' = \left\{\frac{\partial \mu}{\partial d}\right\}_{d=0} \tag{1.47}$$

It can be easily checked that the displacement at the external boundary $r = b$ is given by :

$$U(b) = \frac{T(4\, b^3\mu_s + 3\, k\, {a_0}^3)}{12\, k\, \mu_s\, (b^3 - {a_0}^3)} b \tag{1.48}$$

As in [124], it is classical to verify that T, as defined before by the value of the radial stress $\boldsymbol{\sigma}_{rr}(b)$, and $\frac{U(b)}{(b)}$ are the generalized quantities which allow representing the overall stress-strain response of the structure.

- **The damage regime**
  Beyond the threshold $T = T_{el}$, the hollow sphere passes from the linear elastic regime to the elastic-damage regime where the radius $r = c$ is the boundary between the damaging zone and the elastic zone. In the damage regime we can therefore see the hollow sphere separated into two zones:
  - $a_0 < r < c$: damage zone
  - $c < r < b$: elastic zone

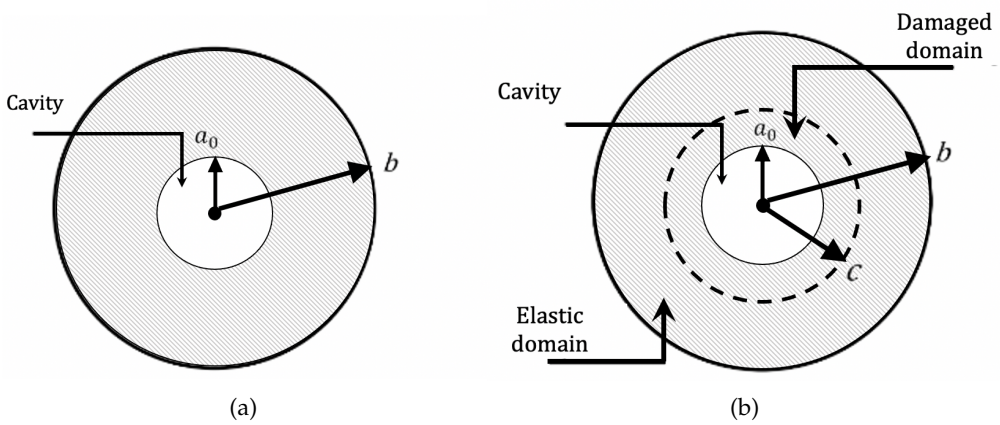

FIGURE 1.1: Repesentation of the hollow sphere in the two distinct regimes : (A) Linear elastic regime, (B) Elasto-damageable regime

1.4.3 Closed-form solutions for the damage model with $\mu(d) = \mu_s \frac{1+Qd}{1+Q'd}$ [30]

We consider now a first model which relies on the expression of the shear modulus established by Ponte-Castañeda and Willis [121] as an upper bound of effective shear modulus. This type of bounds, which accounts for both interaction between microcracks and their spatial distribution (considered here as spherical), provides :

$$\mu(d) = \mu_s \frac{1+Q\,d}{1+Q'\,d} \quad \text{where} \quad Q \leq Q' \tag{1.49}$$

in which Q and Q' are two scalar constants that depend only on the Poisson ratio of the sound material (constituting here the solid matrix).
Note that for comparison purposes, we will also examine the case $Q = 0$ which corresponds to the prediction of the so-called Mori-Tanaka scheme which does not account for microcracks spatial distribution.

By reporting the expression (1.49) of the shear modulus in (1.44), one gets

$$\frac{\partial U}{\partial r} - \frac{U}{r} = \zeta\,(1 + Q'\,d) \qquad \text{where} \qquad \zeta = \epsilon\sqrt{\frac{3\mathcal{Y}_c}{2\mu_s\,(Q'-Q)}} \tag{1.50}$$

with $\epsilon = \pm 1$.
ζ is a material characteristic that is readily seen to depend on the elastic properties of the sound material and of its damage characteristics $\mathcal{Y}_c$.

The solution to the above differential equation in $U(r)$ reads :

$$U(r) = u_0\,r + r\int_{a_0}^{r} \zeta(1+Q'd(\rho))\frac{d\rho}{\rho} \tag{1.51}$$

Introducing then (1.51) into (1.43), and using (1.49), the differential equation in $d(r)$ takes the form :

$$\frac{\partial d}{\partial r} = -\frac{3}{r}\left(d + \frac{3k + 4\mu_s}{3kQ' + 4\mu_s Q}\right) \tag{1.52}$$

It follows that the damage distribution has a closed-form expression :

$$d(r) = \frac{3k + 4\mu_s}{3kQ' + 4\mu_s Q}\left(\left(\frac{c}{r}\right)^3 - 1\right) \tag{1.53}$$

The shear modulus remains positive if the condition $d(r) \leq -1/Q$ is verified. If $Q < 0$, the condition becomes $d(r) = -1/Q$, for which the solution is given by $r = \tilde{a}(c)$

$$\tilde{a}(c) = \mathcal{G}c \qquad \text{where} \qquad \mathcal{G} = \left(\frac{1 + \dfrac{4\mu_s}{3k}}{1 - \dfrac{Q'}{Q}}\right)^{\frac{1}{3}} \tag{1.54}$$

if $\tilde{a} < a_0$ then the condition on the shear modulus of rigidity $\mu(d) > 0$ is satisfied over the whole sphere.
If $\tilde{a} > a_0$ then the region $a_0 < r < \tilde{a}$ is totally damaged and the boundary condition $\boldsymbol{\sigma}_{rr} = 0$ is then satisfied on $r = \tilde{a}$. We thus note a the value of r for the boundary condition $\boldsymbol{\sigma}_{rr}(a) = 0$. The expression of a will then depend on c:

$$a = \left\{ \begin{array}{lll} a_0 & \text{if} & \tilde{a}(c) < a_0 \\ \tilde{a}(c) & \text{if} & \tilde{a}(c) > a_0 \end{array} \right\} \tag{1.55}$$

The displacement field $U(r)$ is readily obtained by inserting (1.53) into (1.51). The resolution of the problem is completed by considering the boundary condition $\boldsymbol{\sigma}_{rr}(a) = 0$. Once $U(r)$ is fully determined, $\boldsymbol{\sigma}_{rr}$ can be computed from (1.41) :

$$\boldsymbol{\sigma}_{rr} = \frac{12k(Q' - Q)\zeta\mu_s}{3kQ' + 4\mu_s Q}\log\frac{a}{r} + \frac{4\mu_s\zeta Q(3k + 4\mu_s)}{3(3kQ' + 4\mu_s Q)}\frac{c^3}{a^3}\left(\frac{a^3}{r^3} - 1\right) \tag{1.56}$$

and from (1.42), we obtain the following expression of $\boldsymbol{\sigma}_{\theta\theta}$:

$$\boldsymbol{\sigma}_{\theta\theta} = \left(\frac{4c^3\zeta\mu_s Q\left(\frac{a^3}{r^3}-1\right)(3k+4\mu_s)}{3a^3\left(3kQ'+4\mu_s Q\right)} + \frac{12\zeta k\mu_s\left(Q'-Q\right)\log\left(\frac{a}{r}\right)}{3kQ'+4\mu_s Q} \right) - 2\zeta\mu(r)\left(\frac{Q'\left(\frac{c^3}{r^3}-1\right)(3k+4\mu_s)}{3kQ'+4\mu_s Q} + 1 \right) \tag{1.57}$$

The shear modulus would eventually take the following form by replacing $d(r)$ by its expression (1.53):

$$\mu(r) = \mu_s \frac{1 + Q\frac{(3k+4\mu_s)}{3kQ'+4\mu_s Q}\left(\frac{c^3}{r^3}-1\right)}{1 + Q'\frac{(3k+4\mu_s)}{3kQ'+4\mu_s Q}\left(\frac{c^3}{r^3}-1\right)} \tag{1.58}$$

The expressions (1.56) and (1.57) are used in the damaged domain only. In the elastic zone, by putting to use the boundary condition on $r = b$, we obtain the displacement on $r = b$:

$$U(b) = \frac{Tb}{3k} - c^3\zeta\frac{3k+4\mu_s}{9kb^2} \tag{1.59}$$

the stress components take the following form :

$$r > c: \qquad \sigma_{rr} = T + \frac{4}{3}\mu_o\zeta c^3\left(\frac{1}{r^3}-\frac{1}{b^3}\right) \tag{1.60}$$

$$\sigma_{\theta\theta} = T - \frac{2c^3\zeta\left(b^3+2r^3\right)\mu_o}{3b^3r^3} \tag{1.61}$$

Finally the load T can be linked to c through the following expression (one can refer to [30] for further details):

$$T = \frac{4}{3}\zeta\mu_s\left(\frac{3k(Q'-Q)}{3kQ'+4\mu_s Q}\left(3\log\frac{a}{c}-1\right) + \frac{c^3}{b^3} - \frac{c^3}{a^3}\frac{Q(3k+4\mu_s)}{3kQ'+4\mu_s\,Q}\right) \tag{1.62}$$

At this stage, further discussion can be helpful according to the possible cancellation of the shear modulus at a high level of damage and the necessity to update the geometry of the hollow sphere whose internal radius will be noted a. For a such detailed discussion, one may refer to [30]. Now, if $\tilde{a} > a_0$, then $c > c_{cr}$, (with $c < b$), the ratio a/c in (1.62) is such that (see [30]) T can be written as :

$$\tilde{a} > a_0 : \qquad \frac{T}{\mu_s} = \frac{4\zeta(Q'-Q)(3k+4\mu_s)}{3kQ'+4\mu_s Q}\log\mathcal{G} - 4\frac{U(b)}{b} \tag{1.63}$$

Ponte-Castañeda-Willis bound

Let us start with the Ponte-Castañeda-Willis (PCW) upper bound of the effective stiffness of a randomly microcracked medium. The typical stress-strain curve for the corresponding damage model for simple shear is depicted in Fig. 1.2.

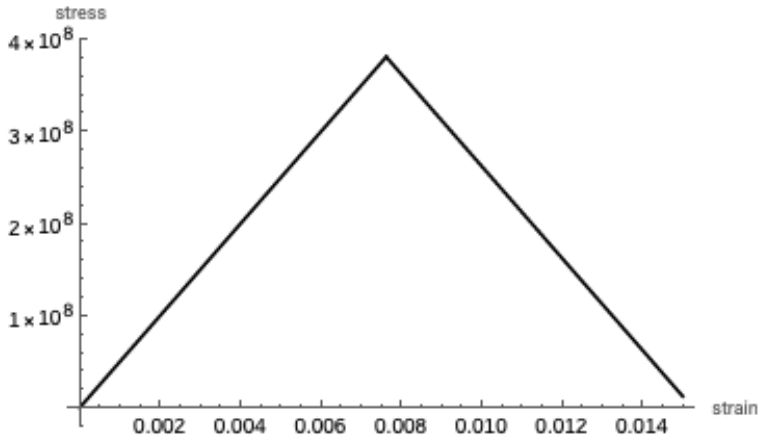

(a)

FIGURE 1.2: Typical stress-strain curve for simple shear in a material point for an isotropic damage model based on the PCW scheme

Results corresponding to the Ponte-Castañeda and Willis bound are displayed in figures 1.3 for two values of the ratio $\frac{k}{\mu_s}$: $\frac{k}{\mu_s} = 3$ (on left) and $\frac{k}{\mu_s} = 30$ (on right). These figures represent the macroscopic stress T as function of the overall volumetric strain $U(b)/b$.
Three regimes are distinguishable on these figures :

- Phase (1) : $T < T_{el}$ - in this regime the entire hollow sphere has a linear elastic behavior, the volumetric strain being given then by the classical expression (1.48).
- Phase (2) : $c_{cr} < c < b$ - this corresponds to the damage regime in which the $r \in [a_0, c]$ zone is subjected to partial damage while the $r \in [c, b]$ still behaves linear elastically. The equations (1.62) with $a = a_0$ and (1.59) govern this regime.
- Phase (3) : $a_0 < c < c_{cr}$ - softening occurs in this regime, the domain $r \in [a_0, \tilde{a}(c)]$ is completely damaged (in the sense that the shear modulus cancels), and this regime is described by (1.63) with $a = \tilde{a}$.

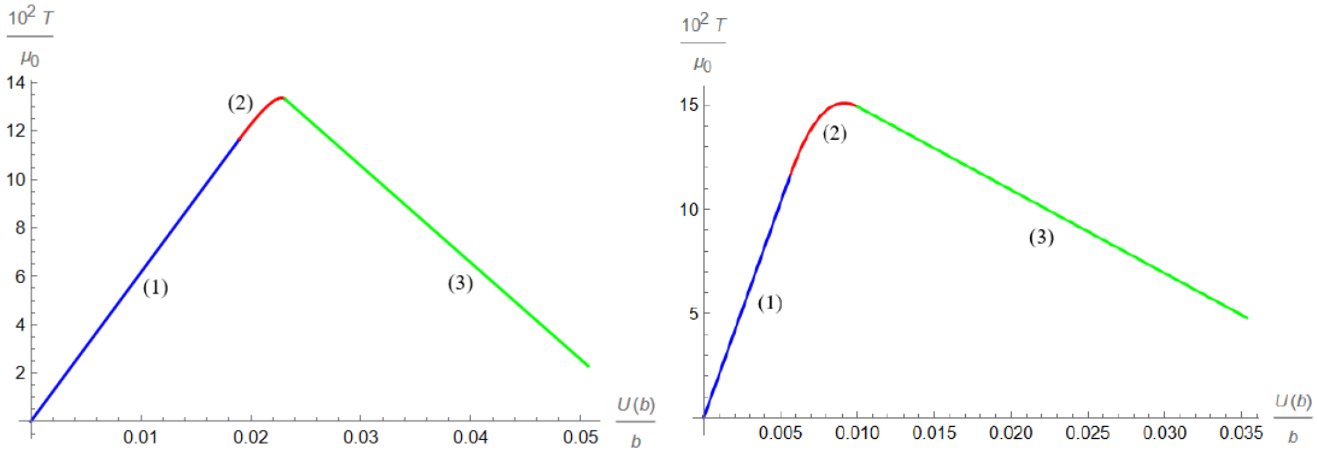

(a) $\frac{k}{\mu_s} = 3$ (b) $\frac{k}{\mu_s} = 30$

FIGURE 1.3: Macroscopic response of the hollow sphere : T with respect to $\frac{U(b)}{b}$ for different $\frac{k}{\mu_s}$. $\zeta = -0.1$, $b/a = 2$, $Q' = -Q = 1$ for the model based on the PCW upper bound

For completeness, we present in Fig.1.4 the distribution of the stress field components in the hollow sphere, that is as a function of the ratio r/a_0. The example shown here concerns the evolution of $\boldsymbol{\sigma}_{rr}$ and $\boldsymbol{\sigma}_{\theta}$ in regime (2) for the peak stress loading level $T = T_{max}$ (already shown on Fig.1.3). The continuity of the radial stress at the limit between the damaged zone and the linear elastic zone is easily verified in agreement with the continuity of the stress vector. Moreover, the distribution of the orthoradial stress component $\boldsymbol{\sigma}_{\theta\theta}$ is also observed. This is explained by the fact that the local damage criterion can be expressed as $\boldsymbol{\sigma}_{\theta\theta} - \boldsymbol{\sigma}_{rr} = constant$ and is then continuous at $r = c$. The continuity of $\boldsymbol{\sigma}_{\theta\theta}$ follows then as a consequence of the radial stress continuity.

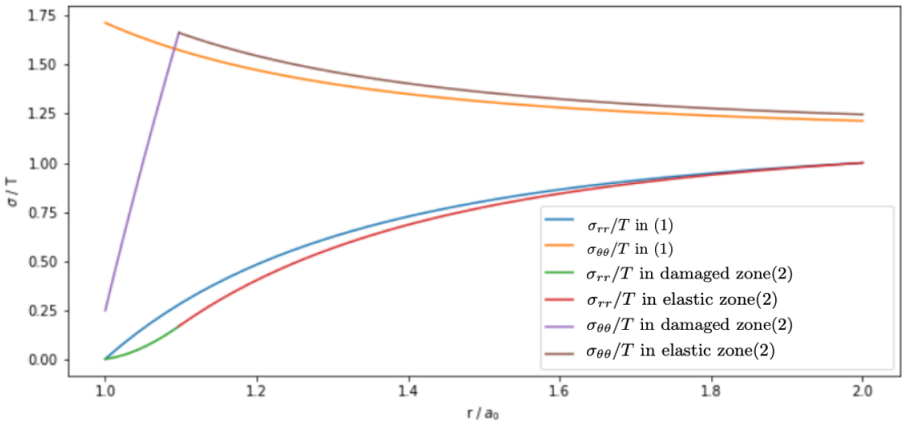

FIGURE 1.4: Evolution of $\frac{\boldsymbol{\sigma}_{rr/\theta\theta}}{T}$ in the damaged hollow sphere as a function of $\frac{r}{a_0}$ for the model based on the PCW upper bound

Mori-Tanaka scheme

As previously announced, let us come now to the Mori-Tanaka (MT) scheme-based expression of the degradation function $\mu(d)$. As also mentioned before, this is a particular case of the PCW-type bound with $Q = 0$:

$$\mu(d) = \frac{\mu_s}{1 + Q'\,d} \qquad \text{with} \qquad Q' > 0 \tag{1.64}$$

The typical stress-strain curve for the corresponding damage model for simple shear is depicted on Fig. 1.5.

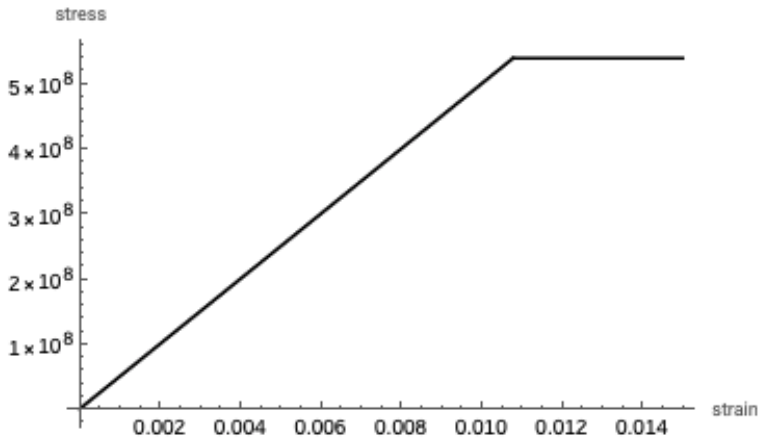

(a)

FIGURE 1.5: Typical stress-strain curve for simple shear in a material point for an isotropic damage model based on the MT scheme

The procedure of derivation of the solutions follows the same set of equations. But, as we will illustrate that, the specific observation is that this scheme does not predict any softening phase during the damage regime. The main analytical in this damage regime are summarized by :

$$\begin{cases} d(r) = \dfrac{3k + 4\mu_s}{3kQ'}\left(\left(\dfrac{c}{r}\right)^3 - 1\right) & \text{(1.65a)} \\ U(r) = u_0\, r - \dfrac{\zeta}{9k}\left(12\mu_s r \log r + (3k + 4\mu_s)\dfrac{c^3}{r^2}\right) \qquad \text{where} \qquad u_0 = \dfrac{4\zeta\mu_s}{3k}\, log(a_0) & \text{(1.65b)} \\ \boldsymbol{\sigma}_{rr} = 4\zeta\mu_s \log\dfrac{a_0}{r} & \text{(1.65c)} \\ \boldsymbol{\sigma}_{\theta\theta} = 2\zeta\mu_s\left(log\left(\dfrac{a_0}{r}\right)^2 - 1\right) & \text{(1.65d)} \\ T = \dfrac{4}{3}\zeta\left(-1 + \dfrac{c^3}{b^3} + 3\, log\left(\dfrac{a_0}{c}\right)\right)\mu_s & \text{(1.65e)} \end{cases}$$

Based on the above equations, and unlike Fig.1.3, it is seen that the Mori-Tanaka model consists of only two regimes, without softening:

- Phase (1) : $T < T_{el}$ - the first phase corresponds to the elastic regime and the volumetric strain is still given by (1.48).
- Phase (2) : $a_0 < c < b$ - this phase represents the damage regime in which the $r \in [a_0, c]$ domain is subjected to partial damage while the $r \in [c, b]$ domain is still linear elastic. The stress-strain response in this regime is provided by equations (1.65e) and (1.59).

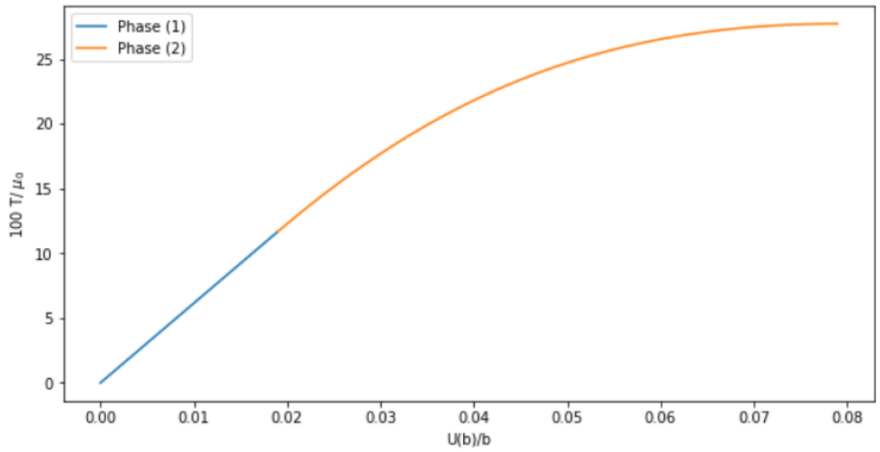

FIGURE 1.6: Macroscopic response of the hollow sphere : T with respect to $\frac{U(b)}{b}$ for $\frac{k}{\mu_s} = 3.\ \zeta = -0.1, b/a = 2, Q' = 1$ for the MT scheme

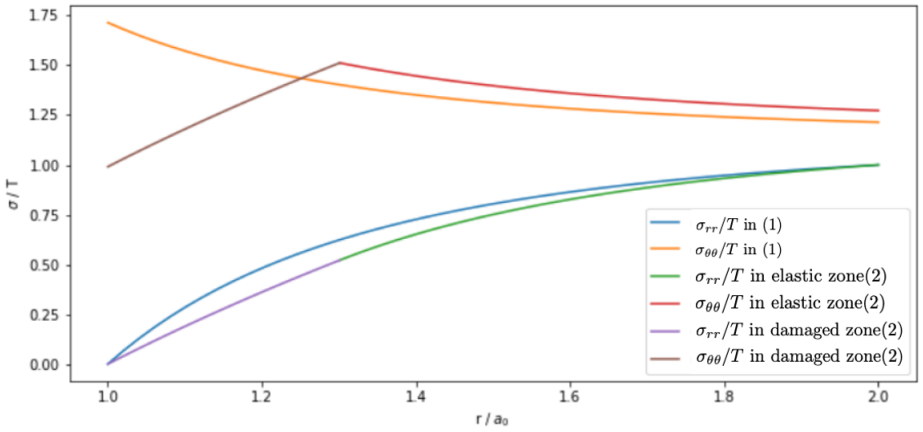

FIGURE 1.7: Evolution of $\frac{\boldsymbol{\sigma}_{rr/\theta\theta}}{T}$ in the damaged hollow sphere as a function of $\frac{r}{a_0}$ for the model based on the MT scheme

1.4.4 Closed-form solutions for the damage model with $\mu(d) = (1-d)^2\mu_s$

We consider now the degradation function $\mu(d) = \mu_s(1-d)^2$ which corresponds to the one usually used in the recent literature devoted to the gradient damage model (we will come back to this point in the next chapters). By reporting this expression of the shear modulus in

(1.45), one gets :

$$\frac{\partial U}{\partial r} - \frac{U}{r} = \zeta \sqrt{\frac{1}{1-d(r)}} \qquad \text{where} \qquad \zeta = \epsilon \sqrt{\frac{3\mathcal{Y}_c}{4\mu_s}} \tag{1.66}$$

which seems to be a little more complicated than the two previous ones (see 1.50), since the damage field $d(r)$ appears in the second member in a non-affine form.

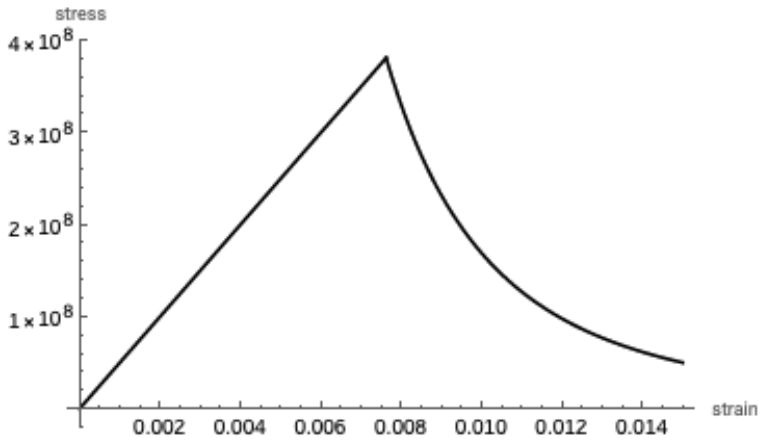

(a)

FIGURE 1.8: Typical stress-strain curve for simple shear in a material point for an isotropic damage model based on the $(1-d)^2$ degradation function

Nevertheless, this new coupled partial a differential equation can be also solved by first considering that $U(r)$, is the unknown. One gets :

$$U(r) = r\,u_0 + r \int_{a_0}^{r} \zeta \sqrt{\frac{1}{1-d(\rho)}}\,\frac{d\rho}{\rho} \tag{1.67}$$

The introduction of (1.67) into (1.43) remarkably provides the following differential equation in $d(r)$

$$\frac{\partial d}{\partial r} - 6\frac{d(r)}{r} + \frac{6}{r} = 0 \tag{1.68}$$

The solution to this equation is obtained, knowing that $d(c) = 0$, and takes the following form for the damage distribution in the zone $r \in [ao, c]$ (the relation between T and c will be given below):

$$d(r) = 1 - \left(\frac{r}{c}\right)^6 \tag{1.69}$$

which can be compared to the distribution obtained for the previous degradation functions, namely the one given by (1.53).
By inserting (1.69) into (1.67), and taking into account the boundary condition at the inner

boundary, one gets $u_0 = -r\dfrac{\zeta(3kc^{12} + 4\mu_s {a_0}^{12})}{9kc^9 {a_0}^3}$ and $U(r)$ in the form

$$U(r) = \frac{1}{3} r\zeta c^3 \left(\frac{1}{{a_0}^3} - \frac{1}{r^3}\right) - r\frac{\zeta(3kc^{12} + 4\mu_s {a_0}^{12})}{9kc^9 {a_0}^3} \tag{1.70}$$

which can be simplified as

$$U(r) = -\frac{\zeta}{3}\frac{c^3}{r^2} - \frac{\zeta}{3}\frac{4\,\mu_s\, a_0^9}{3\,k\,c^9} r \tag{1.71}$$

Therefore, one gets the stress components $\boldsymbol{\sigma}_{rr}$ and $\boldsymbol{\sigma}_{\theta\theta}$ by introducing the above expression of $U(r)$ in (1.41) and (1.42) :

$$\boldsymbol{\sigma}_{rr} = \frac{4}{3}\,\zeta\,\mu_s \left(\frac{r^9}{c^9} - \frac{a_0^9}{c^9}\right) \tag{1.72}$$

and

$$\boldsymbol{\sigma}_{\theta\theta} = -\frac{2\,\zeta\,\mu_s}{3} \left(\frac{r^9}{c^9} - \frac{2\,a_0^9}{c^9}\right) \tag{1.73}$$

Recall that the equations (1.71), (1.72), and (1.73) are for the damaged domain $a_0 < r < c$. The radial stress in the elastic domain $c < r < b$ is the same as equation (1.60). The continuity of the radial stress at the boundary of the damaged zone and the elastic zone in $r = c$ gives us the relation between T and c by associating (1.72) and (1.60).

$$T = \frac{4\,\zeta\,\mu_s}{3} \left(\frac{c^3}{b^3} - \frac{a_0^9}{c^9}\right) \tag{1.74}$$

Two regimes can be distinguished:

- Phase 1: it represents the elastic regime for which the result (1.48) for the elastic volumetric strain is still valid
- Phase 2: $a_0 < c < b$: we are here in the damage regime in which the zone $r \in [a_0, c]$ is again subjected to partial damage while the $r \in [c, b]$ domain remains linear elastic. Equations (1.74) and (1.59) provide the overall response in this regime. It can be noted that in regime 2 of the present model, damage and softening occur simultaneously.

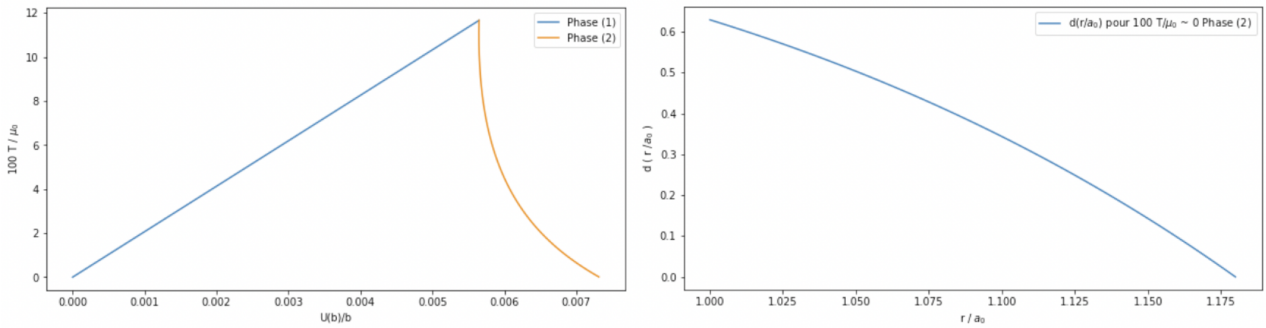

(a) (b)

FIGURE 1.9: (a) Macroscopic response of the hollow sphere with the model based on $\mu(d) = \mu_s(1-d)^2 : T$ with respect to $\frac{U(b)}{b}$ for $\frac{k}{\mu_s} = 30$. $\zeta = -0.1$, $b/a = 2$, (b) Damage evolution with respect to the radius

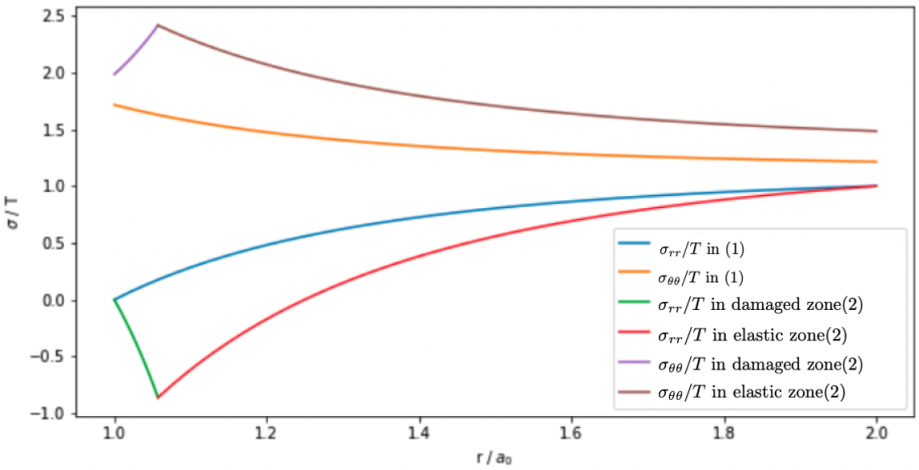

FIGURE 1.10: Evolution of $\frac{\boldsymbol{\sigma}_{rr/\theta\theta}}{T}$ as a function of $\frac{r}{a_0}$, for the model based on $\mu(d) = \mu_s(1-d)^2$

1.5 Conclusion

This chapter has been devoted to two issues :

- First, to recall and present a standard thermodynamics-based formulation of the isotropic local elastic damage model. This has been done by relying on the General Standard Materials (GSM) framework in which the elastic damage model, based on the use of a scalar internal variable, is formulated from a thermodynamics potential and a dissipation potential. The standard formulation recalled here, includes (based on literature) the so-called unilateral effects (related to microcracks closure phenomena) and which generally induce a partial deactivation of damage effects.
  Taking advantage of the GSM framework, simple variational principles can be obtained (see [109], [97], [123], etc.) and may be useful in the damage context for the

proposal of two-fields variational principles early suggested by [34] for simple dissipative structures (see [33]) or by [39]. Note that these variational formulations appear now as particular cases of the one introduced by [19] in the context of regularized damage model.

- Derivation of closed-form solutions for a hollow sphere made up of an elastic damage matrix. The used procedure follows the study by [30] (see also [31]), with the aim of producing simple and basic exact solutions that will be used for a first assessement of the nonlinear homogenization that will be constructed in the next chapter. From this study, it appears that, depending on the considered degradation function, the overall behavior can exhibit, or not, a hardenable first stage (structural effect) before the occurrence of a softening regime.
  It must be emphasized that the closed-form results presented in section 1.4 can be extended to a composite sphere by taking advantage of a recent study on a matrix-inclusion configuration by [26] which also follows [30].

Again, it must be repeated, that even the established solutions do not strictly constitute homogenization results, they are licit to be considered for comparison purposes with theoretical nonlinear homogenization models which lack in literature, except the very recent work of [43] which provides original results relying on recent tools both from homogenization theory and from some gradient damage models. The construction and assessment of such new homogenization models for quasi-brittle composites with an elastic damage matrix is the subject of the next chapters.

Chapter 2

An Effective Internal Variable approach for quasi-brittle composites

Contents

We begin in section 2.1 with a general presentation of some nonlinear homogenization methods including incremental variational approaches whose general framework is detailed in section 2.2. Based on the thermodynamics framework of Generalized Standard Materials

(GSM) theory, already recalled in chapter 1, we then introduce the main elements of the Effective Internal Variable (EIV) homogenization approach proposed by Lahellec and Suquet [75]. This method relies on the incremental variational formulation of [109] (see also [94]). Since the novelty of this chapter lies in the adaptation of the EIV method to composites with elasto-damageable constituents, we detail the corresponding theoretical development in section 2.3. To this end, we proceed to a simple linearization of the incremental potential and then solve the resulting homogenization problem. Finally, the developed model is implemented for a two-phase composite, made of spherical linear elastic particles randomly and isotropically distributed in an elasto-damageable matrix. The required numerical solution procedures are presented. The chapter ends with some preliminary predictions of the model.

2.1 Nonlinear homogenization methods for composites

2.1.1 Available nonlinear homogenization procedures

Several methodologies and results have been proposed for composites with elastic linear constituents for which estimates and bounds are available since the work of Eshelby [35]. Among the different homogenization schemes in this framework, one can mention the Mori-Tanaka [100], the Hashin-Shtrikman bounds [54], the Ponte Castañeda and Willis [120] or the self-consistent scheme [69]. The linear homogenization theory has been extended to the linear thermo-elastic case in which thermal strain can be treated as free strain. This extension is based on the fact that the equations are linear, which allows the use of the superposition principle. Note that due to the linearity of the behavior, the constitutive thermoelastic law of the phases can be applied to the field averages per phase called first-order moment. For homogenization of linear thermoelastic heterogeneous media, the reader can for instance refer to [78], [134]. An interesting survey on continuum micromechanics can be also found in [137].

The case of nonlinear composites induces new difficulties since the principle of superposition is no longer valid. In this context, new approaches have been proposed since the 1980s with the introduction of new variational formulations (one can refer to [119]). With the exception of the last 12 years, most of this work has focused on composites made up of phases whose behavior is governed by a unique nonlinear potential: the free energy in the case of nonlinear elasticity, and the dissipation potential in the case of purely viscoplastic materials without threshold. For such composite materials, nonlinear homogenization theories are generally based on two steps: a linearization step followed by a homogenization step . The first step is to approach the nonlinear composite by an elastic fictitious linear comparison composite (LCC) by linearizing the local constitutive laws around a value of reference. This LCC is in a second step homogenized by using a linear homogenization scheme.

The first approaches developed within this approach, implicitly or explicitly, choose the average by phase (or first-order moment) of the strain or stress tensor as the reference value around which the linearization is performed. The pioneering incremental method introduced by Hill [57] for nonlinear homogenization of elasto(visco)plastic composites can be seen as an incremental linearization around the phase-averaged fields. Afterwards, the secant method (Berveiller and Zaoui [10]), constructed as an alternative to the incremental formulation of Hill for elasto-plasticity in the context of proportional loadings as well as the affine approach for elasto(visco)plasticity (Masson and Zaoui [91]), visco-plasticity or elasto-plasticity (Masson et al. [89]), are based on a similar principle. Nevertheless, in a general way, it has been noticed that the use of first-order moments as a representation of the deformation state of the phases often leads to predictions that are too stiff (see for instance Gilormini [46]) and does not properly account for the nonlinear mechanical responses.

On the basis of variational formulations and arguments of a physical nature, different authors have shown the importance of considering quantities that do not neglect the heterogeneity of the fields within the phases. Among these quantities, the most generally used are the second-order moments (see for example Ponte Castañeda [118], Suquet [119], Ponte Castañeda and Suquet [119]). An alternative and complementary way of taking these fluctuations into account is to discretize the composite into subdomains (see Bilger et al. [11, 12], Michel and Suquet [95]). These approaches have significantly increased the accuracy of the models. Moreover, it has been shown [126] that the choice of second-order moments is optimal with respect to the variational formulation introduced by Ponte-Castañeda [116]. Currently, the most sophisticated models take into account both first and second-order moments to define the LCC (Ponte Castañeda [117]). The effectiveness of such models has been shown through numerous theoretical and numerical studies (Idiart et al. [58], Idiart and Ponte Castañeda [59]) based in particular on the comparison of the predictions of these mean fields approaches with numerical simulations which serve as reference solutions. The comparisons concern both the effective behavior as well as the inter and intra-phase heterogeneities of the local fields (i.e. the first and second-order moments).

2.1.2 Methods based on incremental variational approaches

In 1986, Mialon [94] was the first to introduce a variational principle close to the one used in this thesis. He applies this principle to the cases of structures made up of elasto-plastic materials whose behavior is governed by two potentials. Later, Ortiz and Stainier [109] proposed another variational principle, similar to that of Mialon, but in the context of elasto(visco)plastic materials. Lahellec and Suquet, [75] and [74], developed two homogenization schemes based on these variational principles which will be presented below.

Studies [73, 75], which introduce an incremental variational approach for nonlinear composites, opened new research directions in the homogenization of nonlinear behaviors governed

by two potentials. The local variational principle used in this approach is based on the introduction of a single potential, the condensed incremental potential, which accounts for both conservative and dissipative effects in the composite. This potential is constructed as the sum of the two potentials which define the local behavior in the GSM framework, namely the free energy and the dissipation potential. From this local variational principle, these authors obtained a macroscopic incremental variational principle allowing them to estimate the responses of the nonlinear composites. This variational principle makes it possible to extend most of the methods developed within the framework of composites governed by a single potential to composites whose phase's behavior can be described by means of two potentials. Based on this observation, Lahellec and Suquet [73, 75] applied the main idea of the variational procedure introduced by Ponte Castañeda [118] to their macroscopic incremental variational principle in order to estimate the effective behavior of composites consisting of elasto(visco)plastic phases. To this end, they used two approximations. The behavior of each constituent phase is first linearized by introducing a uniform secant viscosity per phase through the variational procedure. Additionally, the inelastic heterogeneous strains at time t_n are approximated by a homogeneous effective internal variable in each phase. These two approximations lead to the definition of a thermo-elastic LCC (as introduced by Ponte Castañeda [118]) whose effective behavior can then be obtained using any appropriate linear homogenization scheme for the considered microstructure. This procedure, called Effective Internal Variables (EIV), was first applied to nonlinear elasto(visco)plastic composites without threshold or hardening and led to accurate estimates of the macroscopic behavior in the case of nonlinear behaviors.
The same year, Lahellec and Suquet [76] used another linearization scheme. They proposed a modified version of the second order method (Ponte Castañeda [115]) by applying it to the dissipation potential, which leads to replace, at each time step, the nonlinear viscoelastic composite with a linear visco-elastic composite.

In 2013, Lahellec and Suquet [74] introduced modified incremental variational principles in a rate form in order to get estimates of the local and global behavior for composites made of elasto(visco)plastic phases with both isotropic and linear kinematic hardening. Their new approach, called the Rate Variational Procedure (RVP), still relies on two approximations. The first one consists in using the variational procedure to linearize the constitutive laws and provides again a secant approximation of the behavior. For the second one, at the difference with Lahellec and Suquet [75], it is now the heterogeneous stress field – and not the heterogeneous plastic strain field – at time t_n which is approximated by effective homogeneous internal variables in each individual phase. For that, they make use of a similar method to the one proposed by Lahellec et al. [72], which is also based on the variational procedure but relies on a new definition of an LCC with uniform coefficients per phase which depend on the first and second-order moments of the stress field. In order to assess their new model, Lahellec and Suquet [74] carry out Fast Fourier Transform (FFT) simulations on a heterogeneous material made of an elasto(visco)plastic matrix reinforced by 50 elastic isotropic spherical particles randomly distributed. A good agreement is observed between the model predictions and the FFT simulations for elastic ideally-plastic matrix or elasto-plastic matrix

with isotropic or linear kinematic hardening under radial and non-radial loadings.

As previously mentioned, these homogenization models are limited to elasto(visco)plastic composites exhibiting kinematic hardening, linear or nonlinear, and possibly coupled with isotropic hardening. In the present study, we focus on the homogenization of composites whose constituents' behavior results from a coupling between elasticity and damage and presents a stress softening. The latter is able to lead to the ultimate step of fracture occurrence due to the strong localization of the damage.
Although significant progress has been made in recent years in the modeling of damage and the resulting fracture processes, the consideration of this damage in homogenization approaches of composites is still a work in progress and at its very first stages (see for instance the recent study by [43]). The study presented hereafter aims at establishing a framework for modeling elasto-damageable composites based on the Effective Internal Variable approach as initially introduced by Lahellec and Suquet and developed/extended in the literature for elasto(visco)plastic composites with or without hardening (see [18], [2], [84], [128] or [83]).

2.2 General framework of the incremental variational approach

2.2.1 The incremental potential

We focus now on the development of the incremental variational approach for the study of nonlinear composites. To this end, we make use of the incremental variational principle, already briefly presented and described within the GSM framework, and as used by Lahellec and Suquet [75]. Hereafter, we'll be presenting the general framework of the incremental variational approach for composite materials, the internal variable being denoted in a generic manner by α (scalars, second order tensors, etc.) for the sections 2.2 and 2.2.2.

Following what has been already introduced in section(1.3), the constitutive behavior of any GSM can be described by the following set of equations (see (1.15)):

$$\boldsymbol{\sigma} = \frac{\partial w}{\partial \boldsymbol{\varepsilon}}(\boldsymbol{\varepsilon}, \alpha), \qquad \frac{\partial w}{\partial \alpha}(\boldsymbol{\varepsilon}, \alpha) + \frac{\partial \varphi}{\partial \dot{\alpha}}(\dot{\alpha}) = 0 \tag{2.1}$$

The second equation in (2.1) is mostly known as the Biot equation [13] (see also in [104], [125]).

For the introduction of the incremental potential, the starting point is the incremental variational principle presented in section 1.2.2

The incremental formulation we rely on goes through a discretization of the time interval of the study $[0, T]$ in N time steps that are not necessarily of the same duration. The initial state of the material at time $t = 0$ is known and we aim to obtain its response to a loading history imposed on the interval $[0, T]$. To simplify the notations, the value $f(t_n)$ of the function f at

time t_n will be denoted f_n and the subscript $n+1$ will be omitted for variables calculated at time t_{n+1} (i.e. $\boldsymbol{\varepsilon} \equiv \boldsymbol{\varepsilon}_{n+1}$). Furthermore, we define the time increment Δt as $\Delta t = t_{n+1} - t_n$. The time discretization according to an implicit Euler scheme of equation (2.1) leads to the following equation

$$\boldsymbol{\sigma}_{n+1} = \frac{\partial w}{\partial \boldsymbol{\varepsilon}_{n+1}}(\boldsymbol{\varepsilon}_{n+1}, \alpha_{n+1}) \, ; \quad \frac{\partial w}{\partial \alpha_{n+1}}(\boldsymbol{\varepsilon}_{n+1}, \alpha_{n+1}) + \frac{\partial \varphi}{\partial \dot{\alpha}_{n+1}}\left(\frac{\alpha_{n+1} - \alpha_n}{\Delta t}\right) = 0 \tag{2.2}$$

Similar to Lahellec and Suquet we introduce the condensed incremental potential J such that the equation $(2.2)_2$ corresponds to the Euler-Lagrange equations providing the solution of the variational problem:

$$\begin{cases} w_\Delta(x, \boldsymbol{\varepsilon}) = \inf\limits_{\alpha} J(x, \boldsymbol{\varepsilon}, \alpha) \quad \text{where :} \\ J(x, \boldsymbol{\varepsilon}, \alpha) = w(\boldsymbol{\varepsilon}, \alpha) + \Delta t \varphi\left(\dfrac{\alpha - \alpha_n}{\Delta t}\right) \end{cases} \tag{2.3}$$

The stress defined by $(2.2)_1$ is then obtained by the derivation of the unique condensed potential w_Δ

$$\boldsymbol{\sigma} = \frac{\partial w_\Delta}{\partial \boldsymbol{\varepsilon}}(x, \boldsymbol{\varepsilon}) \tag{2.4}$$

2.2.2 Effective behavior of nonlinear composite materials

Local problem

We consider now a Representative Volume Element (RVE) Ω of a composite made of N phases occupying domains $\Omega^{(r)} (r = 1, \ldots, N)$ such that $\Omega = \cup_{r=1}^{N} \Omega^{(r)}$. The volume fraction of phase r is denoted $c(r)$ with $c(r) = |\Omega(r)|/|\Omega|$. The phase distribution is described by means of the characteristic functions $\chi^{(r)}$ such as

$$\chi^{(r)}(x) = \begin{cases} 1 \text{ if } x \in \Omega^{(r)} \\ 0 \text{ otherwise} \end{cases} \tag{2.5}$$

Each phase r, assumed to be of generalized standard type, is governed by equations (2.1) applied to the potentials $w^{(r)}$ and $\varphi^{(r)}$. The free energy w and the dissipation potential φ at each position $x \in \Omega$ are given by

$$w(\boldsymbol{\varepsilon}, \alpha) = \sum_{r=1}^{N} w^{(r)}(\boldsymbol{\varepsilon}, \alpha) \, \chi^{(r)}(x) \quad ; \quad \varphi(\dot{\alpha}, \alpha) = \sum_{r=1}^{N} \varphi^{(r)}(\dot{\alpha}, \alpha) \, \chi^{(r)}(x) \tag{2.6}$$

The RVE is subjected to a history of loading in macroscopic deformation $E(t)$ and the local problem which determines the local fields $\boldsymbol{\sigma}(x,t)$, $\boldsymbol{\varepsilon}(x,t)$ and α within the RVE is written:

$$\begin{cases} \boldsymbol{\sigma} = \dfrac{\partial w}{\partial \boldsymbol{\varepsilon}}(\boldsymbol{\varepsilon},\alpha); \quad \dfrac{\partial w}{\partial \alpha}(\boldsymbol{\varepsilon},\alpha) + \dfrac{\partial \varphi}{\partial \dot{\alpha}}(\dot{\alpha}) = 0 \ \forall (x,t) \in \Omega \times [0,T] \\ \operatorname{div}(\boldsymbol{\sigma}) = 0 \ \forall (x,t) \in \Omega \times [0,T] \\ \langle \boldsymbol{\varepsilon}(t) \rangle = \boldsymbol{E}(t) + \text{Boundary conditions on } \partial\Omega \end{cases} \tag{2.7}$$

The fields $\boldsymbol{\sigma}$, $\boldsymbol{\varepsilon}$ and α depend on x and t. The brackets $\langle . \rangle$ represent the spatial average on Ω. Assuming macro homogeneous boundary conditions, there is no need to specify the details of these. The effective or macroscopic response of the composite along the deformation loading macroscopic history $E(t)$ is given by the macroscopic stress $\boldsymbol{\Sigma}(t)$, where $\boldsymbol{\Sigma}(t) = \langle \boldsymbol{\sigma}(x,t) \rangle$.

Effective incremental potential

Thanks to the variational principle (2.3), the discretized local problem allowing to determine the local stress and strain fields in the RVE is written

$$\begin{cases} \operatorname{div}(\boldsymbol{\sigma}_{n+1}) = 0 \quad \forall (x) \in \Omega \\ \boldsymbol{\sigma}_{n+1} = \dfrac{\partial w_\Delta}{\partial \boldsymbol{\varepsilon}}(\boldsymbol{\varepsilon}_{n+1}) \quad \forall (x) \in \Omega \\ \langle \boldsymbol{\varepsilon}_{n+1} \rangle = \boldsymbol{E}_{n+1} + \text{Boundary conditions on } \partial\Omega \end{cases} \tag{2.8}$$

where

$$\begin{cases} w_\Delta(x,\boldsymbol{\varepsilon}) = \inf\limits_{\alpha} J(x,\boldsymbol{\varepsilon},\alpha) \quad \text{with:} \\ J(x,\boldsymbol{\varepsilon},\alpha) = \sum\limits_{r=1}^{N} J^{(r)}(x,\boldsymbol{\varepsilon},\alpha)\chi^{(r)}(x) \quad \text{and:} \\ J^{(r)}(x,\boldsymbol{\varepsilon},\alpha) = w^{(r)}(\boldsymbol{\varepsilon},\alpha) + \Delta t \varphi^{(r)}\left(\dfrac{\alpha - \alpha_n}{\Delta t}\right) \end{cases} \tag{2.9}$$

A variational characterization of the local problem can be obtained by noting that the strain field $\boldsymbol{\varepsilon}$ is the solution of the following potential energy minimization problem for the composite

$$\inf_{\boldsymbol{\varepsilon}/\langle \boldsymbol{\varepsilon} \rangle = E} \langle w_\Delta(\boldsymbol{\varepsilon}) \rangle = \inf_{\boldsymbol{\varepsilon}/\langle \boldsymbol{\varepsilon} \rangle = E} \langle \inf_{\alpha} J(\boldsymbol{\varepsilon},\alpha) \rangle \tag{2.10}$$

Finally, the effective condensed incremental potential $\tilde{w}_\Delta(E)$ takes the form:

$$\tilde{w}_\Delta(\boldsymbol{E}) = \inf_{\boldsymbol{\varepsilon}/\langle \boldsymbol{\varepsilon} \rangle = E} \langle w_\Delta(\boldsymbol{\varepsilon}) \rangle \tag{2.11}$$

Lahellec and Suquet have shown, using the relation $\boldsymbol{\sigma} = \dfrac{\partial w_\Delta}{\partial \boldsymbol{\varepsilon}}$ and Hill's lemma, that the macroscopic stress $\boldsymbol{\Sigma} = \langle \boldsymbol{\sigma} \rangle$ is given by:

$$\boldsymbol{\Sigma} = \frac{\partial \tilde{w}_\Delta}{\partial \boldsymbol{E}}(\boldsymbol{E}) \tag{2.12}$$

Field statistics

In addition to the determination of the macroscopic stress tensor $\boldsymbol{\Sigma}(t)$, it is of great interest to characterize as well the local field statistics at any time t of the loading history. These field statistics, which will be very useful for the assessment of the proposed models by comparison to full-field simulations (EF) results, are the first and second-order moments as well as the averages of the field fluctuations over each (r) phase.

Let us consider then a second order tensor a with a non-zero trace. As classically, notation $a_m = \dfrac{1}{3} tr(a)$ corresponds to the spherical part of a and $a_d = a - a_m \mathbb{1}$ its deviatoric part, with $\mathbb{1}$, the second order identity tensor.
The first order moment of this tensor on phase r represents the spatial average on that phase and is denoted $\langle a \rangle^{(r)} = a(r)$.
In homogenization methods, in order to characterize field statistics, the second-order moments are often used (see for example Ortiz and Molinari [108], Kreher [67], Kreher and Molinari [68]), which for the a_d tensor on the r phase is defined as

$$\overline{\overline{a_d}}^{(r)} = \sqrt{\varrho \langle a_d : a_d \rangle^{(r)}} \tag{2.13}$$

where $\varrho = \dfrac{2}{3}$ if a is a deformation variable and $\varrho = \dfrac{3}{2}$ if a is a force variable. Similarly, the second moment of a_m on phase r is written

$$\overline{\overline{a_m}}^{(r)} = \sqrt{\langle (a_m)^2 \rangle^{(r)}} \tag{2.14}$$

The last fields statistics quantity that we will analyze is the phase average of the field fluctuations which will be denoted $\mathcal{C}^{(r)}(a)$ and defined as

$$\mathcal{C}^{(r)}(a) = \left\langle \left(a - \overline{a}^{(r)}\right) \otimes \left(a - \overline{a}^{(r)}\right) \right\rangle^{(r)} = \langle a \otimes a \rangle^{(r)} - \overline{a}^{(r)} \otimes \overline{a}^{(r)} \tag{2.15}$$

These fluctuations will be quantified through the following expression :

$$\begin{cases} \sqrt{\mathcal{C}^{(2)}(\boldsymbol{\sigma}) :: \mathbb{K}} \;=\; \sqrt{\dfrac{2}{3}\left[\left(\overline{\overline{\boldsymbol{\sigma}}_d}^{(2)}\right)^2 \;-\; \left(\overline{\boldsymbol{\sigma}_d}^{(2)}\right)^2_{eq}\right]} \\ \text{where}: \;\left(\overline{\boldsymbol{\sigma}_d}^{(2)}\right)_{eq} \;=\; \sqrt{\dfrac{3}{2}\,\overline{\boldsymbol{\sigma}_d}^{(2)} : \overline{\boldsymbol{\sigma}_d}^{(2)}} \end{cases} \tag{2.16}$$

2.3 Formulation of an incremental variational model for elasto-damageable composites

2.3.1 The local damage model in the context of composites

Let us consider now a Representative Volume Element (RVE) Ω of a composite material consisting of N-phases with $\Omega^{(r)}$ the volume of each phase : $r(r = 1, \ldots, N)$, the phases being assumed to have elasto-damageable behavior as modeled in the Generalized Standard Materials (GSM) framework (see section 1.2.1). Thus, the mechanical behavior model of these phases can be formulated by considering the state variables deformation $\boldsymbol{\varepsilon}$ and an internal variable d (chosen as a positive scalar, so as to consider only isotropic damage processes) and by choosing two convex potentials that we will specify later.
The following characteristic function is used to specify the phase distribution :

$$\chi^{(r)}(x) \;=\; \begin{cases} 1 \text{ if } x \in \Omega^{(r)} \\ 0 \text{ otherwise} \end{cases} \tag{2.17}$$

Reversible effects are associated with a free-energy density that depends only on the state variables of the material, the strain $\boldsymbol{\varepsilon}$ and the damage d :

$$\begin{cases} w\left(\boldsymbol{\varepsilon}, d\right) \;=\; \displaystyle\sum_{r=1}^{N} w^{(r)}\left(\boldsymbol{\varepsilon}, d\right)\, \chi^{(r)}(x) \quad \text{with}: \\ w^{(r)}\left(\boldsymbol{\varepsilon}, d\right) \;=\; \dfrac{1}{2}\boldsymbol{\varepsilon} : \mathbb{C}^{(r)}(d) : \boldsymbol{\varepsilon} \end{cases} \tag{2.18}$$

where $\mathbb{C}^{(r)}(d)$ represents the elasticity tensor of the damaged material. In the case of isotropic elastic behavior of the phases, the elasticity tensor takes the form

$$\mathbb{C}^{(r)}(d) \;=\; 3\,k^{(r)}(d)\,\mathbb{J} \;+\; 2\,\mu^{(r)}(d)\,\mathbb{K} \tag{2.19}$$

where, as already seen in chapter 1, we recall that $\mathbb{K} = \mathbb{I} - \mathbb{J}$ represents the deviatoric projector of isotropic fourth-order tensors having the symmetries of an elasticity tensor, while $\mathbb{I}$ is the symmetric fourth-order identity tensor and $\mathbb{J}$ the spherical projector whose expressions are respectively $\mathbb{I}_{ijkl} = \dfrac{1}{2}\left(\delta_{ik}\delta_{jl} \;+\; \delta_{il}\delta_{jk}\right)$ and $\mathbb{J} = \dfrac{1}{3}\delta_{ij}\delta_{kl}$.
For simplicity, we consider for the damage model the following degradation function widely

used in recent literature[1] concerning damage mechanics :

$$\mathbb{C}^{(r)}(d) \;=\; g(d)\,\mathbb{C}_s^{(r)} \;=\; (1-d)^2\;\mathbb{C}_s^{(r)} \tag{2.20}$$

where $\mathbb{C}_s^{(r)}$ represents the stiffness tensor of the undamaged material.
For the developments that will be presented below, the dissipation potential $\varphi^{(r)}(\dot{d},d)$ of a phase r is taken in the form :

$$\begin{cases} \varphi(\dot{d},d) \;=\; \displaystyle\sum_{r=1}^{N} \varphi^{(r)}(\dot{d},d)\,\chi^{(r)}(x) \quad \text{with :} \\ \varphi^{(r)}(\dot{d},d) \;=\; \mathcal{Y}_c\,\dot{d} \;+\; \Psi_c(\dot{d}) \end{cases} \tag{2.21}$$

with $\Psi_c(\dot{d}) : \{\dot{d} \geq 0\}$ the irreversibility condition and the constant $\mathcal{Y}_c$ is a characteristic of the elastic damageable material.

2.3.2 Incremental variational principle

Methodology

In order to determine the effective condensed incremental potential $\tilde{w}_\Delta$, we apply the incremental variational procedure proposed by Lahellec and Suquet and based on the approach introduced by Ponte Castañeda for nonlinear composites.
We recall the variational problem :

$$\begin{cases} w_\Delta(x,\boldsymbol{\varepsilon}) \;=\; \inf\limits_{d} J(x,\boldsymbol{\varepsilon},d) \quad \text{with:} \\ J(x,\boldsymbol{\varepsilon},d) \;=\; \displaystyle\sum_{r=1}^{N} J^{(r)}(x,\boldsymbol{\varepsilon},d)\chi^{(r)}(x) \quad \text{and:} \\ J^{(r)}(x,\boldsymbol{\varepsilon},d) = w^{(r)}(\boldsymbol{\varepsilon},d) \;+\; \Delta t\varphi^{(r)}\left(\dfrac{d-d_n}{\Delta t}\right) \end{cases} \tag{2.22}$$

Following [75, 74], the linearization of the local behavior and the accounting for the heterogeneity of the incremental potential within the phases are addressed simultaneously[2].
In our case, due to the coupling of elasticity and damage, the incremental potential J is approximated by a linearized incremental potential J_0 chosen in the form :

$$\begin{cases} J_0(x,\boldsymbol{\varepsilon},d) \;=\; \displaystyle\sum_{r=1}^{N} J_0^{(r)}(\boldsymbol{\varepsilon},d)\chi^{(r)}(x) \\ J_0^{(r)} \;=\; \dfrac{1}{2}\,(1-d)^2\,\mathcal{A}_0^{(r)} \;+\; \dfrac{1}{2}\boldsymbol{\varepsilon} : \mathbb{C}_0^{(r)} : \boldsymbol{\varepsilon} \;+\; \mathcal{Y}_c\,(d-d_n) \;+\; \Delta t\,\Psi_c\left(\dfrac{d\;-\;d_n}{\Delta t}\right) \end{cases} \tag{2.23}$$

[1] We will see later that this choice of degradation function corresponds to the model classically considered in the literature for simulation of damage and fracture phenomena by means of the so-called Phase field approach.

[2] addressing these two steps separately, as in [2, 83, 84], could be a perspective, an overall discussion over it is available in Appendix[B.2]

where $\mathcal{A}_0^{(r)}$ is a uniform per phase scalar and $\mathbb{C}_0^{(r)}$ is a fourth-order tensor having the symmetries of an elasticity tensor, also uniform per phase.
The approximation of the condensed incremental potential is done by adding and subtracting to the potential J the linearized incremental potential J_0 *i.e.* $J = J_0 + J - J_0$, so that, on the one hand, the first term J_0 can be homogenized using classical homogenization schemes, and on the other hand, the difference $J - J_0$ can be estimated semi-analytically. The difference $\Delta J = J - J_0$ of the potentials is then written

$$\begin{cases} \Delta J(x,\boldsymbol{\varepsilon},d) \;=\; \displaystyle\sum_{r=1}^{N} \Delta J^{(r)}(\boldsymbol{\varepsilon},d)\chi^{(r)}(x) \\ \Delta J^{(r)} \;=\; \dfrac{1}{2}(1-d)^2\left[\boldsymbol{\varepsilon} : \mathbb{C}_s^{(r)} : \boldsymbol{\varepsilon} \;-\; \mathcal{A}_0^{(r)}\right] \;-\; \dfrac{1}{2}\boldsymbol{\varepsilon} : \mathbb{C}_0^{(r)} : \boldsymbol{\varepsilon} \end{cases} \tag{2.24}$$

By replacing J with its expression in the variational problem, the effective condensed incremental potential is expressed as (see (2.11))

$$\tilde{w}_\Delta(\boldsymbol{E}) \;=\; \inf_{\boldsymbol{\varepsilon}/\langle\boldsymbol{\varepsilon}\rangle=E}\left[\inf_{d/\Psi_c(\dot{d})} \langle J_0(\boldsymbol{\varepsilon},d) \;+\; \Delta J(\boldsymbol{\varepsilon},d)\rangle\right] \tag{2.25}$$

the expressions of $J_0(\boldsymbol{\varepsilon},d)$ and $\Delta J(\boldsymbol{\varepsilon},d)$ to be considered being given in (2.23) and (2.24) respectively.
As in Lahellec and Suquet, a rigorous upper bound on $\tilde{w}_\Delta$ can be obtained by taking a supremum condition of ΔJ with respect to $(\boldsymbol{\varepsilon},d)$:

$$\tilde{w}_\Delta(\boldsymbol{E}) \leq \inf_{\boldsymbol{\varepsilon}/\langle\boldsymbol{\varepsilon}\rangle=E}\left[\inf_{d/\Psi_c(\dot{d})} \langle J_0(\boldsymbol{\varepsilon},d)\rangle \;+\; \sup_{\boldsymbol{\varepsilon}^*,d^*}\langle \Delta J(\boldsymbol{\varepsilon},d)\rangle\right] \tag{2.26}$$

Moreover, they have shown that this upper bound may be too stiff in some cases. As in Ponte Castañeda and Willis in 1999 [120] and Ponte Castañeda in 2002 [117], this upper bound can be relaxed by replacing the supremum condition with a stationarity condition. Finally, the optimization with respect to the parameters introduced in J_0 provides the final estimate of $\tilde{w}_\Delta$:

$$\tilde{w}_\Delta(\boldsymbol{E}) \;\approx\; \underset{\mathcal{A}_0^{(r)},\mathbb{C}_0^{(r)}}{\operatorname{stat}}\left[\inf_{\boldsymbol{\varepsilon}/\langle\boldsymbol{\varepsilon}\rangle=E}\left(\inf_{d/\Psi_c(\dot{d})} \langle J_0(\boldsymbol{\varepsilon},d)\rangle \;+\; \underset{\boldsymbol{\varepsilon}^*,d^*}{\operatorname{stat}}\langle \Delta J(\boldsymbol{\varepsilon},d)\rangle\right)\right] \tag{2.27}$$

Note : In this procedure, the internal variable d will be approximated by resolving the infimum problem $\inf_{d/\Psi_c(\dot{d})} \langle J_0(\boldsymbol{\varepsilon},d)\rangle$. And the reference variables that were introduced in the linearization procedure will be approximated by solving the stationarity problem $\underset{\boldsymbol{\varepsilon}^*,d^*}{\operatorname{stat}}\langle \Delta J(\boldsymbol{\varepsilon},d)\rangle$. The added $(.)^*$ aims at distinguishing the solution minimizing the first infimum problem from the one that is the solution to the stationarity problem.

Stationarity conditions

We now propose to develop all the stationarity conditions appearing in (2.27). We will first write the stationarity of ΔJ with respect to d^* and $\boldsymbol{\varepsilon}^*$ which will provide an expression for

$\mathcal{A}_0^{(r)}$ and $\mathbb{C}_0^{(r)}$. The stationarity with respect to these two quantities will then allow completing their expressions. Finally, the stationarity of J_0 with respect to d will provide an expression of the damage as a function of $\boldsymbol{\varepsilon}$.

1. Stationarity of ΔJ

The stationarity of ΔJ (2.24) with respect to $\boldsymbol{\varepsilon}^*$ can be written as :

$$\frac{\partial}{\partial \boldsymbol{\varepsilon}^*}\left\{\frac{1}{2}\left(1-d^*\right)^2\left[\boldsymbol{\varepsilon}^* : \mathbb{C}_s^{(r)} : \boldsymbol{\varepsilon}^* - \mathcal{A}_0^{(r)}\right] - \frac{1}{2}\boldsymbol{\varepsilon}^* : \mathbb{C}_0^{(r)} : \boldsymbol{\varepsilon}^*\right\} = 0 \tag{2.28}$$

which implies

$$\Longrightarrow \quad \mathbb{C}_0^{(r)} = \left(1-d^*\right)^2 \mathbb{C}_s^{(r)} \tag{2.29}$$

Similarly, the stationarity condition of ΔJ over d^* reads :

$$\frac{\partial}{\partial d^*}\left\{\frac{1}{2}\left(1-d^*\right)^2\left[\boldsymbol{\varepsilon}^* : \mathbb{C}_s^{(r)} : \boldsymbol{\varepsilon}^* - \mathcal{A}_0^{(r)}\right] - \frac{1}{2}\boldsymbol{\varepsilon}^* : \mathbb{C}_0^{(r)} : \boldsymbol{\varepsilon}^*\right\} = 0 \tag{2.30}$$

This leads to an expression for the first parameter introduced in J_0 :

$$\Longrightarrow \quad \mathcal{A}_0^{(r)} = \boldsymbol{\varepsilon}^* : \mathbb{C}_s^{(r)} : \boldsymbol{\varepsilon}^* \tag{2.31}$$

The two relations (2.29) and (2.31) show that the two unknowns $\mathcal{A}_0^{(r)}$ and $\mathbb{C}_0^{(r)}$ depend on the variables $\boldsymbol{\varepsilon}^*$ and d^* which remain to be determined.

2. Minimization of $J_0^{(r)}$

We obtain a Linear Comparison Composite (LCC) by minimizing $J_0^{(r)}$ with respect to d. And due to the stationarity of ΔJ with respect to the strain tensor, we can then write:

$$\tilde{w}_\Delta(\boldsymbol{E}) \approx \underset{\mathcal{A}_0^{(r)},\mathbb{C}_0^{(r)}}{\operatorname{stat}}\left[\inf_{\boldsymbol{\varepsilon}/\langle\boldsymbol{\varepsilon}\rangle=E}\langle w_0(\boldsymbol{\varepsilon})\rangle + \underset{\boldsymbol{\varepsilon}^*,d^*}{\operatorname{stat}}\langle\Delta J(\boldsymbol{\varepsilon},d)\rangle\right] \tag{2.32}$$

where $w_0(\boldsymbol{\varepsilon})$ is the energy associated with the resulting LCC such that :

$$w_0(\boldsymbol{\varepsilon}) = \inf_{d/\Psi_c(\dot{d})} J_0(\boldsymbol{\varepsilon},d) \tag{2.33}$$

The infimum of $J_0(\boldsymbol{\varepsilon},d)$ with respect to d is given with account of the irreversibility constraint on damage, which is written using the Karush-Kuhn-Tucker (KKT) optimality conditions:

$$\begin{cases} \dfrac{\partial}{\partial d}\left(J_0(\boldsymbol{\varepsilon},d) + \lambda\,\Psi(\dot{d})\right) = 0 \\ \lambda\,\dot{d} = 0 \\ \lambda \le 0\,, \quad \dot{d} \ge 0 \end{cases} \tag{2.34}$$

which can be rewritten over each phase as :

$$\begin{cases} \dfrac{\partial}{\partial d}\left\{\dfrac{1}{2}(1-d)^2\,\mathcal{A}_0^{(r)} + \dfrac{1}{2}\boldsymbol{\varepsilon} : \mathbb{C}_0^{(r)} : \boldsymbol{\varepsilon} + \mathcal{Y}_c\,(d-d_n)\right\} + \lambda = 0 \\ \lambda\left(\dfrac{d-d_n}{\Delta t}\right) = 0 \\ \lambda \leq 0 \quad ; \dfrac{d-d_n}{\Delta t} \geq 0 \end{cases} \tag{2.35}$$

Case 1. $\lambda < 0$. According to $(2.35)_2$, this assumption leads to $d = d_n$ which is the same as the elastic case without the presence or evolution of damage. This case will therefore not be retained.

Case 2. $\lambda = 0$. The latter corresponds to $d - d_n > 0$, which correlates to the case of evolving damage. It is therefore this case that we retain. From $(2.35)_1$, this assumption leads to:

$$\frac{\partial}{\partial d}\left\{\frac{1}{2}(1-d)^2\,\mathcal{A}_0^{(r)} + \frac{1}{2}\boldsymbol{\varepsilon} : \mathbb{C}_0^{(r)} : \boldsymbol{\varepsilon} + \mathcal{Y}_c\,(d-d_n)\right\} = 0 \tag{2.36}$$

The resulting expression of the damage variable is as follows :

$$d_{opt}^{(r)} = 1 - \frac{\mathcal{Y}_c}{\mathcal{A}_0^{(r)}} \tag{2.37}$$

which turns out to be uniform per phase. Though this uniformity of the optimal damage field $d_{opt}^{(r)}$ in the phase r, it will be shown below that $d_{opt}^{(r)}$ may depend on the strain heterogeneity in phase r via its link with $\mathcal{A}_0^{(r)}$.

The energy associated with the LCC (see its definition by (2.33), with J_0 given by (2.23)) is then written as :

$$w_0^{(r)}(\boldsymbol{\varepsilon}) = \frac{1}{2}\left(1-d_{opt}^{(r)}\right)^2 \mathcal{A}_0^{(r)} + \frac{1}{2}\boldsymbol{\varepsilon} : \mathbb{C}_0^{(r)} : \boldsymbol{\varepsilon} + \mathcal{Y}_c\left(d_{opt}^{(r)} - d_n\right) \tag{2.38}$$

The resulting $w_0^{(r)}$ is the LCC's linear thermoelastic potential with piecewise uniform parameters and, unlike the EIV formulation in [75], this potential does not involve a polarization $\tau_0^{(r)}$.

The effective potential, given by (2.32), can be written by applying the minimization condition with respect to $\boldsymbol{\varepsilon}$ as :

$$\tilde{w}_\Delta(\boldsymbol{E}) \approx \underset{\mathcal{A}_0^{(r)},\mathbb{C}_0^{(r)}}{\text{stat}}\left[\tilde{w}_0(E) + \underset{\boldsymbol{\varepsilon}^*,d^*}{\text{stat}}\langle \Delta J(\boldsymbol{\varepsilon},d)\rangle\right] \tag{2.39}$$

where

$$\tilde{w}_0(E) = \inf_{\boldsymbol{\varepsilon}/\langle\boldsymbol{\varepsilon}\rangle = E}\langle w_0(\boldsymbol{\varepsilon})\rangle \tag{2.40}$$

and represents the effective energy of the LCC.

We are ready now to write the last optimality conditions, which will allow to determine the expressions of the remaining quantities $\mathcal{A}_0^{(r)}$ and $\mathbb{C}_0^{(r)}$.

3. Stationarity of $\left\langle J_0^{(r)} + \Delta J^{(r)} \right\rangle^{(r)}$

Optimality with respect to $\mathcal{A}_0^{(r)}$ and $\mathbb{C}_0^{(r)}$ allows to obtain the missing link between $(\boldsymbol{\varepsilon}^*, d^*)$ and the variables $(\boldsymbol{\varepsilon}, d)$:

$$\underset{\mathcal{A}_0^{(r)}}{\text{stat}} \left\langle J_0^{(r)} + \Delta J^{(r)} \right\rangle^{(r)} \Longrightarrow \left\langle (1-d)^2 \right\rangle^{(r)} = \left\langle (1-d^*)^2 \right\rangle^{(r)} \tag{2.41}$$

$$\underset{\mathbb{C}_0^{(r)}}{\text{stat}} \left\langle J_0^{(r)} + \Delta J^{(r)} \right\rangle^{(r)} \Longrightarrow \begin{cases} \langle \boldsymbol{\varepsilon} : \mathbb{K} : \boldsymbol{\varepsilon} \rangle^{(r)} = \langle \boldsymbol{\varepsilon}^* : \mathbb{K} : \boldsymbol{\varepsilon}^* \rangle^{(r)} \\ \\ \langle \boldsymbol{\varepsilon} : \mathbb{J} : \boldsymbol{\varepsilon} \rangle^{(r)} = \langle \boldsymbol{\varepsilon}^* : \mathbb{J} : \boldsymbol{\varepsilon}^* \rangle^{(r)} \end{cases} \tag{2.42}$$

for which it is recalled that $\mathbb{K}$ represents the isotropic deviatoric projector and $\mathbb{J}$ the isotropic spherical projector.
By denoting $\langle a \rangle^{(r)}$ the average of the quantity a considered on the phase (r), from (2.31) and (2.42), it is readily seen that $\mathcal{A}_0^{(r)}$ can then be determined using the second-order moment estimate of the strain field :

$$\mathcal{A}_0^{(r)} = \left\langle \boldsymbol{\varepsilon} : \mathbb{C}_s^{(r)} : \boldsymbol{\varepsilon} \right\rangle^{(r)} \tag{2.43}$$

which is the average over the r phase of the elastic energy of the undamaged material.
Using the result (2.43), one can rewrite (2.37) in the following form

$$\left(1 - d_{opt}^{(r)}\right) \left\langle \boldsymbol{\varepsilon} : \mathbb{C}_s^{(r)} : \boldsymbol{\varepsilon} \right\rangle^{(r)} - \mathcal{Y}_c = 0 \tag{2.44}$$

The relation (2.37) can thus be interpreted as follows: the damage $d_{opt}^{(r)}$, homogeneous and associated with the phase r, results from the saturation on average over phase r of the damage criterion.

The optimal damage value reads then :

$$d_{opt}^{(r)} = 1 - \frac{\mathcal{Y}_c}{\left\langle \boldsymbol{\varepsilon} : \mathbb{C}_s^{(r)} : \boldsymbol{\varepsilon} \right\rangle^{(r)}} \tag{2.45}$$

Finally, using the results (2.41) and (2.43), and carrying (2.37) into (2.29), one gets the expression of $\mathbb{C}_0^{(r)}$

$$\mathbb{C}_0^{(r)} = \left(1 - d_{opt}^{(r)}\right)^2 \mathbb{C}_s^{(r)} = \left(\frac{\mathcal{Y}_c}{\left\langle \boldsymbol{\varepsilon} : \mathbb{C}_s^{(r)} : \boldsymbol{\varepsilon} \right\rangle^{(r)}} \right)^2 \mathbb{C}_s^{(r)} \tag{2.46}$$

which represents the elasticity tensor of the Linear Comparison Composite (LCC) described by $w_0(\boldsymbol{\varepsilon})$ (2.38).

Effective response of the elasto-damageable composite

Once all the parameters are known, the effective behavior of the composite can be specified. In order to do so, we proceed to the minimization of $\tilde{w}_\Delta$ defined by (2.27), with respect to $\boldsymbol{\varepsilon}$. This functional is stationary with respect to $\mathcal{A}_0^{(r)}$, $\mathbb{C}_0^{(r)}$ and d and the term ΔJ of this functional is stationary with respect to $\boldsymbol{\varepsilon}^*$ and d^*. Given this, we can define the local problem that corresponds to the Euler-Lagrange equations providing the solution to the variational problem:

$$\begin{cases} \operatorname{div}\boldsymbol{\sigma}(x) \;=\; 0 & \forall x \in \Omega \\ \boldsymbol{\sigma}(x) = \mathbb{C}_0^{(r)} \;:\; \boldsymbol{\varepsilon}(x) & \forall x \in \Omega \\ \langle \boldsymbol{\varepsilon}(x) \rangle \;=\; \boldsymbol{E} \qquad + & \text{Boundary conditions on } \partial\Omega \end{cases} \tag{2.47}$$

The effective behavior of the nonlinear composite can then be estimated as :

$$\begin{aligned} \boldsymbol{\Sigma} \;&=\; \langle \boldsymbol{\sigma}(x) \rangle \;=\; \frac{\partial \tilde{w}_\Delta}{\partial \boldsymbol{E}}(\boldsymbol{E}) \approx \frac{\partial \tilde{w}_0}{\partial \boldsymbol{E}}(\boldsymbol{E}) \\ &= \sum_{r=1}^{N} c^{(r)}\, \mathbb{C}_0^{(r)} \;:\; \langle \boldsymbol{\varepsilon}(x) \rangle \;=\; \sum_{r=1}^{N} c^{(r)}\, \mathbb{C}_0^{(r)} \;:\; \left[\mathbb{A}^{(r)} : \boldsymbol{E} \right] \end{aligned} \tag{2.48}$$

where $\mathbb{A}^{(r)}$ is a fourth-order tensor that corresponds to the strain localization tensor in the phase (r). And $c^{(r)}$ is the volume fraction of the phase (r) such that: $c^{(r)} \;=\; \dfrac{|\Omega^{(r)}|}{|\Omega|}$.

Elasto-damageable matrix reinforced by elastic particles

The above-developed procedure is now particularized to the case of a two-phase particulate composite (N=2 being the number of phases), composed of an elasto-damageable matrix reinforced by randomly and isotropically distributed elastic spherical particles. The subscripts (1) and (2) represent the inclusion and the matrix, respectively. For this purpose, in order to estimate the effective behavior of the composite as well as the first and second-order moments of the different fields in each phase, we made use of the Hashin-Shtrikman bounds. Regarding the first-order moment of the strain $\boldsymbol{\varepsilon}$ upon the phases, it can be expressed as:

$$\bar{\boldsymbol{\varepsilon}}^{(1)} \;=\; \mathbb{A}^{(1)} \;:\; E\,, \quad \bar{\boldsymbol{\varepsilon}}^{(2)} \;=\; \frac{1}{c^{(2)}} \left(\boldsymbol{E} \;-\; c^{(1)} \bar{\boldsymbol{\varepsilon}}^{(1)} \right) \tag{2.49}$$

For a two-phase composite (N=2), the strain localization tensors associated with the Hashin-Shtrikman estimates are classically given by :

$$\mathbb{A}^{(1)} \;=\; \left(\mathbb{I} \;+\; c^{(2)} \mathbb{P}_0^{(2)} \;:\; \Delta\mathbb{C}_0 \right)^{-1}, \quad \mathbb{A}^{(2)} \;=\; \frac{1}{c^{(2)}} \left(\mathbb{I} - c^{(1)} \mathbb{A}^{(1)} \right) \tag{2.50}$$

where $\Delta\mathbb{C}_0 \;=\; \mathbb{C}_0^{(1)} - \mathbb{C}_0^{(2)}$, and $\mathbb{P}_0^{(2)}$ is Hill tensor associated with the matrix phase of the LCC in the case of isotropically distributed spherical particles. Under these conditions, the

tensor $\mathbb{P}_0^{(2)}$ is written as

$$\mathbb{P}_0^{(2)} = \frac{\alpha_0^{(2)}}{3\,k_0^{(2)}}\mathbb{J} + \frac{\beta_0^{(2)}}{2\,\mu_0^{(2)}}\mathbb{K}, \text{ with } \alpha_0^{(2)} = \frac{3\,k_0^{(2)}}{3k_0^{(2)} + 4\mu_0^{(2)}},\ \beta_0^{(2)} = \frac{6\left(k_0^{(2)} + +2\mu_0^{(2)}\right)}{5\left(3k_0^{(2)} + 4\mu_0^{(2)}\right)} \tag{2.51}$$

Given these expressions, in order to obtain the first-order moment of the strain tensor within each constitutive phase, we need to determine $\mathbb{C}_0^{(r)}$. The latter, as we saw in (2.46), can be obtained with the use of the second-order moment of the strain tensor, which is estimated with the following expression :

$$\langle \boldsymbol{\varepsilon} \otimes \boldsymbol{\varepsilon} \rangle^{(r)} = \frac{1}{c^{(r)}} \frac{\partial \tilde{w}_0}{\partial \mathbb{C}_0^{(r)}} \tag{2.52}$$

In this two-phase case, the elasticity of the inclusion is given by: $\mathbb{C}_0^{(1)} = \mathbb{C}_s^{(1)}$ as it remains undamaged. In the matrix phase, the expression of $\mathbb{C}_0^{(2)}$ which characterizes the MLC w_0 is obtained from (2.46).
The nonlinear problem is reduced to the solution of a system of equations defined by two coupled functions whose unknowns are $\mathcal{A}_0^{(r)}$ and $\mathbb{C}_0^{(2)}$:

$$\begin{cases} F_1\left(\mathcal{A}_0^{(2)}, \mathbb{C}_0^{(2)}\right) = \mathcal{A}_0^{(2)} - \left\langle \boldsymbol{\varepsilon} : \mathbb{C}_s^{(2)} : \boldsymbol{\varepsilon} \right\rangle^{(2)} = 0 \\ F_2\left(\mathcal{A}_0^{(2)}, \mathbb{C}_0^{(2)}\right) = \mathbb{C}_0^{(2)} - \left(\frac{\mathcal{Y}_c}{\left\langle \boldsymbol{\varepsilon} : \mathbb{C}_s^{(2)} : \boldsymbol{\varepsilon} \right\rangle^{(2)}} \right)^2 \mathbb{C}_s^{(2)} = 0 \end{cases} \tag{2.53}$$

The resolution of this system allows to determine the damage level and then the behavior locally and globally.

2.4 Numerical implementation

2.4.1 Algorithm's structure

We now consider the numerical implementation of the developed theoretical model. The aim here is to describe the algorithm allowing to determine, for a given loading history defined in terms of prescribed macroscopic strain E at all times t_n, the effective stress $\boldsymbol{\Sigma}$ and the first and second-order moments of the local fields in the phases. This problem will be solved iteratively by determining the solution at t_{n+1} from the known solution at the previous time step t_n. The algorithm's structure goes as follows :

- At the current time step $t = t_{n+1}$, the macroscopic strain $\boldsymbol{E}_n$, the field statistics at step t_n are known. An increment $\Delta\boldsymbol{E}$ is applied. At each step we aim at determining the macroscopic stress $\boldsymbol{\Sigma}_{n+1}$, the local field statistics (namely the first and second order moments) at time step t_{n+1}. The coupled nonlinear system (2.53) is therefore solved at t_{n+1}. The equation associated with F_2 of this system can be decomposed into spherical

and deviatoric parts

$$\begin{cases} F_1\left(\mathcal{A}_0^{(2)},\mathbb{C}_0^{(2)}\right) = \mathcal{A}_0^{(2)} - \left(3\,k_s^{(2)}\left(\overline{\overline{\boldsymbol{\varepsilon}}}_m^{(2)}\right)^2 + 3\,\mu_s^{(2)}\left(\overline{\overline{\boldsymbol{\varepsilon}}}_d^{(2)}\right)^2\right) = 0 \\ F_2^{sph}\left(\mathcal{A}_0^{(2)},\mathbb{C}_0^{(2)}\right) = k_0^{(2)} - \left(\dfrac{\mathcal{Y}_c}{\mathcal{A}_0^{(2)}}\right)^2 k_s^{(2)} = 0 \\ F_2^{dev}\left(\mathcal{A}_0^{(2)},\mathbb{C}_0^{(2)}\right) = \mu_0^{(2)} - \left(\dfrac{\mathcal{Y}_c}{\mathcal{A}_0^{(2)}}\right)^2 \mu_s^{(2)} = 0 \end{cases} \tag{2.54}$$

with $\overline{\overline{\boldsymbol{\varepsilon}}}_m^{(2)}$ the second moment of the spherical part of the deformation tensor, and $\overline{\overline{\boldsymbol{\varepsilon}}}_d^{(2)}$ that of its deviatoric part [3]. These quantities are obtained through (2.49) and (2.52), the resulting expressions depend on $k_0^{(2)}$ and $\mu_0^{(2)}$.
Solving the system (2.54) provides the elastic characteristics of the LCC $\mathcal{A}_0^{(2)}$, $k_0^{(2)}$ and $\mu_0^{(2)}$. For this purpose, we use the function LEAST_SQUARES on Python which allows the nonlinear resolution of the system using the Levenberg-Marquardt algorithm, making it possible to determine the energy $w_0^{(r)}$ (2.38) of the LCC with phase-homogeneous properties as well as the values of the matrix damage (2.37).

- The second step consists in calculating the homogenized parameters $\left(\tilde{\mu}_0,\tilde{k}_0\right)$ defining the energy $\tilde{w}_0$, by implementing a Hashin-Shtrikman type bound. Once all these parameters are determined, we can proceed to the calculation of the macroscopic stress $\boldsymbol{\Sigma}$ which is obtained using the equation (2.48).

- All the quantities are then updated at the end of the current time step, and used for the following time step $(.)_{n+1} \longrightarrow (.)_n$

2.4.2 Numerical accuracy

As previously mentioned, the proposed analytical model undergoes a time discretization over the time interval $[0,T]$, where the time increment Δt as $\Delta t = t_{n+1} - t_n$.
We now propose a first analysis of the influence of the time step discretization on the model predictions. To this end, we have performed simulations on a two-phase composite for different values of the time step Δt. This composite consists of an elasto-damageable matrix reinforced with linear elastic spherical particles.
The chosen material parameters are the same as those of Fantoni et al. ([36]), which is composed of an Aluminum matrix exhibiting damage and linear elastic inclusions corresponding to Silicon carbide :

$$\begin{aligned} \text{Inclusion} : c^{(1)} &= 25\%\,,\ E^{(1)} = 340\,\text{GPa}\,,\ \nu^{(1)} = 0.18 \\ \text{Matrix} : E^{(2)} &= 60\,\text{GPa}\,,\ \nu^{(2)} = 0.3\,,\ \mathcal{Y}_c = 2.9\text{MPa} \end{aligned} \tag{2.55}$$

[3] $\boldsymbol{\varepsilon}_m = 1/3,\text{tr}(\boldsymbol{\varepsilon})$ $\quad \boldsymbol{\varepsilon}_d = \boldsymbol{\varepsilon} - \boldsymbol{\varepsilon}_m\mathbf{I}$ $\quad \mathbf{I}$: identity tensor of order 2

The composite is subjected to an isochoric macroscopic deformation of the form

$$E(t) = E_{33}(t)\left(-\frac{1}{2}(e_1 \otimes e_1 + e_2 \otimes e_2) + e_3 \otimes e_3\right)$$

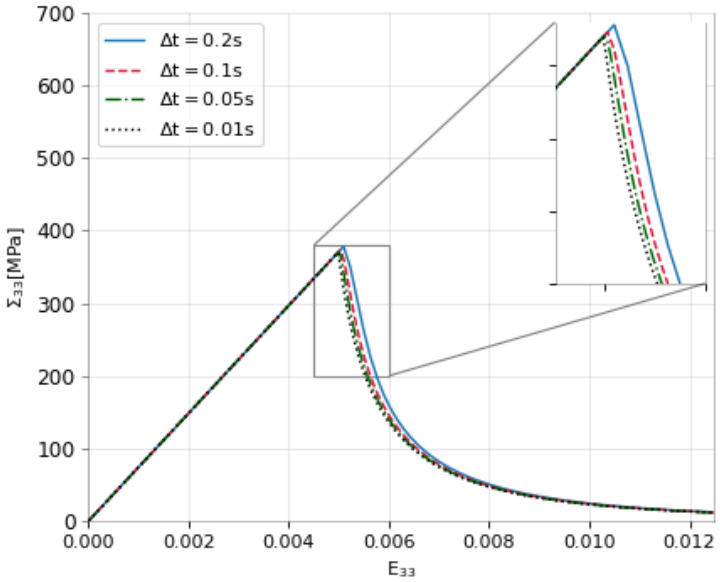

FIGURE 2.1: Influence of the time step discretization on the effective response of the model in terms of macroscopic behavior for an isochoric load (damageable matrix, elastic particle).

Fig.2.1 shows the evolution of the macroscopic axial stress versus the macroscopic axial strain for different time steps ($\Delta t = 0.2s, 0.1s, 0.05s, 0.01s$). On the same figure is provided a zoom on the transition zone between the linear elastic regime and the softening regime. It can be seen in these figures that the four curves in the elastic regime, each corresponding to a different Δt, are practically stacked, unlike the softening regime where a relatively more important difference is observed starting from the transition zone.
As the accuracy of the response does not improve significantly as the time step decreases for $\Delta t < 0.05s$ the latter is set to $\Delta t = 0.01s$ for all simulations throughout the remainder of this dissertation.

2.5 Model predictions

As discussed in the previous section, obtaining the macroscopic behavior as well as averages of local fields requires solving the nonlinear system (2.54). We consider here a composite material made of an elasto-damageable matrix reinforced by elastic spherical particles. The material parameters used are those introduced in (2.55).

Within this study, different loadings have been considered, but as a starting point, we'll first focus on an isochoric macroscopic strain

$$E(t) = E_{33}(t)\left(-\frac{1}{2}(e_1 \otimes e_1 + e_2 \otimes e_2) + e_3 \otimes e_3\right) \tag{2.56}$$

This model is characterized by a pure elastic regime until a threshold, after which the softening regime takes place. Fig.2.2a illustrates the macroscopic response of the composite under isochoric loading as well as the evolution of the average stress in the matrix and in the inclusion. Fig.2.2b shows the evolution of the constitutive behaviors of the composite, the matrix, and the inclusion.

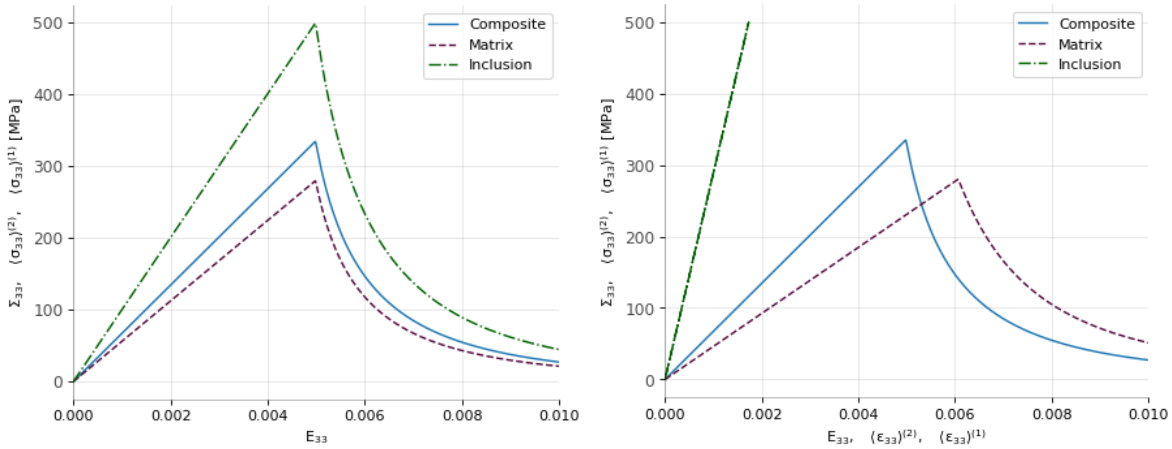

(a) (b)

FIGURE 2.2: (a) Macroscopic stress and average stress in each phase under an isochoric loading with respect to the effective load E_{33} for each phase and the composite., (b) Constitutive behaviors of the composite, matrix, and inclusion

The first figure clearly shows how the presence of the inclusion reinforces the matrix in its capacity to uphold higher levels of stress before softening takes place, which is due to the evolution of damage in the matrix. A remarkable point is the decrease of the average stress in the inclusion from the moment corresponding to the softening in the matrix, whereas the inclusion has a linear elastic behavior, as can be seen in Fig.2.2b illustrates the mechanical stress-strain relations in the matrix and inclusions together the composite behavior.

An examination of the evolution of the average strains in the inclusion indicates that it is indeed an unloading of the inclusion simultaneously with the softening behavior of the matrix. This is clearly illustrated in Fig.2.3 showing the evolution of the average strain in the inclusion together with the evolution of damage in the matrix with respect to the macroscopic strain.

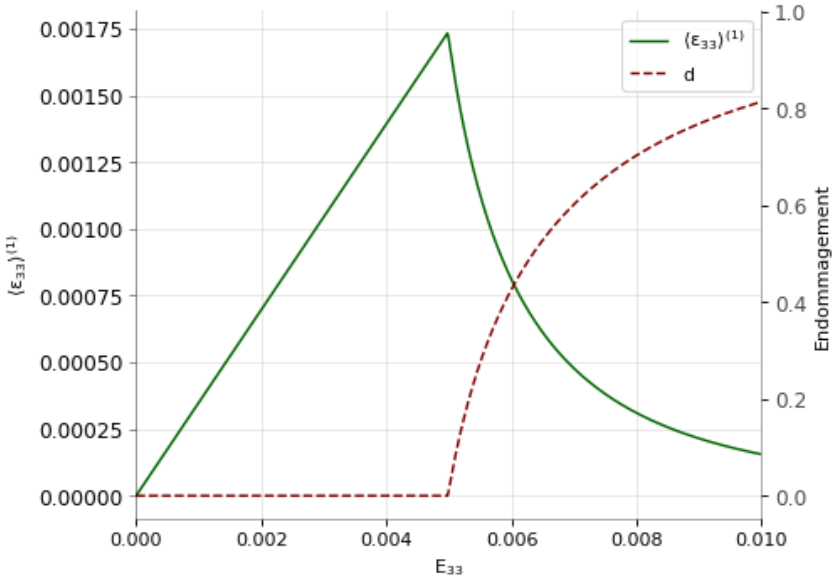

FIGURE 2.3: Evolution of the average local strain in the inclusion $< \boldsymbol{\varepsilon}_{33} >^{(1)}$ and damage in the matrix with respect to the macroscopic strain E_{33}

2.6 The case of a porous material

In this section, we propose a simple comparison of the homogenization model predictions to the closed-form solutions already presented in chapter 1 as a reference result. Let us recall that these solutions have been detailed in section 1.4. For comparison purposes, we consider here a two-phase composite as before, but with the spherical linear elastic inclusions replaced by spherical voids. The matrix is still elasto-damageable.

The considered isotropic loading consists of a uniform radial displacement $u_r = E \times b/3$ on the external boundary $r = b$, which corresponds to a macroscopic strain tensor $E = \dfrac{E}{3}\mathrm{Id}$. As a reminder, the bulk modulus is not affected by damage, and the shear damage function is taken in the form $\mu(d) = (1-d)^2\mu_s$. As in chapter 1, the constant ζ in (1.66) is equal to -0.1. For the same reason, a ratio of the bulk modulus and the shear modulus $\dfrac{k_s}{\mu_s} = 30$ (this corresponds to a Poisson ratio equal to 0.48 -in other words, for a sound matrix nearly elastic incompressible.
Owing to the fact the hollow sphere was set with a ratio $b/a_0 = 2$, we consider a porosity $c^1 = 1/8 = 0.125$.
The comparison is shown on Fig.2.4a in terms of macroscopic stress as function of the volumetric strain.
Discrepancies between both curves are observed past $E_{33} = 0.0075$. The overall agreement between the two approaches is found to be quite satisfactory in both regimes.

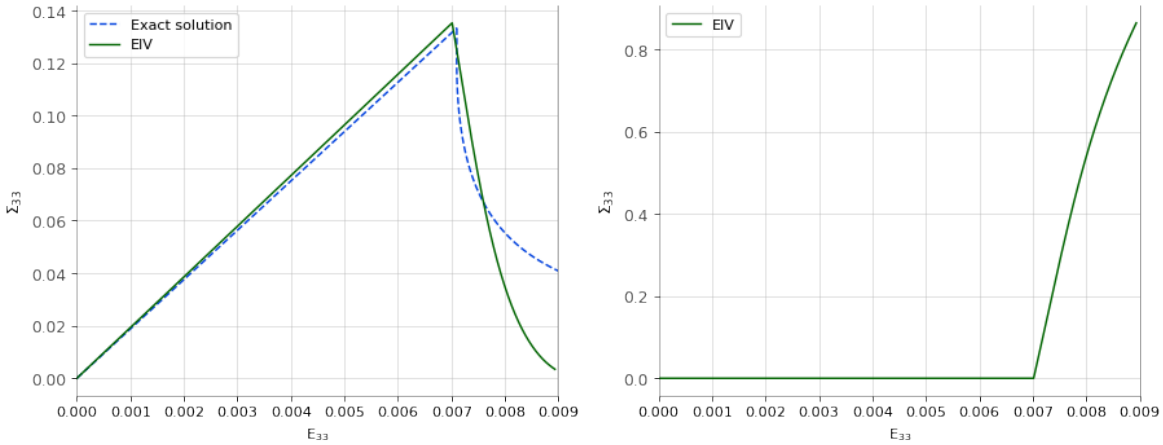

(a) (b)

FIGURE 2.4: (a) Radial behavior of a damaging hollow sphere submitted to a uniform radial displacement on its external envelope, (b) damage evolution obtained via the theoretical model

2.7 The Effective Internal Variable approach for a damage model based on the Mori-Tanaka scheme

2.7.1 Incremental variational procedure

In the previous section, we considered a particular degradation function (2.20), this choice of degradation function corresponds to a model classically considered in the literature for the numerical simulation of damage processes. However, it is completely within our reach to study the effective behavior of elasto-damageable composite using different degradation functions.
In this section, we'll be considering a non-softening damage law for which the expression of the degradation function $g(d)$ takes the following form :

$$\mathbb{C}^{(r)}(d) \;=\; g(d)\,\mathbb{C}_s^{(r)} \;=\; \frac{1}{1+Q'd}\,\mathbb{C}_s^{(r)} \tag{2.57}$$

The free energy and the dissipation potential will be considered as (2.18) and (2.21) respectively.

Linearization of the local behavior

We follow the same steps introduced in section (2.3.2). The incremental potential J $(2.9)_3$ is approximated by a linearized incremental potential J_0 :

$$\begin{cases} J_0(x,\boldsymbol{\varepsilon},d) \;=\; \displaystyle\sum_{r=1}^{N} J_0^{(r)}(\boldsymbol{\varepsilon},d)\chi^{(r)}(x) \\ J_0^{(r)} \;=\; \dfrac{1}{2(1+Q'\,d)}\,\mathcal{A}_0^{(r)} \;+\; \dfrac{1}{2}\boldsymbol{\varepsilon} : \mathbb{C}_0^{(r)} : \boldsymbol{\varepsilon} \;+\; \mathcal{Y}_c\,(d-d_n) \;+\; \Delta t\,\Psi_c\left(\dfrac{d-d_n}{\Delta t}\right) \end{cases} \tag{2.58}$$

where $\mathcal{A}_0^{(r)}$ is a uniform per phase scalar and $\mathbb{C}_0^{(r)}$ is a uniform per phase fourth-order tensor. This approximation consists of rewriting J as $J = J_0 + \Delta J$ where ΔJ corresponds to the difference between the two potentials such as :

$$\begin{cases} \Delta J(x,\boldsymbol{\varepsilon},d) \;=\; \displaystyle\sum_{r=1}^{N} \Delta J^{(r)}(\boldsymbol{\varepsilon},d)\chi^{(r)}(x) \\ \Delta J^{(r)} \;=\; \dfrac{1}{2(1+Q'\,d)}\left[\boldsymbol{\varepsilon} : \mathbb{C}_s^{(r)} : \boldsymbol{\varepsilon} \;-\; \mathcal{A}_0^{(r)}\right] \;-\; \dfrac{1}{2}\boldsymbol{\varepsilon} : \mathbb{C}_0^{(r)} : \boldsymbol{\varepsilon} \end{cases} \tag{2.59}$$

By replacing J by its expression in the variational problem $(2.9)_1$, then considering a rigorous upper bound on $\tilde{w}_\Delta$, and finally replacing the supremum condition by a stationarity condition, we obtain an estimate of $\tilde{w}_\Delta$ of the form :

$$\tilde{w}_\Delta(\boldsymbol{E}) \;\approx\; \underset{\mathcal{A}_0^{(r)},\mathbb{C}_0^{(r)}}{\text{stat}} \left[\inf_{\boldsymbol{\varepsilon}/\langle\boldsymbol{\varepsilon}\rangle=E} \left(\inf_{d/\Psi_c(\dot{d})} \langle J_0(\boldsymbol{\varepsilon},d)\rangle \;+\; \underset{\boldsymbol{\varepsilon}^*,d^*}{\text{stat}} \langle \Delta J(\boldsymbol{\varepsilon},d)\rangle \right) \right] \tag{2.60}$$

Stationarity conditions

Following the steps introduced previously in section (2.3.2), we will write the stationarity of ΔJ with respect to d^* and $\boldsymbol{\varepsilon}^*$ providing an expression for the parameters $\mathcal{A}_0^{(r)}$ and $\mathbb{C}_0^{(r)}$. The stationarity with respect to these parameters will complete their expressions. And finally, the stationarity of J_0 with respect to d will provide an expression of the damage as a function of $\boldsymbol{\varepsilon}$.

1. Stationarity of ΔJ

The stationarity of ΔJ (2.59) with respect to $\boldsymbol{\varepsilon}^*$ can be written as :

$$\frac{\partial}{\partial\boldsymbol{\varepsilon}^*}\left\{ \frac{1}{2(1+Q'\,d^*)}\left[\boldsymbol{\varepsilon}^* : \mathbb{C}_s^{(r)} : \boldsymbol{\varepsilon}^* \;-\; \mathcal{A}_0^{(r)}\right] \;-\; \frac{1}{2}\boldsymbol{\varepsilon}^* : \mathbb{C}_0^{(r)} : \boldsymbol{\varepsilon}^* \right\} = 0 \tag{2.61}$$

which implies

$$\Longrightarrow \quad \mathbb{C}_0^{(r)} \;=\; \frac{1}{(1+Q'\,d^*)}\,\mathbb{C}_s^{(r)} \tag{2.62}$$

Similarly, the stationarity condition of ΔJ over d^* reads :

$$\frac{\partial}{\partial d^*}\left\{ \frac{1}{2(1+Q'\,d^*)}\left[\boldsymbol{\varepsilon}^* : \mathbb{C}_s^{(r)} : \boldsymbol{\varepsilon}^* \;-\; \mathcal{A}_0^{(r)}\right] \;-\; \frac{1}{2}\boldsymbol{\varepsilon}^* : \mathbb{C}_0^{(r)} : \boldsymbol{\varepsilon}^* \right\} = 0 \tag{2.63}$$

This leads to an expression for the first parameter introduced in J_0 :

$$\Longrightarrow \quad \mathcal{A}_0^{(r)} = \boldsymbol{\varepsilon}^* : \mathbb{C}_s^{(r)} : \boldsymbol{\varepsilon}^* \tag{2.64}$$

The two relations (2.62) and (2.64) show that the two unknowns $\mathcal{A}_0^{(r)}$ and $\mathbb{C}_0^{(r)}$ depend on the variables $\boldsymbol{\varepsilon}^*$ and d^* which remain to be determined.

2. Minimization of $J_0^{(r)}$

We obtain a Linear Comparison Composite (LCC) by minimizing $J_0^{(r)}$ with respect to d. And due to the stationarity of ΔJ with respect to the strain tensor, we can then write:

$$\tilde{w}_\Delta(\boldsymbol{E}) \approx \underset{\mathcal{A}_0^{(r)},\mathbb{C}_0^{(r)}}{\text{stat}} \left[\inf_{\boldsymbol{\varepsilon}/\langle\boldsymbol{\varepsilon}\rangle=E} \langle w_0(\boldsymbol{\varepsilon})\rangle + \underset{\boldsymbol{\varepsilon}^*,d^*}{\text{stat}} \langle \Delta J(\boldsymbol{\varepsilon},d)\rangle \right] \tag{2.65}$$

where $w_0(\boldsymbol{\varepsilon})$ is the energy associated with the resulting LCC such that :

$$w_0(\boldsymbol{\varepsilon}) = \inf_{d/\Upsilon_c(\dot{d})} J_0(\boldsymbol{\varepsilon},d) \tag{2.66}$$

The infimum of $J_0(\boldsymbol{\varepsilon},d)$ with respect to d is given with account of the irreversibility constraint on damage, which is written using the Karush-Kuhn-Tucker (KKT) optimality conditions:

$$\begin{cases} \dfrac{\partial}{\partial d}\left\{ \dfrac{1}{2(1+Q'\,d)}\,\mathcal{A}_0^{(r)} + \dfrac{1}{2}\boldsymbol{\varepsilon} : \mathbb{C}_0^{(r)} : \boldsymbol{\varepsilon} + \mathcal{Y}_c\,(d-d_n) \right\} + \lambda = 0 \\ \lambda \left(\dfrac{d-d_n}{\Delta t} \right) = 0 \\ \lambda \le 0 \quad ; \dfrac{d-d_n}{\Delta t} \ge 0 \end{cases} \tag{2.67}$$

Case 1. $\lambda < 0$. According to $(2.67)_2$, this assumption leads to $d = d_n$ which is the same as the elastic case without the presence or evolution of damage. This case will therefore not be retained.

Case 2. $\lambda = 0$. From $(2.67)_1$, this assumption leads to:

$$\frac{\partial}{\partial d}\left\{ \frac{1}{2(1+Q'\,d)}\,\mathcal{A}_0^{(r)} + \frac{1}{2}\boldsymbol{\varepsilon} : \mathbb{C}_0^{(r)} : \boldsymbol{\varepsilon} + \mathcal{Y}_c\,(d-d_n) \right\} = 0 \tag{2.68}$$

It is this case that we retain.

The resulting expression of the damage variable is as follows :

$$d_{opt}^{(r)} = \sqrt{\frac{\mathcal{A}_0^{(r)}}{2\,Q'\,\mathcal{Y}_c}} - \frac{1}{Q'} \tag{2.69}$$

The energy associated with the LCC, with J_0 given by (2.58), is then written as :

$$w_0^{(r)}(\boldsymbol{\varepsilon}) = \frac{1}{2\left(1+Q'\,d_{opt}^{(r)}\right)}\,\mathcal{A}_0^{(r)} + \frac{1}{2}\boldsymbol{\varepsilon} : \mathbb{C}_0^{(r)} : \boldsymbol{\varepsilon} + \mathcal{Y}_c\left(d_{opt}^{(r)} - d_n\right) \tag{2.70}$$

3. Stationarity of $\left\langle J_0^{(r)} + \Delta J^{(r)}\right\rangle^{(r)}$

Optimality with respect to $\mathcal{A}_0^{(r)}$ and $\mathbb{C}_0^{(r)}$ allows to obtain the missing link between $(\boldsymbol{\varepsilon}^*, d^*)$ and the variables $(\boldsymbol{\varepsilon}, d)$:

$$\underset{\mathcal{A}_0^{(r)}}{\text{stat}}\left\langle J_0^{(r)} + \Delta J^{(r)}\right\rangle^{(r)} \Longrightarrow \left\langle \frac{1}{(1+Q'\,d)}\right\rangle^{(r)} = \left\langle \frac{1}{(1+Q'\,d^*)}\right\rangle^{(r)} \tag{2.71}$$

$$\underset{\mathbb{C}_0^{(r)}}{\text{stat}}\left\langle J_0^{(r)} + \Delta J^{(r)}\right\rangle^{(r)} \Longrightarrow \begin{cases} \langle \boldsymbol{\varepsilon} : \mathbb{K} : \boldsymbol{\varepsilon}\rangle^{(r)} = \langle \boldsymbol{\varepsilon}^* : \mathbb{K} : \boldsymbol{\varepsilon}^*\rangle^{(r)} \\ \langle \boldsymbol{\varepsilon} : \mathbb{J} : \boldsymbol{\varepsilon}\rangle^{(r)} = \langle \boldsymbol{\varepsilon}^* : \mathbb{J} : \boldsymbol{\varepsilon}^*\rangle^{(r)} \end{cases} \tag{2.72}$$

$\mathcal{A}_0^{(r)}$ can then be determined using the second-order moment estimate of the strain field:

$$\mathcal{A}_0^{(r)} = \left\langle \boldsymbol{\varepsilon} : \mathbb{C}_s^{(r)} : \boldsymbol{\varepsilon}\right\rangle^{(r)} \tag{2.73}$$

Using the result (2.73), one can rewrite (2.69) in the following form

$$\frac{1}{2\left(1+Q'\,d_{opt}^{(r)}\right)}\left\langle \boldsymbol{\varepsilon} : \mathbb{C}_s^{(r)} : \boldsymbol{\varepsilon}\right\rangle^{(r)} - \mathcal{Y}_c = 0 \tag{2.74}$$

Finally, using the results (2.71) and (2.73), and carrying (2.69) into (2.62), one gets the expression of $\mathbb{C}_0^{(r)}$

$$\mathbb{C}_0^{(r)} = \frac{1}{\left(1+Q'\,d_{opt}^{(r)}\right)}\,\mathbb{C}_s^{(r)} = \sqrt{\frac{2\,\mathcal{Y}_c}{Q'\left\langle \boldsymbol{\varepsilon} : \mathbb{C}_s^{(r)} : \boldsymbol{\varepsilon}\right\rangle^{(r)}}}\,\mathbb{C}_s^{(r)} \tag{2.75}$$

which represents the elasticity tensor of the Linear Comparison Composite (LCC) described by $w_0(\boldsymbol{\varepsilon})$ (2.70).

Effective response of the elasto-damageable composite

Once all the parameters are known, the effective behavior of the composite can be specified. In order to do so, we proceed to the minimization of (2.60) with respect to $\boldsymbol{\varepsilon}$. This functional is stationary with respect to $\mathcal{A}_0^{(r)}$, $\mathbb{C}_0^{(r)}$ and d and the term ΔJ of this functional is stationary with respect to $\boldsymbol{\varepsilon}^*$ and d^*. Given this, we can define the local problem that corresponds to

the Euler-Lagrange equations providing the solution to the variational problem:

$$\begin{cases} \operatorname{div}\boldsymbol{\sigma}(x) \;=\; 0 & \forall x \in \Omega \\ \boldsymbol{\sigma}(x) = \mathbb{C}_0^{(r)} \;:\; \boldsymbol{\varepsilon}(x) & \forall x \in \Omega \\ \langle \boldsymbol{\varepsilon}(x) \rangle \;=\; E \qquad + & \text{Boundary conditions on } \partial\Omega \end{cases} \tag{2.76}$$

The effective behavior of the nonlinear composite can then be approximated from the estimate :

$$\begin{aligned} \boldsymbol{\sigma} \;&=\; \langle \boldsymbol{\sigma}(x) \rangle \;=\; \frac{\partial \tilde{w}_\Delta}{\partial \boldsymbol{E}}(\boldsymbol{E}) \approx \frac{\partial \tilde{w}_0}{\partial \boldsymbol{E}}(\boldsymbol{E}) \\ &= \sum_{r=1}^{N} c^{(r)}\, \mathbb{C}_0^{(r)} \;:\; \langle \boldsymbol{\varepsilon}(x) \rangle \;=\; \sum_{r=1}^{N} c^{(r)}\, \mathbb{C}_0^{(r)} \;:\; \left[\mathbb{A}^{(r)} : E \right] \end{aligned} \tag{2.77}$$

where $\mathbb{A}^{(r)}$ is the fourth-order tensor which corresponds to the strain localization tensor in the phase (r).

We consider yet again the case of a two-phased composite (N=2 being the number of phases) composed of an elasto-damageable matrix reinforced by randomly and isotropically distributed elastic spherical particles. The subscripts (1) and (2) represent the inclusion and the matrix, respectively.

The nonlinear problem is reduced to the solution of a two-function system of unknowns $\mathcal{A}_0^{(r)}$ and $\mathbb{C}_0^{(2)}$:

$$\begin{cases} F_1\left(\mathcal{A}_0^{(2)}, \mathbb{C}_0^{(2)}\right) \;=\; \mathcal{A}_0^{(2)} \;-\; \left\langle \boldsymbol{\varepsilon} : \mathbb{C}_s^{(2)} : \boldsymbol{\varepsilon} \right\rangle^{(2)} \;=\; 0 \\ F_2\left(\mathcal{A}_0^{(2)}, \mathbb{C}_0^{(2)}\right) \;=\; \mathbb{C}_0^{(2)} \;-\; \sqrt{\dfrac{2\,\mathcal{Y}_c}{Q' \left\langle \boldsymbol{\varepsilon} : \mathbb{C}_s^{(r)} : \boldsymbol{\varepsilon} \right\rangle^{(r)}}}\, \mathbb{C}_s^{(2)} \;=\; 0 \end{cases} \tag{2.78}$$

2.7.2 Numerical illustration

We now propose an analysis of the response of such composite with this particular degradation function. To this end, we have performed simulations on a two-phased composite consisting of an elasto-damageable matrix reinforced with linear elastic spherical particles. The material parameters are those given in (2.55). The composite is subjected to an isochoric macroscopic strain (see (2.56)).
As can be seen in Fig.2.5d, the damage evolution shows a steady increase which is due to the non-softening property of the current model.

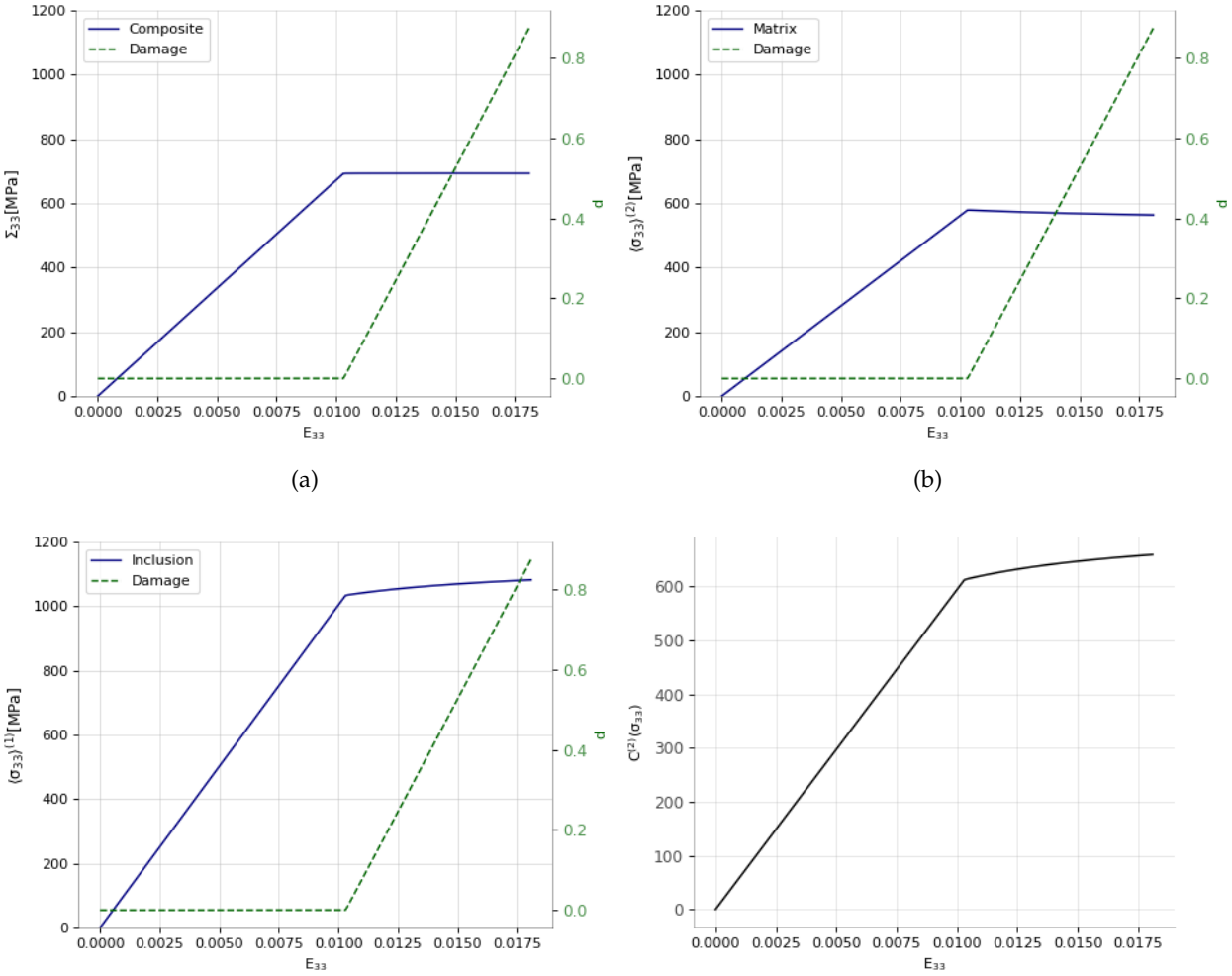

FIGURE 2.5: $Q' = 1$ - Elastically reinforced composite with an elasto-damageable matrix submitted to an isochoric macroscopic strain [MT scheme] (a) Macroscopic axial stress, (b) Average axial stress in the matrix, (c) Average axial stress in the inclusion,(d) Stress fluctuations in the matrix

2.8 Conclusion

In this chapter, after briefly presenting some nonlinear homogenization methods including incremental variational approaches, we introduced the main elements of the Effective Internal Variable homogenization procedure introduced by Lahellec and Suquet [75] by relying on the Generalized Standard Materials framework. Then, we propose an extension of this method to composites with elasto-damageable constituents. To this end, we apply a linearization procedure of the local behavior followed by the resolution of the resulting homogenization problem. The developed homogenization model has been implemented numerically for a two-phased composite. This was followed by a qualitative illustration of the predictions of the homogenization model in the case of an elasto-damageable aluminum matrix reinforced by a linear elastic inclusion made of silicon carbide. It was observed that although the inclusion is linear elastic, it still showed a decrease in the average stress when

represented with respect to the macroscopic strain which is actually a sort of unloading occurring with the evolution of damage in the matrix

Considering a porous material, a first comparison has been made between the nonlinear homogenization model and the closed-form solutions presented in chapter 1 on a hollow sphere. The qualitative agreement between the overall response predicted by the homogenization model and the one issued from the closed-form solution (on the hollow sphere) is remarkable except when the softening regime is well developed.

The chapter ends with the consideration of a different degradation function. The damage law considered in that section has the particularity of showing elastic-perfect damage-like law, that is without softening.

Now that the proposed homogenization model is set up, in the next chapter, our aim is to evaluate its predictions by means of a confrontation with results that will be obtained from full-field simulations.

Chapter 3

Full-field computations and assessment of the EIV approach for elasto-damageable composites

Contents

In this chapter, we aim at evaluating the theoretical homogenization model developed and described in the second chapter. To this end, we performed full-field finite element simulations by relying on the variational commonly referred to now as the phase-field approach, initially introduced by [19] and interpreted later by [112] as regularized gradient damage model. Detail on gradient damage models can be found in several other studies among which [41, 80]. In section 3.1, the choice of gradient damage models for full-field simulations will be first motivated, and a brief presentation of the main elements of the phase field approach in presence of a damage threshold (the so-called AT1 model) will be reminded. The numerical implementation of this variational approach using FEniCS libraries and Python is briefly described following an alternate minimization algorithm as proposed by [19]. This first section ends with a comparison between the theoretical overall behavior issued from the closed-form solutions established on the hollow sphere (see chapter 1, (1.4.4)) and the newly

obtained numerical results. Then, we propose an assessment of the predictive capabilities of the Effective Internal Variable homogenization model through the comparison between its predictions and that of the full-field computations for different macroscopic loading cases, namely isochoric strain, uniaxial extension, and cyclic loadings. Note that, the microstructure studied is constituted by a cube of elasto-damageable matrix containing a spherical linear elastic inclusion.

3.1 Limitations of local damage models : mesh size sensitivity

Pathological limitations of local descriptions of elastic damage models have been well-known for over 30 years. Their main manifestations are a spurious mesh dependency in presence of strong localization of deformations and damage resulting from material softening. As we will see later, several ways are possible in order to circumvent these difficulties : formulation of non-local damage models introducing an internal length; implementation of some mathematical relaxation of energy methods in order to ensure that the corresponding problem is well-posed. (see for instance [40], [50].
In order to confirm the numerical inadequacy of local models by a finite element calculation, we adapt to the local damage context (no internal length) the functional of the variational formulation that will be presented in subsection 3.2.1 for regularized damage model. This leads to the following two fields' minimization problem :

$$\mathcal{E}(u,d) \;=\; \int_\Omega \left(\frac{1}{2}\boldsymbol{\varepsilon} : \mathbb{C}(d) : \boldsymbol{\varepsilon} \;+\; w(d)\right) d\Omega \;-\; W_{\text{ext}} \tag{3.1}$$

where :

$$W_{\text{ext}} \;=\; \int_\Omega f\,\delta u\, d\Omega \;+\; \int_\Omega T\,\delta u\, dS \begin{cases} f \;: & \text{volumetric force in } \Omega \\ T \;: & \text{surface forces in } \partial\Omega \end{cases} \tag{3.2}$$

In this functional, in addition to the elastic energy, one has the term $w(d)$ which corresponds to the total dissipated energy until time t and is such that for the local already presented:

$$w(d) \;=\; \mathcal{Y}_c\, d \tag{3.3}$$

where the material constant $\mathcal{Y}_c$ represents the damage energy release at yield, *i.e.* a parameter of the local damage model which may be obtained from experiences characterizing the material's mechanical behavior.
In what follows, we will briefly investigate the effect of mesh sensitivity on results obtained by means of the local damage model. To this end, we have performed computations on the one-eighth of a 3D cubic cell, with a 3mm side, consisting of an elastic damageable matrix reinforced by an isotropic linear elastic spherical particle at the center whose radius is 2.34mm, the volume fraction considered throughout this study amounts to 25%.

The material properties considered are the ones already introduced in (2.55); the composite is here subjected to an isochoric macroscopic strain :

$$E(t) \;=\; E_{33}(t)\left(-\frac{1}{2}(e_1\otimes e_1 \;+\; e_2\otimes e_2) \;+\; e_3\otimes e_3\right) \tag{3.4}$$

The numerical simulations are performed using FeniCS libraries and the assembly is done via Python programming language.
Hereafter, in order to illustrate mesh sensitivity, we performed three simulations with tetrahedral elements corresponding to three mesh sizes :

	Number of elements	Mesh size (mm)
h1	139 068	0.1
h2	323 339	0.075
h3	608 791	0.06

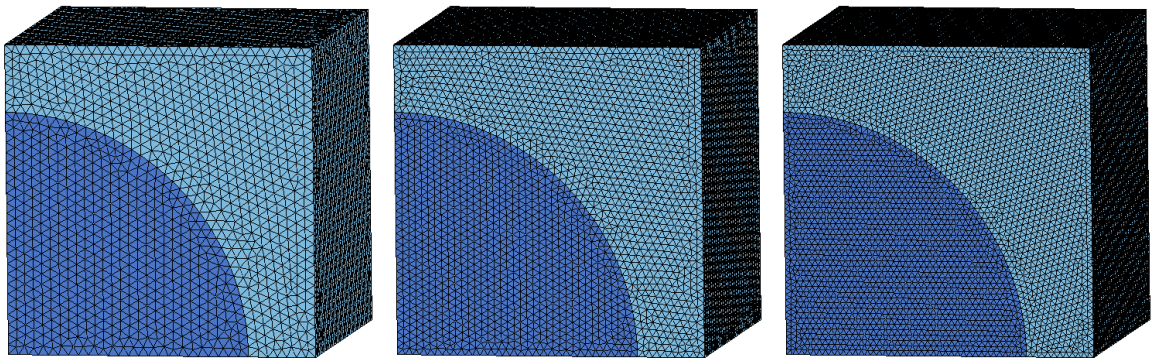

(a) (b) (c)

FIGURE 3.1: Illustrations of the three considered meshes for the local isotropic model, (a) h1, (b) h2, (c) h3

For each of these meshes, we represent in Fig.3.2 the macroscopic response of the composite as well as the averages of the stress field over the matrix phase and the inclusion. Moreover, the evolution of the "mean value" of damage, computed using the expression (2.45)[1]. It can be clearly seen that the composite behavior in the softening regime is strongly mesh size dependent. In Fig.3.3, it is shown how the localized damage zone (at ultimate damage) differs from one mesh to another. This localization of the damage field concentrates in increasingly thin bands for increasing fine meshes. Note that the damage localization in the form of crack is obtained at the occurrence of damage, inducing then a marked softening regime (the damage goes instantaneously from 0 to 1).
A way to correct this pathology, and that we follow in the rest of the study, is to consider non-local formulations in the form of gradient damage-based constitutive laws.

[1]This choice is made in the view of further comparison purpose with the homogenization model.

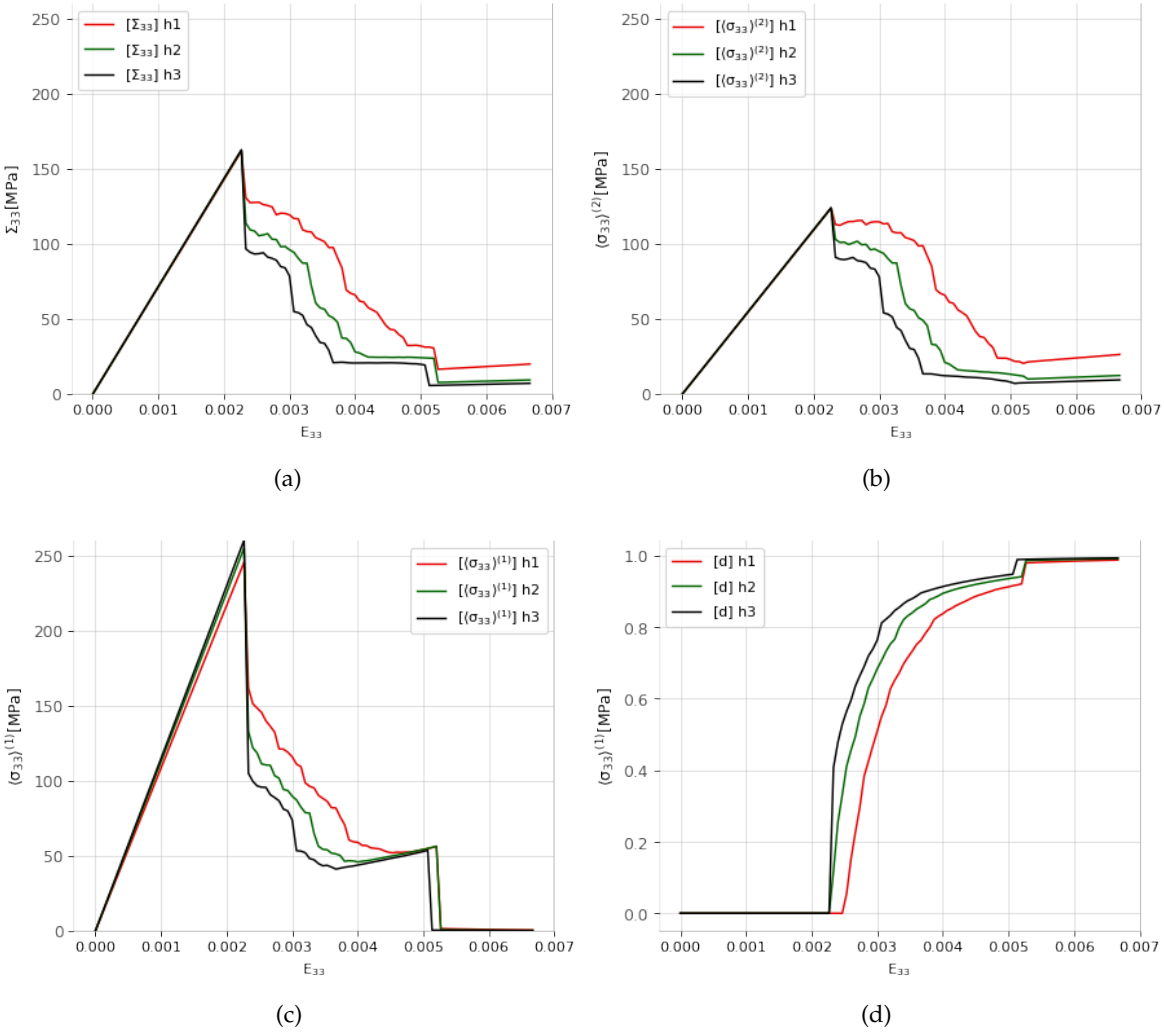

FIGURE 3.2: Predictions of the local isotropic damage model for a composite submitted to an isochoric macroscopic strain. Computations for three different meshes, (a) Macroscopic axial stress, (b) Average axial stress in the matrix, (c) Average axial stress in the inclusion, and (d) the evolution of damage with respect to macroscopic strain E_{33}

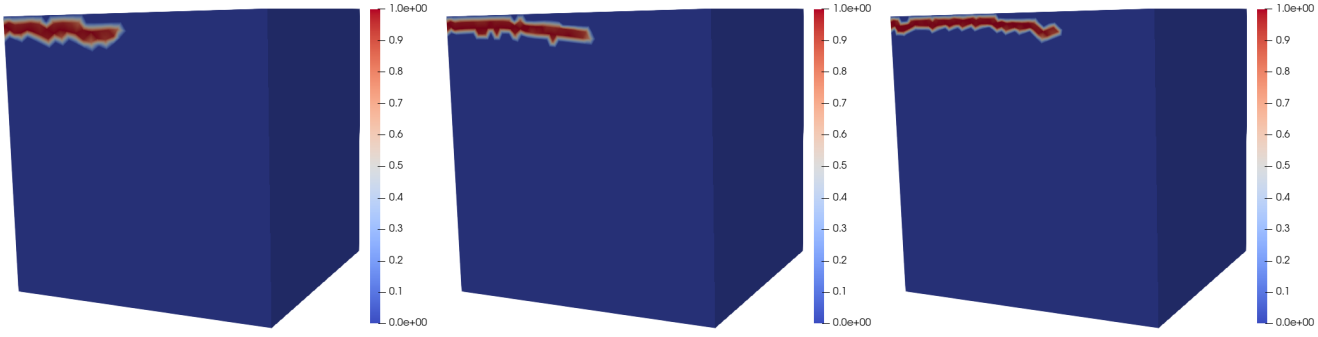

FIGURE 3.3: Damage isovalues showing the distribution of damage localization for the same microstructure. Three different mesh sizes are considered, (a) h1, (b) h2, (c) h3

3.2 A regularized damage approach as a relevant tool of investigation of quasi-brittle composites

In this section, we first present a summary of the variational regularized damage model used for the full-field computations and then the alternate minimization algorithm available for its implementation.

3.2.1 Variational formulation of gradient damage models

As a way of avoiding the pathological problems linked to the Finite Element mesh dependency, we relied on a regularized damage model. This variational approach, introduced by [19] in connection with the study by [3], consists in minimizing a functional with respect to two fields (displacement and damage) on the considered structure. It has been interpreted later as a gradient damage model [88]. Moreover, probably due to their success to describe the transition from damage to fracture phenomena, gradient damage models have opened the way to methods widely recognized and diffused today under the acronym of phase-field methods. As examples of successful applications of gradient damage models mention can be made of [81],[82], [106], [127] to cite few.

Variational formulation

Let us consider a time-dependent loading in which the evolution would be parametrized by a "time" variable t. The variational approach is based on the total energy functional including a gradient of damage term :

$$\mathcal{E}(u,d) = \int_\Omega \Psi(\boldsymbol{\varepsilon}, d, \nabla d)\, d\Omega - \int_\Omega f.u d\Omega - \int_{\partial\Omega} T.u dS \tag{3.5}$$

in which

$$\Psi(\boldsymbol{\varepsilon}, d, \nabla d) = \underbrace{\frac{1}{2}\boldsymbol{\varepsilon} : \mathbb{C}(d) : \boldsymbol{\varepsilon}}_{\text{free energy density}} + \underbrace{w(d) + w_1 l_0^2 \nabla d.\nabla d}_{\text{dissipated energy density}} \tag{3.6}$$

where f and T correspond to external body forces and surface tractions respectively applied at time t.
The dissipated energy density is written as the sum of a local term $w(d)$, also called the damage dissipation function, and a damage gradient term $w_1 l_0^2 \nabla d.\nabla d$ which involves an internal length scale l_0.

Moreover, it should be noted that the field equations of the mechanical problem (equilibrium, damage evolution criterion, and consistency equations) can be obtained from optimality conditions, taking advantage of the fact that the functional to be minimized is separately convex with respect to both u and d. The directional derivative for u describes the linear

variational elasticity problem at fixed d (see [16]):

$$\left.\frac{\partial \mathcal{E}}{\partial u}\right|_{(u,d)}(v,0) \;=\; 0 \longrightarrow \int_\Omega (1-d)^2\, \boldsymbol{\varepsilon}_u \;:\; \mathbb{C}_s \;:\; \boldsymbol{\varepsilon}_v \, d\Omega \;=\; W_{ext}(v) \;\forall v \tag{3.7}$$

And the directional derivative for d gives the variational inequality :

$$\left.\frac{\partial \mathcal{E}}{\partial d}\right|_{(u,d)}(0,\beta-d_n) \;\geq\; 0 \longrightarrow \frac{G_c}{c_w}\int_\Omega \left(\frac{w'(d)}{l_0}\,(\beta-d_n) \;+\; l_0 \nabla d\,(\nabla\beta - \nabla d_n)\right) d\Omega \;\geq 0 \;\; \forall \beta \geq d_n \tag{3.8}$$

which yields the following evolution laws :

$$f(\boldsymbol{\varepsilon},d) \;=\; (1-d)\;\boldsymbol{\varepsilon} \;:\; \mathbb{C}_s \;:\; \boldsymbol{\varepsilon} - \frac{G_c\, w'(d)}{c_w\, l_0} \;+ 2\frac{G_c\, l_0}{c_w}\,\Delta d \;\leq 0 \tag{3.9}$$

The determination of l_0 relies on a classical approach which consists in approximating the regularized damage model to the Griffith model, by postulating that the energy dissipated by damage in the fracture process is equivalent to the Griffith fracture energy. This procedure, for example well described in [88], classically leads for the model considered here to: $l_0 \;=\; \dfrac{3\,G_c}{8\,\mathcal{Y}_c}$ where G_c represents the fracture energy.

In a trivial way, the functional to be minimized then takes the form :

$$\mathcal{E}(u,d) \;=\; \int_\Omega \left(\frac{1}{2}\,(1-d)^2\,\boldsymbol{\varepsilon}(u) : \mathbb{C}_s : \boldsymbol{\varepsilon}(u)\right) d\Omega \;+\; \frac{3}{8}\,G_c \int_\Omega \left(\frac{d}{l_0} \;+\; l_0\,\nabla d.\nabla d\right) d\Omega \tag{3.10}$$

which is the expression of the above functional for the phase field approach known as AT1 in reference to a proposal of Ambrosio and Tortorelli (see [19]), with the choice $\mathbb{C}(d) \;=\; (1-d)^2\mathbb{C}_s$. We will see later in chapter 4 other choices of regularized damage laws including for example the so-called AT2 model.

A brief further comment

In agreement with the GSM framework generally adopted in the thesis, it can be of interest to comment on the possible thermodynamics potentials allowing to retrieve the above functional in link with (1.16). To this end, as in [65], consider the following thermodynamics and dissipation potentials:

$$\begin{cases} w(\boldsymbol{\varepsilon},d) \;=\; \dfrac{1}{2}\,(1-d)^2\,\boldsymbol{\varepsilon} : \mathbb{C} : \boldsymbol{\varepsilon} \\ \varphi(\dot{d},\nabla d) \;=\; \mathcal{Y}_c\,\dot{d} \;+\; 2\,l_0^2\,\mathcal{Y}_c\,\nabla d.\nabla\dot{d} \end{cases} \tag{3.11}$$

Starting from these expressions of the potentials $w(\boldsymbol{\varepsilon},d)$ and $\varphi(\dot{d},\nabla d)$, and noting that the latter corresponds to a simple dissipation structure (see [34, 33])[2], it can be proved that one

[2] **Definition 1.** *system is said to have simple dissipation if the time integral giving the total dissipation depends only on the current value of the state variables.*

gets for the energy functional the following form

$$\mathcal{E}(u,d) \;=\; \int_\Omega \left(\frac{1}{2}\,(1-d)^2\;\boldsymbol{\varepsilon}(u) : \mathbb{C}_s : \boldsymbol{\varepsilon}(u)\right) d\Omega \;+\; \mathcal{Y}_c \int_\Omega \left(d \;+\; l_0^2\,\nabla d.\nabla d\,\right) d\Omega \tag{3.12}$$

in which, compared to (3.6), use has been done of

$$w_1 w(d) \;=\; \int_0^d \mathcal{Y}_c\, d\alpha \tag{3.13}$$

Expression (3.12) corresponds to the functional described by (3.5) with (3.6).

3.2.2 Numerical modeling using gradient damage models

Main features of the numerical implementation

In order to perform Finite Element based numerical simulations with the gradient damage model briefly detailed in the previous paragraphs we made use of Python 3 scripting and FEniCS Libraries[3].
We worked on three-dimensional meshes generated thanks to GMSH [45] and treated via the *mshr* library in FEniCS. We also relied on the multiple-platform visualization tool ParaView. Each mesh is constituted of tetrahedron elements with linear interpolation for the displacement and damage fields.

The minima of the functional $\mathcal{E}(u,d)$ in equation (3.10) is performed thanks to an alternate minimization scheme as in [19], which is briefly summarized in the table hereafter:

Algorithm 1 The alternate minimization algorithm

1: Initial conditions $[u^0_{n+1} = u_n,\; d^0_{n+1} = d_n]$
2: **for** every successive time step **do**
3: **repeat**
4: $u^i_{n+1} = \underset{u}{\operatorname{argmin}}\;\; \mathcal{E}(u, d^i_n)$
5: $d^i_{n+1} = \underset{d/d_n \le d \le 1}{\operatorname{argmin}}\;\; \mathcal{E}(u^i_{n+1}, d)$
6: **Until** $||\;\left(u^i_{n+1}, d^i_{n+1}\right) \;-\; \left(u^{i-1}_{n+1}, d^{i-1}_{n+1}\right)\;|| \le \text{tol}$
7: **end for**

The first step involves solving the weak static equilibrium condition at fixed damage (u-problem). The second step (d-problem) amounts to solving a variational inequality problem in link with the irreversibility constraint. The d-problem is solved using the TAO bound-constraint optimization solver [90] integrated into the PETSc library [6]. At this stage, mention can be made of the study [37] which proposed some improvements to the standard alternate minimization algorithm.

[3] All the simulations were performed on macOS 2,5 GHz Intel Core i5 quad core

Mesh sizes have been carefully considered to be smaller than the characteristic length l_0 to resolve the regularization length scale, which will be disclosed further below for each conducted study. Material properties, as well as specific boundary conditions, will be detailed for each of the considered cases (hollow sphere, two-phase composite) addressed in Sections 3.3 and 3.4.

3.3 Comparison between numerical results and closed-form solutions on a hollow sphere

In this section we consider, once again, the reference case of an elasto-damageable hollow sphere submitted to a uniform radial displacement detailed in Sections 1.4 and 2.6. A finite element simulation of this problem using the regularized gradient damage model is performed and the results are compared to the ones previously established analytically (closed-form solutions) and the incremental variational homogenization approach developed.

Considering the symmetry of the problem, the numerical simulation can be conducted on one-eighth of the sphere. We remind that the sphere's dimensions ratio is $b/a_0 = 2$, $b = 1$mm is the external radius, and $a_0 = 0.5$mm is the internal one (which corresponds to a porosity $f = 0.125$). As previously, the material properties are also chosen as follows: the ratio of the bulk modulus and the shear modulus $k/\mu 0 = 30$ (near an elastic incompressible sound matrix).
The mesh size considered here amounts to $h \approx 0.016$mm, with the total number of elements reaching 67836, and the internal length considered here is equal to $l_0 = 0.1$mm. The threshold $\mathcal{Y}_c = \dfrac{3G_c}{8l_0} = 0.013$MPa is obtained through (1.66).

When it comes to the full-field simulations, a notable difference can be observed in the reached threshold before the softening takes place. Indeed, in the exact solution, there is the purely elastic phase until the threshold is reached and then the damaged phase begins. Whereas in the FEM simulations, it has been observed that damage begins evolving at $E_{33} = 0.0025$, in other words before reaching the highest stress value. Schematically, it is clearly seen from the damage pattern evolution (see Fig. 3.4b, 3.4c, 3.4d) in the numerical simulation that there is a competition between the damaged zone and a linear elastic one, the softening occurring only after a stage of damage development.

As mentioned before, Fig. 3.4b, 3.4c, 3.4d represent the evolution of the damage field within the hollow sphere at three different levels of loading. The first one corresponds to the first occurrence of damage within the matrix, the second level corresponds to the maximum stress level (that is right before the softening regime), and the last one corresponds to the end of the simulation with a damage level ranging from 0.45 -the minimum value for d- to 1. Damage starts from the inner radius and progresses as expected in the sphere when the applied deformation increases.
Despite the non-local character of the numerical model a qualitative agreement is obtained, confirming then an interest in the theoretical results.

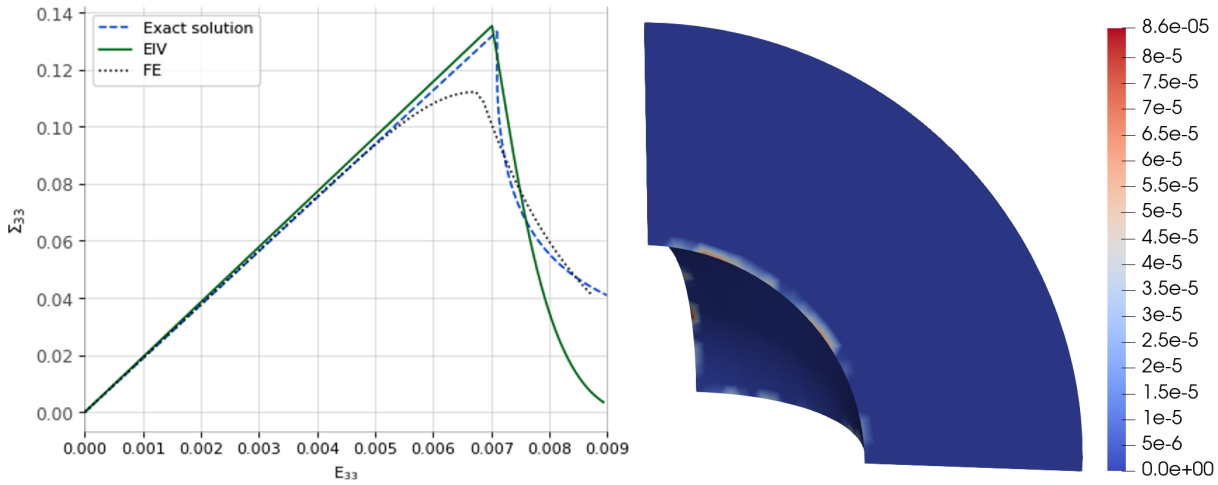

(a) (b) $E_{33} = 0.0028$

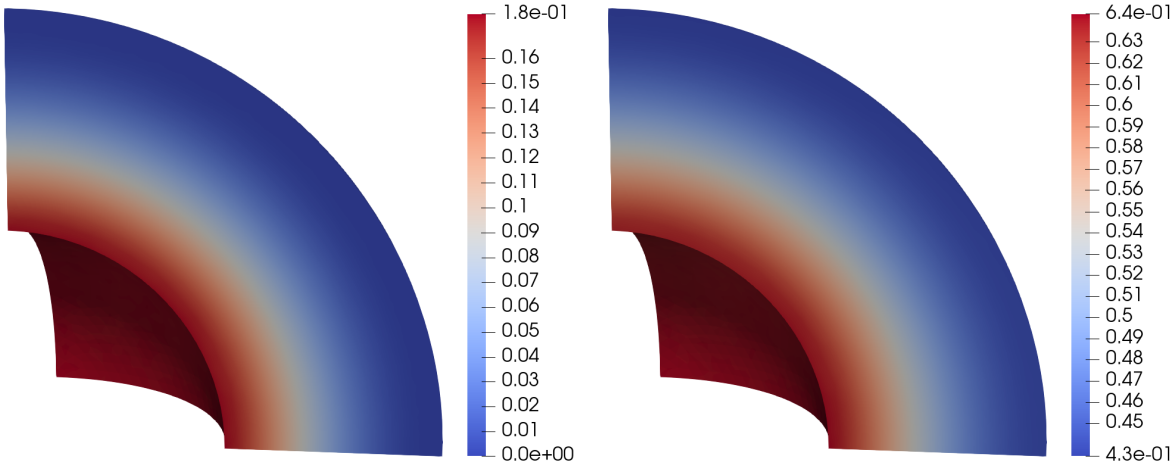

(c) $E_{33} = 0.0068$ (d) $E_{33} = 0.009$

FIGURE 3.4: (a) Comparison of the mechanical responses of a hollow sphere submitted to a uniform radial displacement obtained analytically, with the variational approach developed and thanks to full-field simulations with a gradient damage model. (b)-(c)-(d) Damage local field distribution at different loading levels

3.4 Full-field simulations on a bi-phased composite material

To illustrate the predictions of the proposed nonlinear homogenization model, as well as their evaluation, the studied composite is subjected to different monotonous and cyclic loadings which will be thoroughly discussed hereafter.

We performed FE simulations on one-eighth of a cubic cell composed of a spherical elastic particle at its center surrounded by an elasto-damageable matrix. Throughout the whole study, we made use of a mesh constituted of tetrahedron elements (44965 elements), which is illustrated in Fig.3.5 :

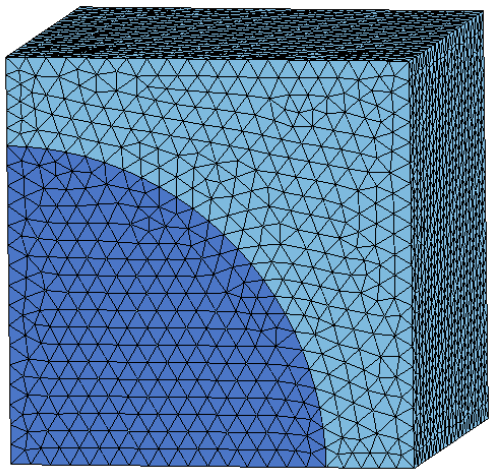

FIGURE 3.5: Mesh illustration

The elastic material properties of the matrix and of the inclusions as well as the volume fraction are given in (2.55). Using $\mathcal{Y}_c$ (2.55) and $G_c = 6\text{N/mm}$, the internal length is thus set to 0.77mm, with the inclusion's radius being roughly 3 times l_0.
For the following simulations, and according to the natural boundary conditions, we do enforce damage to be null on the edges where the loading is applied. This is done in order to prevent damage to localize artificially on the surface where the load is applied [4].

3.4.1 Monotonous Isochoric macroscopic strain loading

The bi-phased composite is first subjected to an isochoric macroscopic strain defined by:

$$E(t) \;=\; E_{33}(t)\left(-\frac{1}{2}(e_1\otimes e_1 \;+\; e_2\otimes e_2) \;+\; e_3\otimes e_3\right) \tag{3.14}$$

In Fig. 3.6a, we represent the macroscopic response of the composite under the considered loading. Regarding Fig. 3.6b and 3.6c, they illustrate respectively the evolution of the average stress in the matrix and in the inclusion phase as a function of the macroscopic strain.
In Fig. 3.6, for both the composite and the matrix, two regimes are distinguished. The first regime corresponds to the initial response which is purely elastic, while the second regime is characterized by a softening response following the development of the matrix damage. We observe in Fig. 3.6 that the predictions of the theoretical model reproduce qualitatively the overall predictions of the FEM simulations regarding the response of the composite and the average local stress in the matrix and in the inclusion. However, the softening behavior in the theoretical approach is systematically induced by the development of uniform damage in the matrix, unlike FE simulations where the softening phase is preceded by a pre-peak positive hardening regime. In addition, it is reminded that the damage criterion (2.44) of the proposed model is saturated on average rather than locally as is the case in FE simulations.

[4] However, for the sake of comprehensive exploration and a deeper understanding, a distinct scenario has been introduced in Appendix C. In this particular scenario, we do not enforce the constraint of null damage on the edges where loading is applied. One can refer to this appendix for further details.

This explains the mismatch observed between the damage threshold stresses observed in the numerical calculation and the theoretical model. In Fig. 3.6d is also represented the evolution of the damage, in an average sense, with the loading. For the sake of comparison, we used in the FE simulations the equation (2.45) allowing us to evaluate the same quantities used to calculate d[5] in the theoretical model. It is important to note that in the proposed homogenization model, the value of the homogeneous damage is determined by saturation of the criterion depending on the second-order moments of the strain in the matrix phase, $\overline{\overline{\boldsymbol{\varepsilon}}}_m^{(2)}$ and $\overline{\overline{\boldsymbol{\varepsilon}}}_m^{(1)}$. It must be recalled that this second-order moment reflects the heterogeneity of the strain field. In the full-field calculation, some heterogeneity of the damage field in the matrix is observed (see Fig. 3.7). This results from the strain field heterogeneity.

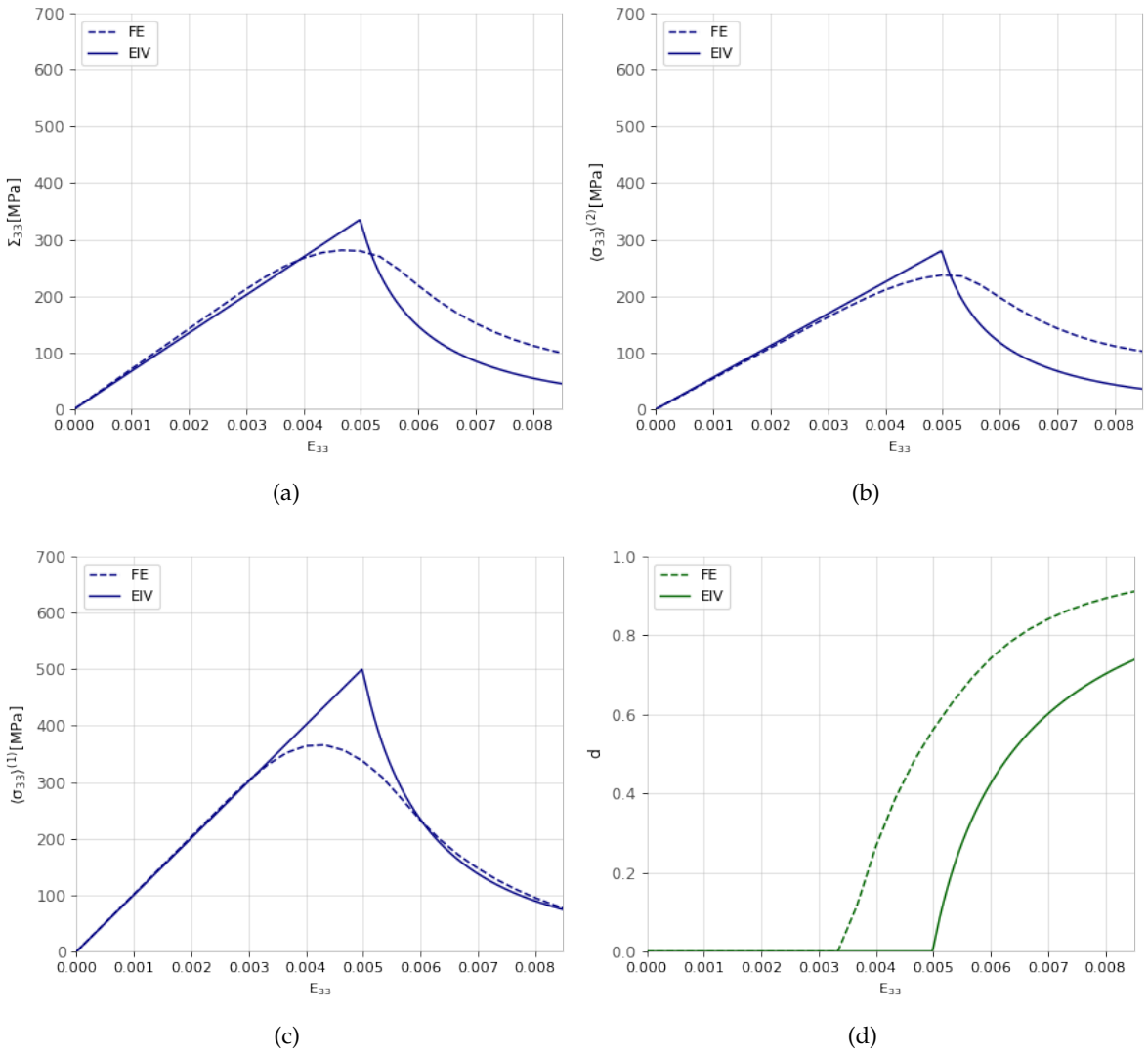

FIGURE 3.6: Elastically reinforced composite with an elasto-damageable matrix submitted to an isochoric macroscopic strain for the AT1 model. (a) Macroscopic axial stress, (b) Average axial stress in the matrix, (c) Average axial stress in the inclusion, (d) Damage evolution

[5] An alternative can be the computation of a spatial average of the damage field, but this wouldn't be very meaningful since the damage field tends to some localization and does not define an extensive quantity.

It is also important to note that the AT1 model implemented here is known to have a relatively rough softening behavior compared to other models, as it exhibits a sharper drop of stress upon reaching its maximum value. As a result, the damage tends to evolve in a localized and heterogeneous way. This constitutes a notable difference when compared to the homogenization model which by construction tends to diffuse damage by retaining a uniform per-phase damage value even determined from the second order moment of the strain field. Moreover, considering the formula (2.45) used to calculate the damage, by comparing their evolution for both approaches in Fig. 3.6d, the proposed analytical systematically underestimates the second order moment of the strain field.

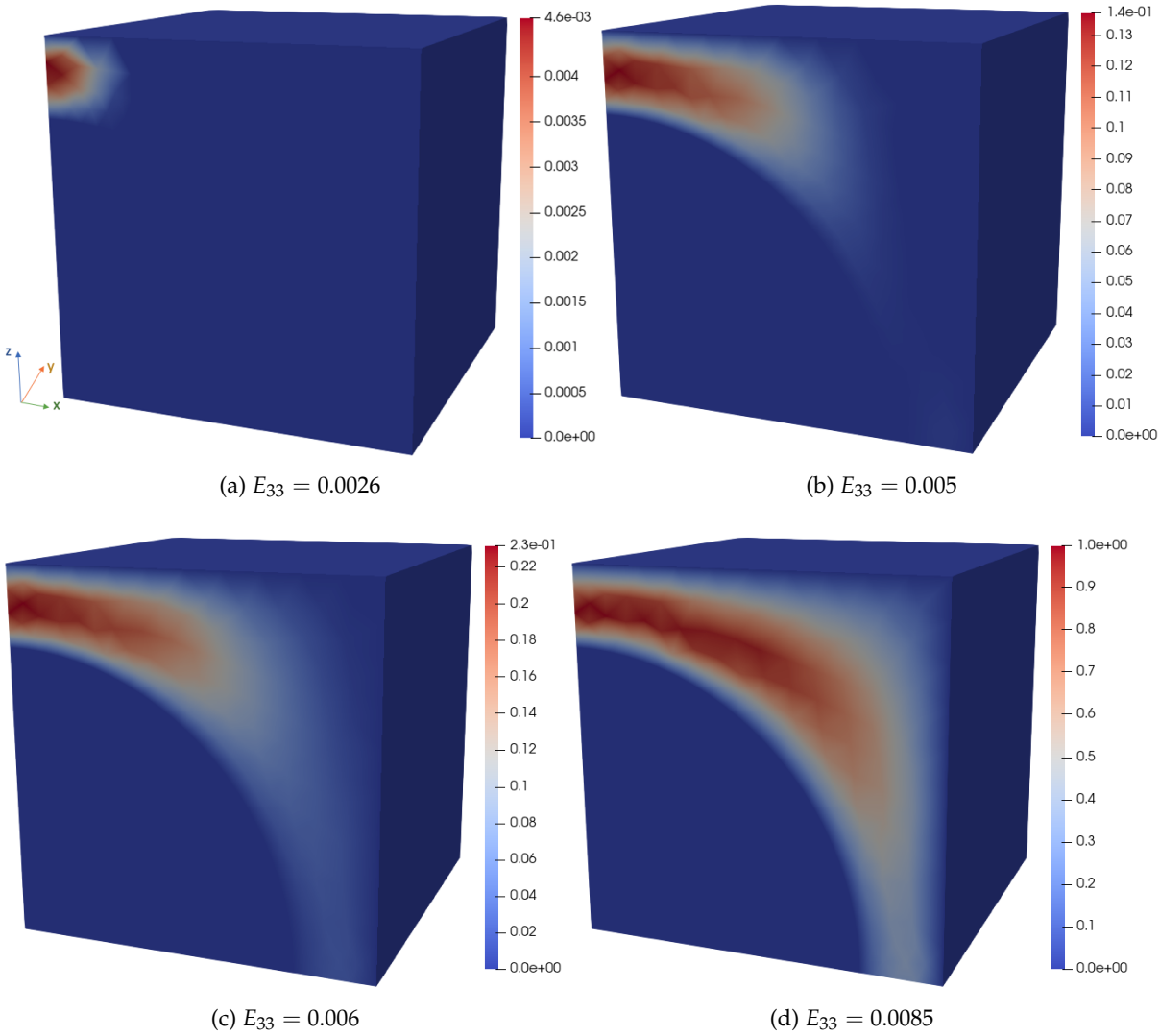

(a) $E_{33} = 0.0026$ (b) $E_{33} = 0.005$

(c) $E_{33} = 0.006$ (d) $E_{33} = 0.0085$

FIGURE 3.7: Damage evolution for the AT1 model at four different loading levels, each corresponding to (a) damage appearance, (b) maximum stress level, (c) softening regime, (d) $d(x) = 1$ locally attained

In Fig. 3.8a are represented the stress fluctuations within the matrix for both the Effective Internal Variable model and the full-field simulations. It can be seen that the loading level corresponding to the start of the softening also corresponds to the decrease of the fluctuations, which is not the case for FE calculations.

The latter is quantified by $\sqrt{\mathcal{C}^{(2)}(\boldsymbol{\sigma}) :: \mathbb{K}}$ (2.16), where $\mathcal{C}^{(2)}(\boldsymbol{\sigma})$ is defined by equation (2.15). To gain a better understanding of the fluctuations' evolution, we represent on Fig. 3.8b the evolution of their two components (see (2.16)), namely $\left(\overline{\overline{\boldsymbol{\sigma}}}_d^{(2)}\right)$ and $\left(\overline{\boldsymbol{\sigma}}_d^{(2)}\right)_{eq}$ for both the homogenization model and the full-field simulations.

The resulting stress fluctuations being directly related to the difference between the two represented components, although they both decrease, we can clearly see that the difference between them increases for the numerical results. Whereas for the homogenization model, beyond the damage threshold, the difference between the two terms seems relatively steady in comparison to FE simulations.

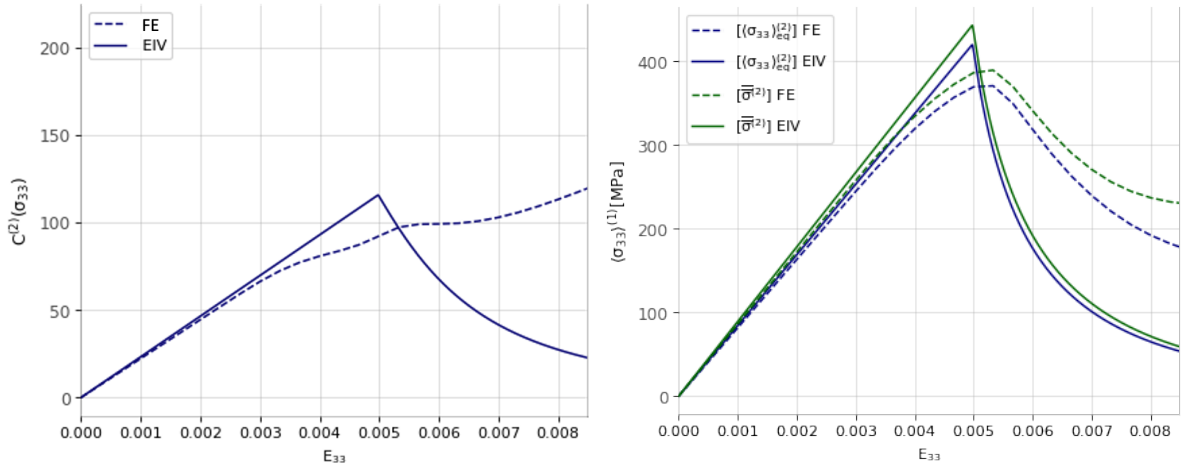

(a) (b)

FIGURE 3.8: Elastically reinforced composite with an elasto-damageable matrix submitted to an isochoric macroscopic strain for the AT1 model. (a) Stress fluctuations, (b) Evolution of the fluctuations' components

We are now interested in the energetic aspects of the damage phenomena in the composite. In particular, we aim at providing some insight on the distribution of the dissipated energy in the composite, by distinguishing its local and non-local parts. We will use the following notation :

$$\begin{cases} \mathcal{E}_f(d) = \dfrac{G_c}{l_0\, c_w}\ \left(w(d) + l_0^2 \nabla d.\nabla d\right) \\ \\ \mathcal{E}_{f-\text{local}}(d) = \dfrac{G_c}{l_0\, c_w}\, w(d) \\ \\ \mathcal{E}_{f-\text{gradient}}(d) = \dfrac{G_c}{l_0\, c_w}\ \left(l_0^2 \nabla d.\nabla d\right) \end{cases} \tag{3.15}$$

It must be first stated that in the case here of the AT1 model in which $w(d) = d$. So, the above $\mathcal{E}_{f-\text{local}}(d) = \mathcal{Y}_c d$ will be just proportional to d and will display the same distribution as for the damage by a factor $\mathcal{Y}_c$ (here $\mathcal{Y}_c = 2.9\,\text{MPa}$). We recall that this dissipated energy density is the unique one that is present in the local damage considered for the Effective Internal Variable model.

In Fig. 3.9 are shown the distribution of the local and non-local components of the dissipated energy density as well as their sum (the total dissipated energy). It is observed that in general, the nonlocal term field reaches much higher values than the local one. In particular, the interface between the matrix and the inclusion constitutes the zone with the highest damage gradient value reaching approximately 47 MPa while the local one is about 2.9 MPa. And in the overall dissipated energy pattern, it can be seen that the regularized term takes over when it comes to the distribution on the cell.

Moreover, in Fig. 3.9, we also represent the evolution of the overall energies; it is observed that the gradient term has relatively important values and it is seen that $\mathcal{E}_{f-\text{local}}(d)$ and $\mathcal{E}_{f-\text{gradient}}(d)$ are of the same order.
Choosing to rely on a gradient damage model for FE simulations allowed us to avoid mesh dependency and thus to obtain a first assessment of the developed model's predictions in terms of effective behavior, average stress over the constitutive phases, or damage evolution. In the case presented here, owing to the relative level of the dissipated energies, the gradient damage model can hardly be considered as a regularization of the local one.

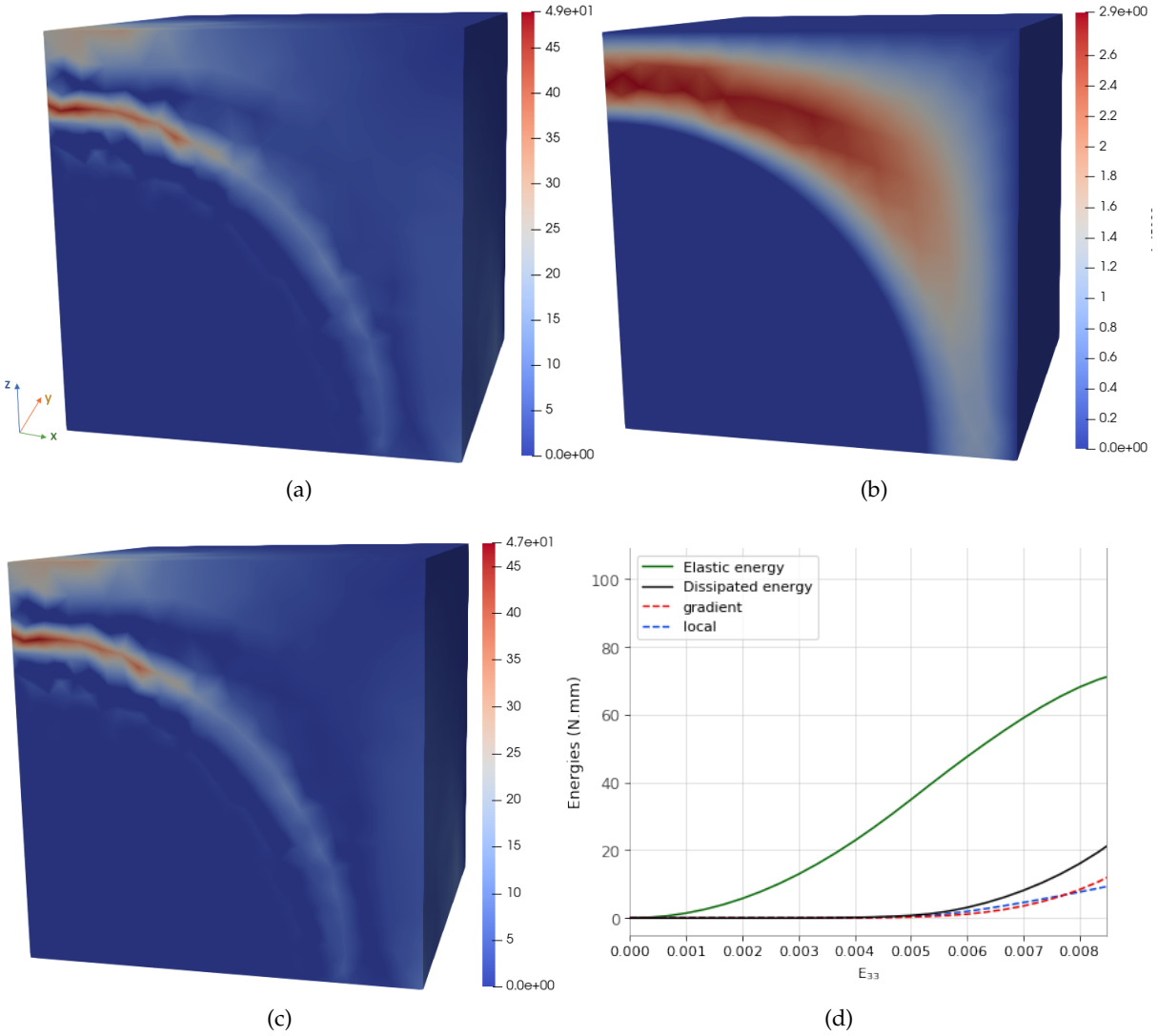

FIGURE 3.9: Elastically reinforced composite with an elasto-damageable matrix submitted to an isochoric macroscopic strain for the AT1 model. (a) Dissipated energy distribution, (b) Local term of the dissipated energy distribution, (c) Regularized term of the dissipated energy distribution, (d) Elastic energy, dissipated energy, and its constitutive terms' evolution

3.4.2 Monotonous Uniaxial extension

We are now concerned with the assessment of the proposed model predictions by comparison to results obtained from the full-field calculations for a non-isochoric strain loading which will trigger both the deviatoric and the spherical parts of the stress and the strain fields. For simplicity, a uniaxial extension along the e_3 direction is considered.

$$E(t) \;=\; E_{33}(t)\, e_3 \otimes e_3 \tag{3.16}$$

Fig. 3.10 shows for this uniaxial extension case the evolution of the axial macroscopic stress, the average stress in the phases, and damage evolution.

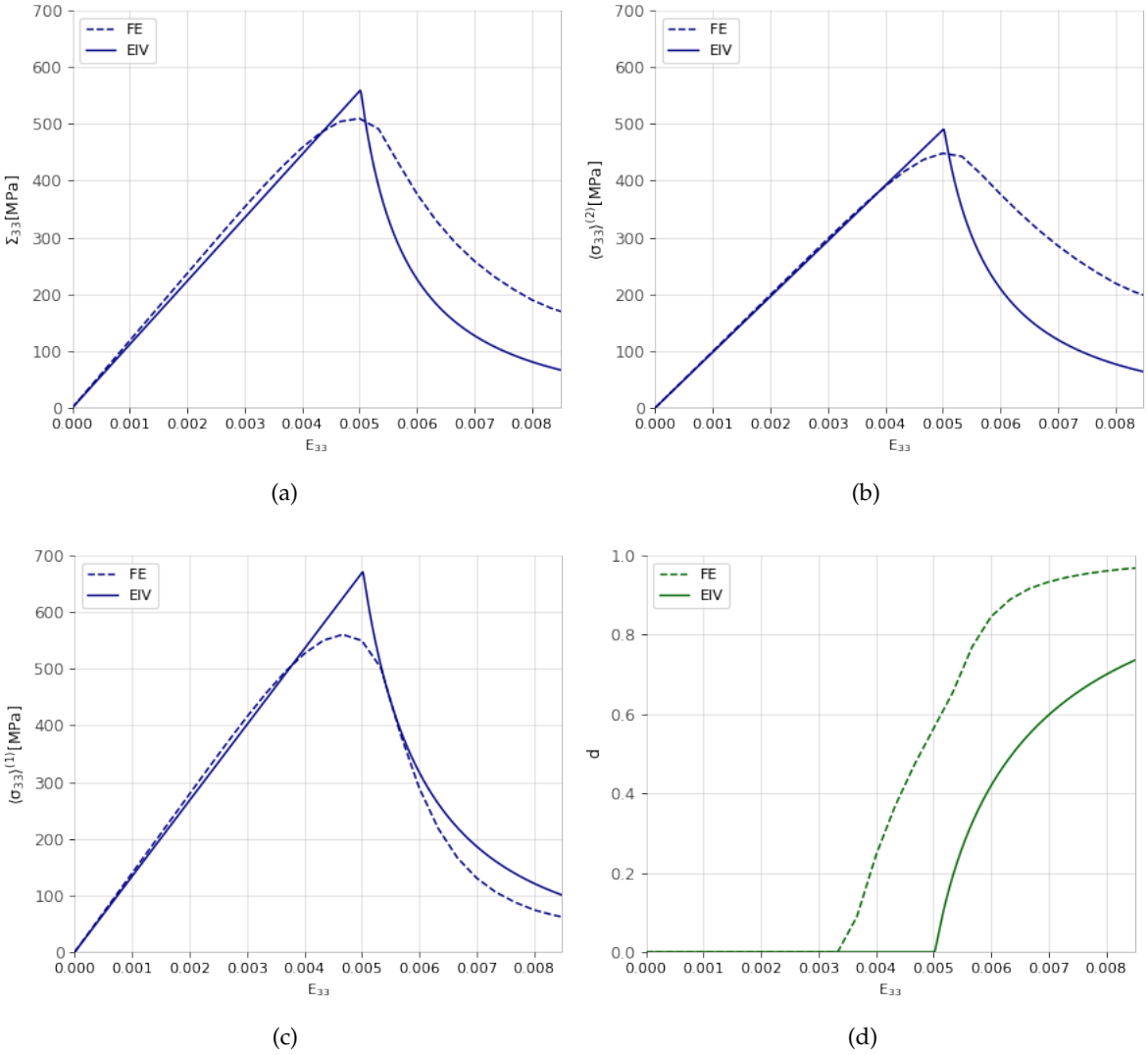

FIGURE 3.10: Elastically reinforced composite with an elasto-damageable matrix submitted to a uniaxial extension for the AT1 model. (a) Macroscopic axial stress, (b) Average axial stress in the matrix, (c) Average axial stress in the inclusion, (d) Damage evolution

Most of the previous comments on the isochoric loading (see subsection 3.4.1), remain valid for the uniaxial extension loading case, except for the damage stress threshold for which the Effective Internal Variable model provides a better agreement with the FEM results than for the previous loading. The damage localization pattern presented in Fig. 3.11 shows also a more diffuse distribution.

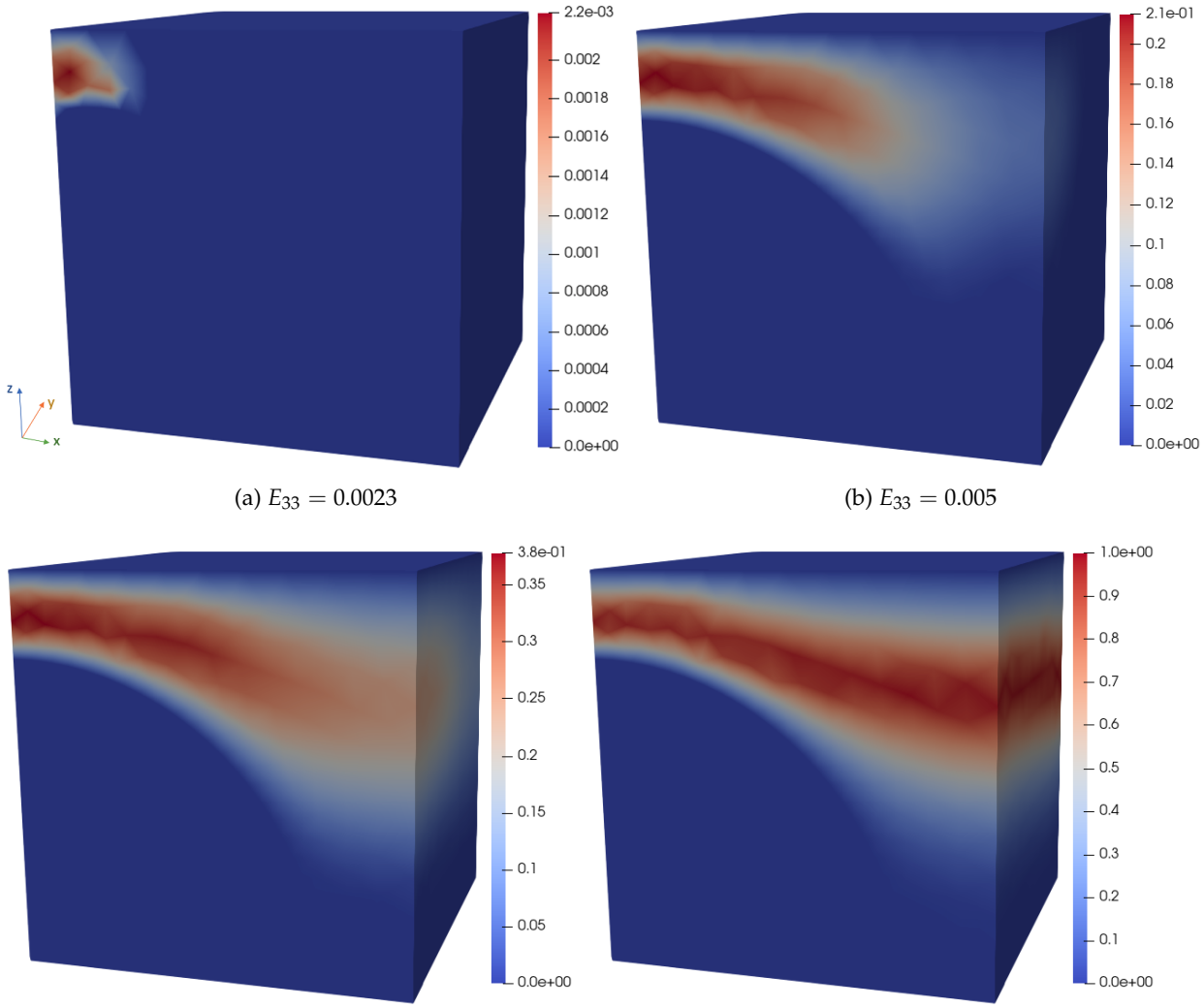

(a) $E_{33} = 0.0023$ (b) $E_{33} = 0.005$

(c) $E_{33} = 0.006$ (d) $E_{33} = 0.01$

FIGURE 3.11: Damage evolution for the AT1 model at four different loading levels, each corresponding to (a) damage appearance, (b) maximum stress level, (c) softening regime, (d) $d(x) = 1$ locally attained

Concerning the stress fluctuations in Fig. 3.12a, right after the peak stress, a sudden drop is observed, followed by an increase. The two components of these stress fluctuations are also shown and confirm the progressive difference between them in for the full-field computations results.

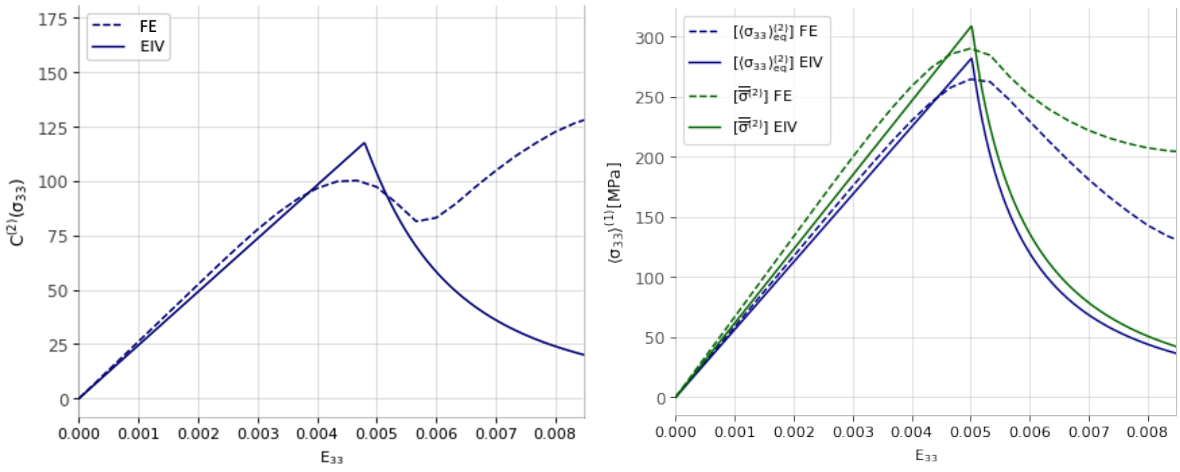

(a) (b)

FIGURE 3.12: Elastically reinforced composite with an elasto-damageable matrix submitted to a uniaxial extension for the AT1 model. (a) Stress fluctuations, (b) Evolution of the fluctuations' constitutive terms

Here as well, by examining the distributions of the dissipated energy the contribution of its nonlocal part reaches higher values in comparison to the local term. It leads to a total dissipated energy distribution of $\mathcal{E}_f$ which is close to $\mathcal{E}_{f-\text{gradient}}$. The evolution of the two terms on the whole composite shows that yet again they are approximately of the same order until $E_{33} = 0.007$. From then on, the damage gradient term takes over and reaches a value twice as high as the local term at the end of the simulation.

In the damage field distribution, we observe a relatively strong localization of the damage following a band pattern above the inclusion with zones that remain undamaged for the current loading.

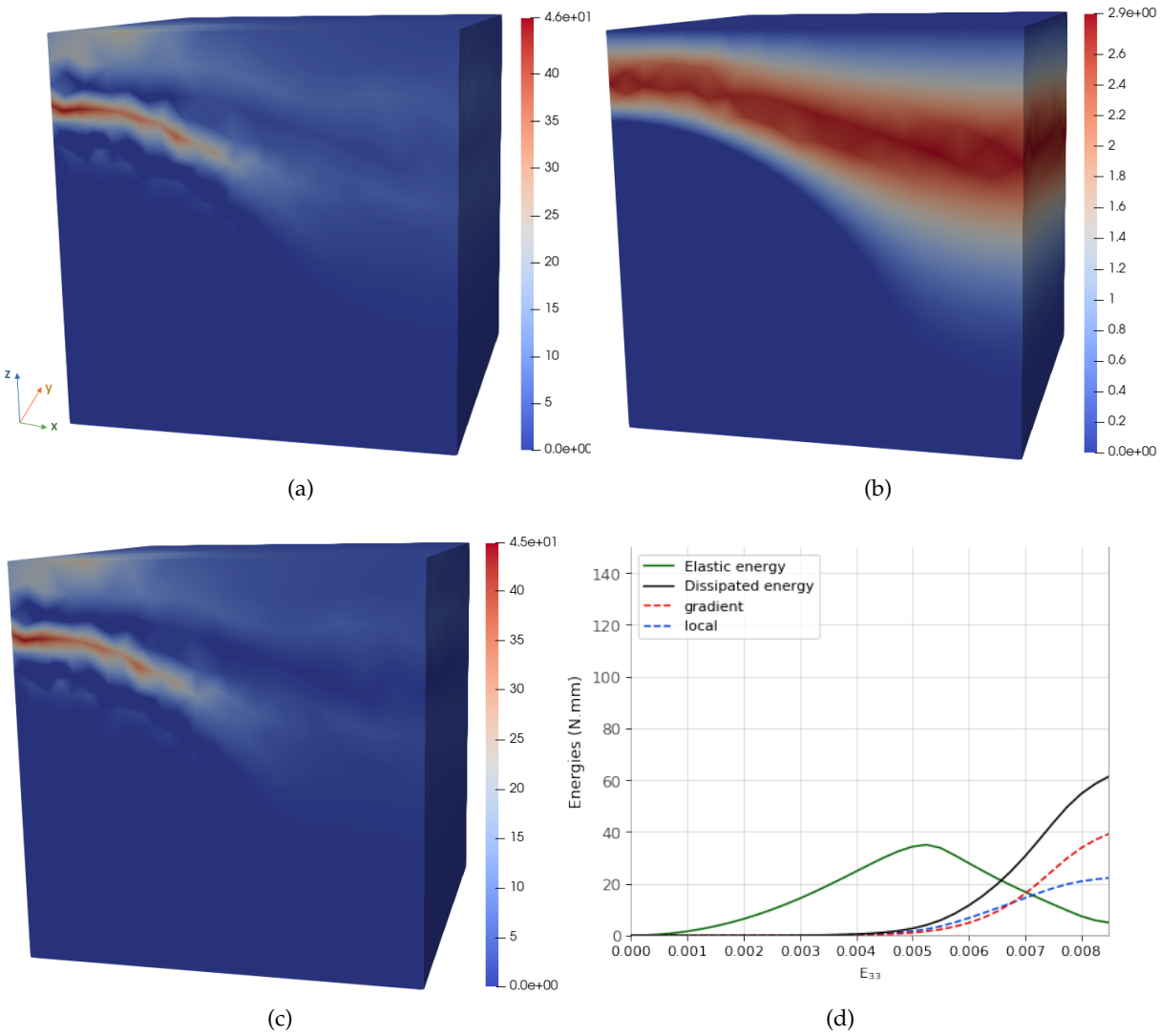

FIGURE 3.13: Elastically reinforced composite with an elasto-damageable matrix submitted to a uniaxial extension for the AT1 model. (a) Dissipated energy distribution, (b) Local term of the dissipated energy distribution, (c) Regularized term of the dissipated energy distribution, (d) Elastic energy, dissipated energy and its constitutive terms' evolution

3.4.3 Cyclic isochoric macroscopic strain Loading

In this section, we investigate the predictions of the homogenization model when the composite is subjected to a multi-cycle loading. Two types of cyclic loading, the first is shown in Fig. 3.14a in which we apply a positive macroscopic strain throughout the loading. The second loading is shown in Fig. 3.14b where a full cycle from positive to negative strains is applied.

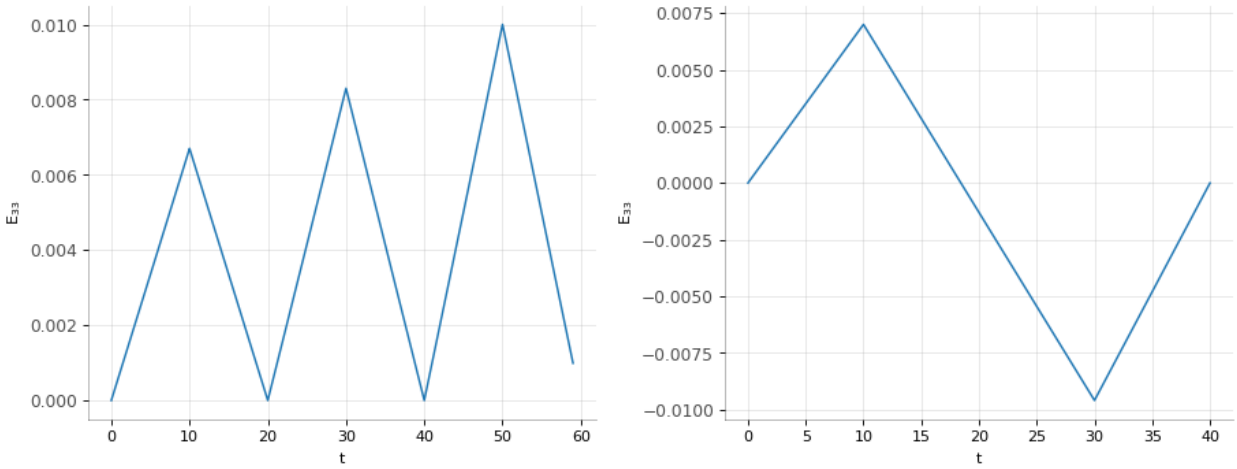

(a) (b)

FIGURE 3.14: Two different cyclic loadings [isochoric macroscopic strain] : (a) Three cycles, (b) One full cycle

The material parameters used are those of (2.55) for an elasto-damageable matrix.

For comparison purposes, we applied the homogenization model to these cyclic loadings and perform also the full-field simulations on the cell already studied.

Fig. 3.15a, 3.15b, 3.15c represent the macroscopic and phase-averaged behaviors over the matrix and over the inclusion, respectively. The model qualitatively reproduces the FE data in the softening part of the composite behavior. The evolutions of the local average stress in the matrix are also in good qualitative agreement. Interestingly a very better agreement is observed for the inclusion phase. As previously mentioned, the damage in the FE calculation does not appear for the same loading level as for the homogenization model.

Fig 3.15d represents the evolution of damage with respect to macroscopic load. But contrary to Fig. 3.6d, we represent, exclusively for the cyclic loadings, the phase-averaged damage within the matrix. The reason being that the damage estimate $\hat{d}$ calculated a posteriori through (2.45) in the numerical simulations do not abide by the irreversibility condition applied to the damage problem resolution. Though the condition $d_{n+1} \geq d_n$ can be explicitly added, this can be an opportunity to confront the average of damage in the matrix obtained through the numerical simulations and the resulting damage through the proposed analytical model.

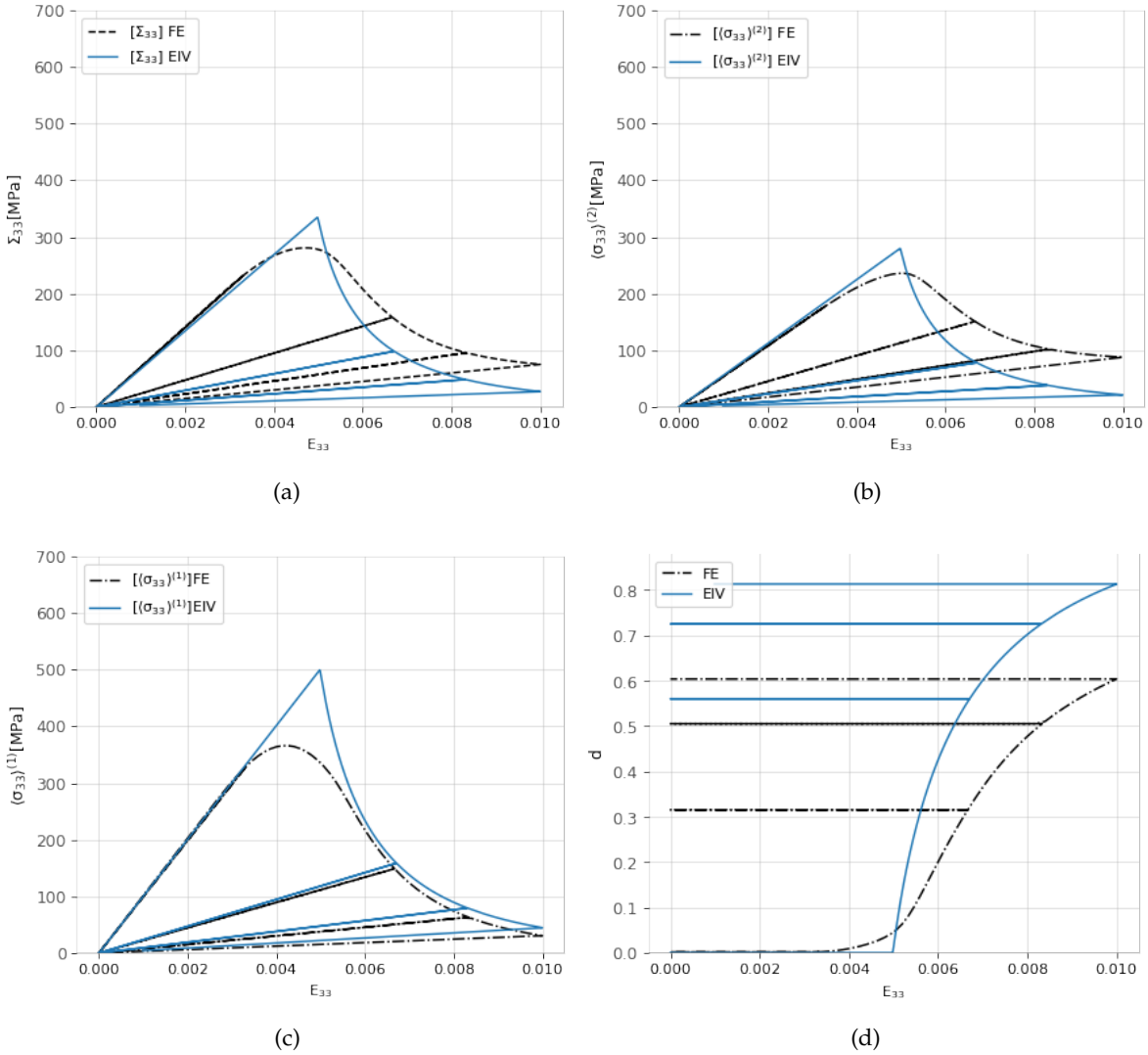

FIGURE 3.15: Elastically reinforced composite with an elasto-damageable matrix submitted to an isochoric macroscopic strain (3-cycle) for the AT1 model. (a) Macroscopic axial stress, (b) Average axial stress in the matrix, (c) Average axial stress in the inclusion, (d) Damage evolution

By looking at the evolution of the damage represented in Fig. 3.15d, we can see that the irreversibility condition is well taken into account in the formulation of the theoretical model. Also, at the first unloading, the level of damage in the homogenization model is about 0.5 as much as the level attained in FE simulations, which consequently affects the softening behavior of the matrix and therefore of the composite.

We examine now the case where a full cycle of macroscopic isochoric strain (3.14b) is applied. This complete cyclic loading allows us to quantify through full-field computations the importance of the unilateral effect on the response of the composite at the local and global levels. In the considered gradient damage model, the unilateral effects has be accounted for by following the proposal of [4] (see also appendix A). It notably consists in rewriting the free energy as in (1.37).

In the meantime, we test the performance of the homogenization model in its current version, that is without the nonlinearity induced by the unilateral effect (see the recent attempt of [99] in a less difficult context).

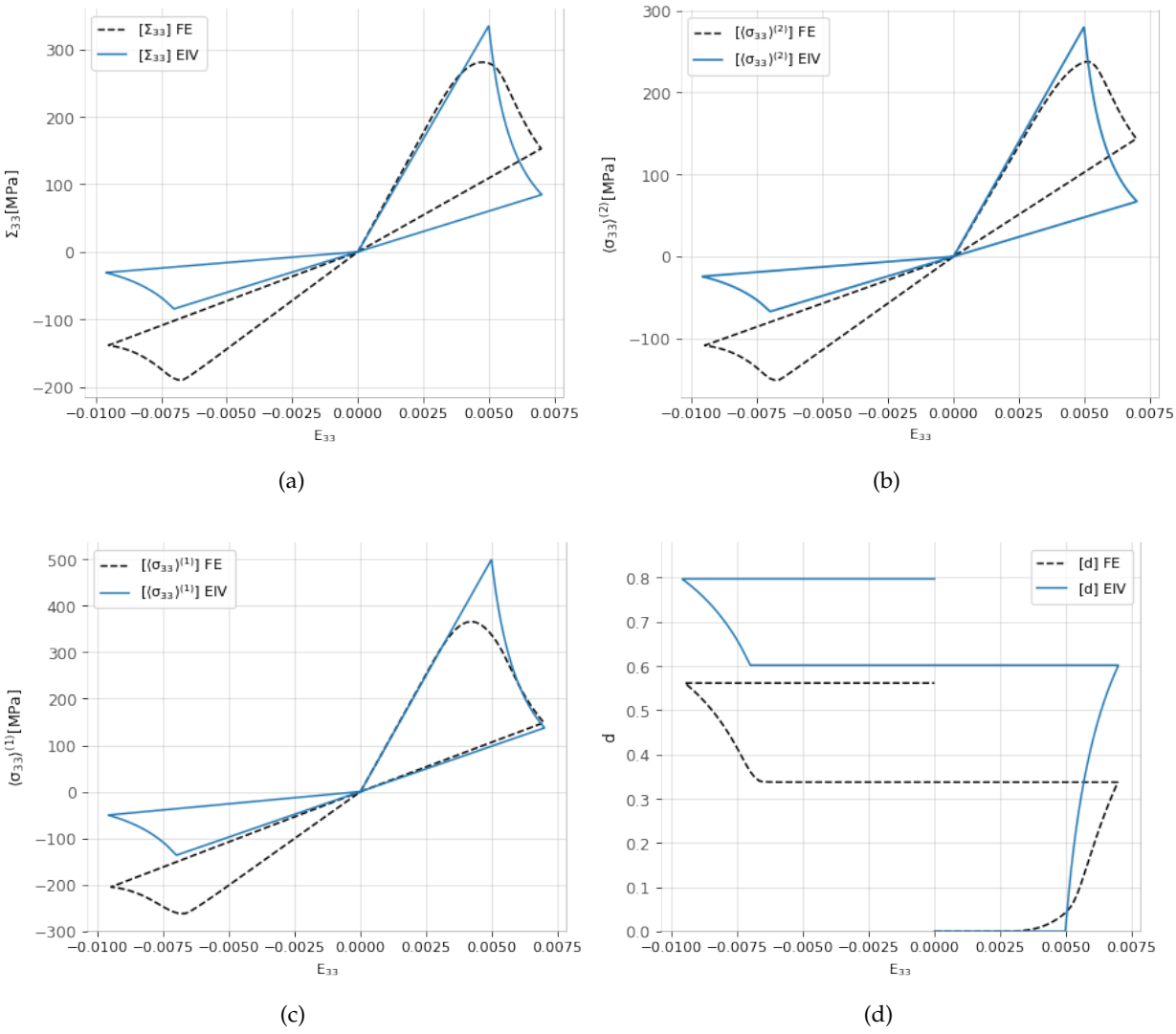

FIGURE 3.16: Elastically reinforced composite with an elasto-damageable matrix submitted to an isochoric macroscopic strain (full cycle) for the AT1 model. (a) Macroscopic axial stress, (b) Average axial stress in the matrix, (c) Average axial stress in the inclusion, (d) Damage evolution

In Fig. 3.16a, 3.16b, 3.16c representing the effective behavior of the composite and the average stress in the constituent, we obtain the same results for the positive macroscopic strains and a notable difference between FE computations and the homogenization model for the negative ones. As expected, in the results obtained by FE calculations, a partial recovery of the damage moduli is noted in the compression regime.

These results clearly show the need to improve the homogenization model by incorporating the unilateral effect description in the incremental variational approach setting. Clearly enough, this is a very difficult task.

3.5 Conclusion

The aim of this chapter was two-fold :

- to perform full-field simulations on nonlinear composites composed of an elastic damage matrix, that is composites with evolving damage
- to take advantage of the above-mentioned simulation in order to assess, at both macroscopic and constituents scales, predictions of the incremental variational approach that was developed in Chapter 2.

To this end, we conducted full-field simulations using the FEM based on variational gradient damage models which were briefly presented. This choice has been motivated by the pathological mesh sensitivity well-known for simulations carried out with local damage models. The resulting simulations allow us to avoid such mesh dependency and provide confidence in the numerical solutions obtained by an alternate minimization of a two-fields functional (see [19, 112]).
Following the first evaluation previously done in Chapter 2 for a hollow sphere made up of an elastic damageable matrix and subjected to a radial loading on its outer boundary, we compare the obtained numerical results to the close-form solution presented in Chapter 1. We observed that the damage yield stress occurs earlier in the FE computations than in the two other approaches. In the softening regime, some agreement is observed before notable differences appear for the highest level of damage.
Then, we focused on bi-phased composites composed of an elasto-damageable matrix reinforced by a linear elastic inclusion. This composite has been submitted to different loadings (monotonous and cyclic). Although the AT1 model implemented here is known for a rather rough softening behavior and considering the difference in the dissipation energy not being negligible, the qualitative agreement, for the composite mechanical response, between predictions of the proposed homogenization model and the results of the full-field simulations seems to be remarkable, even there is room for future improvement. The chapter ends with the application of cyclic loadings (a 3-cycle loading, and 1 full-cycle loading). The full-cycle loading ended up showing a relatively more important difference for the negative macroscopic strains. This is due to the fact that at the present stage of its development the homogenization model does not take into account the unilateral effect. Further future research efforts must be made in this direction, even if not trivial.
As a possible extension of the present version of the model, we will rather propose in the next chapter an Effective Internal Variable homogenization model that will include some hardening-like effects, primarily motivated by some phenomenological evidence.

Chapter 4

An extension of the EIV model accounting for hardening effects in damageable composites

Contents

In this chapter, we investigate the positive hardening effects which accompany damage growth in some composite materials. We begin in section 4.1 with some typical examples of such composites including ceramics matrix reinforced by fibers [42, 5, 23]. We then consider an extended form of the local damage law, following [87] in which the yield quantity $\mathcal{Y}_c$ is affine with the damage level. The mathematical structure of the resulting local damage model requires a slight modification of the previous Effective Internal Variable model that we discussed in section 4.2. Then, we implement this in the Effective Internal Variable setting delivering the macroscopic behavior of the composite materials with hardening.

4.1 Some physical evidences of hardening effects in brittle matrix composites

The very simple objective of this short section is to illustrate some aspects of the mechanical response of brittle matrix composites in order to motivate interest in the implementation of hardening-like phenomena in our previous modelings. We limit here ourselves to the response of this class of composites under cyclic tensile loadings. An example of damage mechanisms in a ceramic-fiber composite can be found in [8] (see Fig. 4.1). Although these mechanisms can generate some anelastic deformation (as will be seen more in the next figure), it is commonly recognized that the first stages of the degradation processes occur in the form of a matrix microcracking.

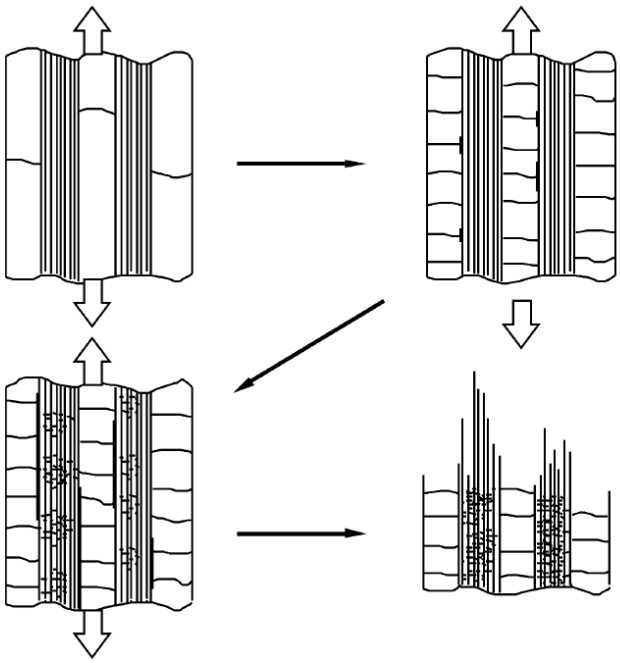

FIGURE 4.1: Damage mechanisms in ceramic-matrix composites [8]

For this class of composite materials, here a Sic-Sic-2D, a typical response under a tensile load applied in the fiber direction as shown in Fig. 4.2. This response corresponds to a hard-enable behavior together with a degradation of the elastic properties of the composite.

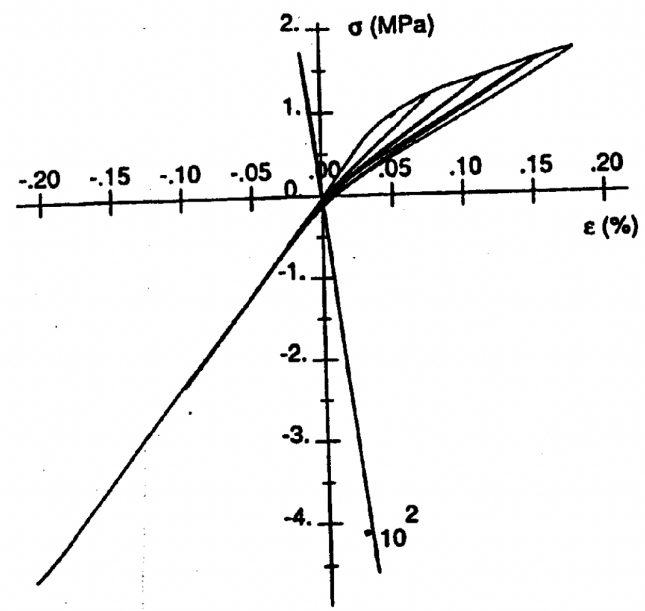

FIGURE 4.2: 0° tension-compression test [42]

For completeness, the response of the same composite to an off-axis loading (here at 45° with respect to the fiber direction) is shown in Fig. 4.3. The difference between the two responses illustrates the material anisotropy which is probably due to a combination of damage-induced anisotropy and that due to the presence of fiber.

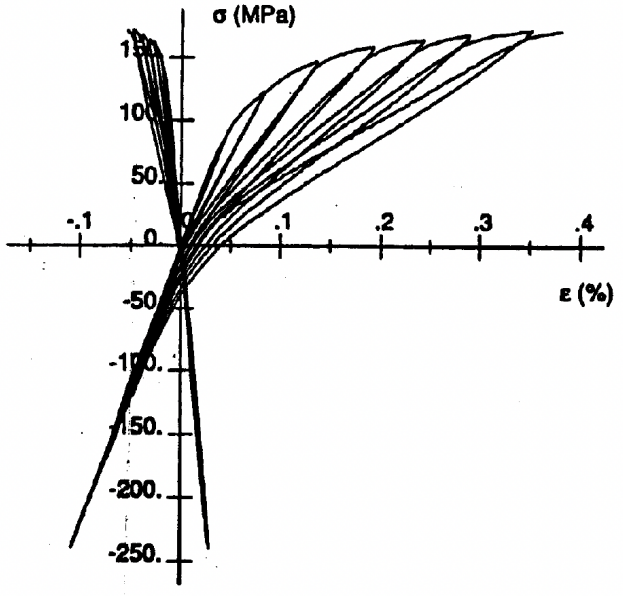

FIGURE 4.3: 45° tension-compression test [42]

Numerous models have been on this class of materials in the framework of Continuum Damage Mechanics, some of them being micromechanically inspired (see for instance [25], [85], etc.). Successful results have been gained by this type of models. However, in absence

of an upscaling procedure, these models are not able to quantitatively couple deformation mechanisms in the reinforcement and the damage in the matrix which is one of the objectives of nonlinear homogenization considered in the present study.
Finally, it must be emphasized in general that, even though the proposed Effective Internal Variable approach has been implemented for spherical reinforcements, there isn't any difficulty to apply it to fiber-reinforced materials.

4.2 Incremental variational principle in presence of hardening

This section is devoted to the adaptation of the Effective Internal Variable approach to the case where hardening is included in the damage model. We restrict ourselves to the main points, that need to be considered for the implementation of this extension.

4.2.1 Local behavior and effective response

The starting point to account for the hardening effects consists simply to consider for the damageable constituents in the composite a variation[1] of $\mathcal{Y}_c$ with d.

Local behavior

In this context, the dissipation potential for a phase r will now takes the following form:

$$\varphi^{(r)}\left(\dot{d};d\right) = \mathcal{Y}_c\left(d\right)\,\dot{d} \tag{4.1}$$

where again the resistance to damage $\mathcal{Y}_c\left(d\right)$ is no longer constant but rather an increasing function of d. Note that in the above writing, the presence of a comma is for recalling that $\dot{d}$ is the unique argument of $\varphi^{(r)}$ and that d serves as a state parameter (see for instance [44], [104]).

Model formulation

Due to the presence of the internal variable d in the dissipation potential, the context is similar to that faced by [83] in a very different context of elastoplasticity with nonlinear kinematics hardening and which requires a slight reformulation of the incremental variational principle that we considered before. With the help of the new form of the dissipation potential (4.1), the constitutive law reads now :

$$\boldsymbol{\sigma} = \frac{\partial w^{(r)}}{\partial \boldsymbol{\varepsilon}}(\boldsymbol{\varepsilon},d), \qquad \frac{\partial w^{(r)}}{\partial d}(\boldsymbol{\varepsilon},d) + \frac{\partial \varphi^{(r)}}{\partial \dot{d}}\left(\dot{d};d\right) = 0 \tag{4.2}$$

Applying the same discretization previously used, the equations (4.2) at time t_{n+1}, for an implicit Euler scheme, are rewritten as :

[1] With the necessary precaution, this is similar to the so-called $\mathcal{R}$-curve in Fracture mechanics see for instance [110]

$$\boldsymbol{\sigma} = \frac{\partial w^{(r)}}{\partial \boldsymbol{\varepsilon}}(\boldsymbol{\varepsilon}, d), \qquad \frac{\partial w^{(r)}}{\partial d}(\boldsymbol{\varepsilon}, d) + \frac{\partial \varphi^{(r)}}{\partial \dot{d}}\left(\frac{d - d_n}{\Delta t}; d\right) = 0 \tag{4.3}$$

Now let us consider the following variational problem :

$$w_\Delta(x, \boldsymbol{\varepsilon}) = \inf_d J(x, \boldsymbol{\varepsilon}, d) \tag{4.4}$$

where

$$\begin{cases} J(x, \boldsymbol{\varepsilon}, d) = \sum_{r=1}^{N} J^{(r)}(x, \boldsymbol{\varepsilon}, d)\chi^{(r)}(x) \quad \text{and:} \\ J^{(r)}(x, \boldsymbol{\varepsilon}, d) = w^{(r)}(\boldsymbol{\varepsilon}, d) + \Delta t \varphi^{(r)}\left(\frac{d - d_n}{\Delta t}; d_n\right) \end{cases} \tag{4.5}$$

in this case, the Euler-Lagrange equations providing the solution to the variational problem are the following :

$$\boldsymbol{\sigma} = \frac{\partial w^{(r)}}{\partial \boldsymbol{\varepsilon}}(\boldsymbol{\varepsilon}, d), \qquad \frac{\partial w^{(r)}}{\partial d}(\boldsymbol{\varepsilon}, d) + \frac{\partial \varphi^{(r)}}{\partial \dot{d}}\left(\frac{d - d_n}{\Delta t}; d_n\right) = 0 \tag{4.6}$$

We thus consider for the remainder of this chapter that the resolution of (4.3) will be approximated by that of equation (4.6).

As previously, the effective potential is defined as :

$$\tilde{w}_\Delta(\boldsymbol{E}) = \inf_{\boldsymbol{\varepsilon}/\langle\boldsymbol{\varepsilon}\rangle = E} \langle w_\Delta(\boldsymbol{\varepsilon})\rangle = \inf_{\boldsymbol{\varepsilon}/\langle\boldsymbol{\varepsilon}\rangle = E} \langle \inf_d J(\boldsymbol{\varepsilon}, d)\rangle \tag{4.7}$$

where w_Δ is defined by (4.4).

The macroscopic response of the composite, with $\boldsymbol{\Sigma} = \langle\boldsymbol{\sigma}\rangle$ follows then :

$$\boldsymbol{\Sigma} = \frac{\partial \tilde{w}_\Delta}{\partial \boldsymbol{E}}(\boldsymbol{E}) \tag{4.8}$$

4.2.2 Construction of the Effective Internal Variable approach for composites with hardenable phases

Linearization of the local behavior

Following what has been introduced above and in chapter 2, the incremental potential J is approximated by a linearized incremental potential J_0 chosen in the form:

$$\begin{cases} J_0(x,\boldsymbol{\varepsilon},d) \;=\; \displaystyle\sum_{r=1}^{N} J_0^{(r)}(\boldsymbol{\varepsilon},d)\chi^{(r)}(x) \\ J_0^{(r)} \;=\; \dfrac{1}{2}\,(1-d)^2\,\mathcal{A}_0^{(r)} \;+\; \dfrac{1}{2}\boldsymbol{\varepsilon} : \mathbb{C}_0^{(r)} : \boldsymbol{\varepsilon} \;+\; \mathcal{Y}_c(d_n)\,(d-d_n) \;+\; \Delta t\,\Psi_c\left(\dfrac{d\;-\;d_n}{\Delta t}\right) \end{cases} \tag{4.9}$$

where, as previously, $\mathcal{A}_0^{(r)}$ is a uniform per phase scalar and $\mathbb{C}_0^{(r)}$ is a fourth-order tensor having the symmetries of the elasticity tensor, also uniform per phase.
Following the idea in section 2.3.2 which consists in subtracting the potential J_0 from the potential J, *i.e.* $J = J_0 + J - J_0$, we replace the incremental potential by its expression in the variational formulation (4.7).

An upper bound on $\tilde{w}_\Delta$ can be obtained by taking a supremum condition of ΔJ with respect to $(\boldsymbol{\varepsilon}, d)$. As seen in chapter 2, the supremum condition can be replaced by a stationarity one. The following estimate of $\tilde{w}_\Delta$ is then obtained :

$$\tilde{w}_\Delta(E) \;\approx\; \underset{\mathcal{A}_0^{(r)},\mathbb{C}_0^{(r)}}{\operatorname{stat}} \left[\inf_{\boldsymbol{\varepsilon}/\langle\boldsymbol{\varepsilon}\rangle=E} \left(\inf_{d/\Psi_c(\dot{d})} \langle J_0(\boldsymbol{\varepsilon},d)\rangle \;+\; \underset{\boldsymbol{\varepsilon}^*,d^*}{\operatorname{stat}} \langle \Delta J(\boldsymbol{\varepsilon},d)\rangle \right) \right] \tag{4.10}$$

Stationary conditions

Following the steps introduced in chapter 2, we will first write the stationarity of ΔJ with respect to d^* and $\boldsymbol{\varepsilon}^*$ which will provide an expression for the parameters $\mathcal{A}_0^{(r)}$ and $\mathbb{C}_0^{(r)}$. The stationarity with respect to these parameters will then allow completing their expressions. Finally, the stationarity of J_0 with respect to d will provide an expression of the damage as a function of $\boldsymbol{\varepsilon}$.

1. Stationarity of ΔJ

The stationarity of $\Delta J = J - J_0$ with respect to $\boldsymbol{\varepsilon}^*$ and d^* respectively imply :

$$\begin{cases} \mathbb{C}_0^{(r)} \;=\; (1-d^*)^2\;\mathbb{C}_s^{(r)} & \text{(4.11a)} \\ \mathcal{A}_0^{(r)} \;=\; \boldsymbol{\varepsilon}^* : \mathbb{C}_s^{(r)} : \boldsymbol{\varepsilon}^* & \text{(4.11b)} \end{cases}$$

This shows that the two unknowns $\mathcal{A}_0^{(r)}$ and $\mathbb{C}_0^{(r)}$ remain unchanged and depend on the state variables $\boldsymbol{\varepsilon}^*$ and d^* which are yet to be determined.

2. Minimization of $J_0^{(r)}$

Moreover, it can be shown that the minimization of $J_0^{(r)}$ with respect to d leads to :

$$\frac{\partial}{\partial d}\left\{ \frac{1}{2}\,(1-d)^2\,\mathcal{A}_0^{(r)} \;+\; \frac{1}{2}\boldsymbol{\varepsilon} : \mathbb{C}_0^{(r)} : \boldsymbol{\varepsilon} \;+\; \mathcal{Y}_c\,(d_n)\,(d-d_n) \right\} \;=\; 0 \tag{4.12}$$

To take simultaneously account of damage yield and/or of hardening effects of damage, one can consider a generalized expression of the local dissipation function by considering $\mathcal{Y}_c(d_n)$ such as :

$$\mathcal{Y}_c(d_n) \;=\; \mathcal{Y}_c\left(\gamma \;+\; 2\,\eta\, d_n\right) \quad ; \quad 0 \leq [\gamma;\eta] < \infty \tag{4.13}$$

where γ and η are positive scalars, we note that η is the parameter controlling the hardening effect (further details will be given in section 4.3).

Using the expression of $\mathcal{Y}_c$ in (4.12), one gets the resulting optimal damage :

$$d_{opt}^{(r)} \;=\; 1 \;-\; \frac{\mathcal{Y}_c\left(\gamma + 2\,\eta\, d_n\right)}{\mathcal{A}_0^{(r)}} \tag{4.14}$$

which is uniform per phase.

The energy associated with the LCC is then written :

$$w_0^{(r)}(\boldsymbol{\varepsilon}) \;=\; \frac{1}{2}\left(1-d_{opt}^{(r)}\right)^2 \mathcal{A}_0^{(r)} \;+\; \frac{1}{2}\boldsymbol{\varepsilon} : \mathbb{C}_0^{(r)} : \boldsymbol{\varepsilon} \;+\; \mathcal{Y}_c\left(\gamma \;+\; 2\,\eta\, d_n\right)\left(d_{opt}^{(r)} - d_n\right) \tag{4.15}$$

The functional (4.10) can be written by applying the minimization condition with respect to $\boldsymbol{\varepsilon}$:

$$\tilde{w}_\Delta(E) \;\approx\; \underset{\mathcal{A}_0^{(r)},\mathbb{C}_0^{(r)}}{\text{stat}} \left[\tilde{w}_0(E) \;+\; \underset{\boldsymbol{\varepsilon}^*,d^*}{\text{stat}} \langle \Delta J(\boldsymbol{\varepsilon},d)\rangle\right] \tag{4.16}$$

where

$$\tilde{w}_0(E) \;=\; \inf_{\boldsymbol{\varepsilon}/\langle\boldsymbol{\varepsilon}\rangle = E} \langle w_0(\boldsymbol{\varepsilon})\rangle \tag{4.17}$$

and represents the effective energy of the LCC.
And finally, considering the upcoming optimality conditions, we will be able to determine the expressions of the remaining parameters $\mathcal{A}_0^{(r)}$ and $\mathbb{C}_0^{(r)}$.

3. Stationarity of $\left\langle J_0^{(r)} \;+\; \Delta J^{(r)}\right\rangle^{(r)}$

Optimality with respect to $\mathcal{A}_0^{(r)}$ and $\mathbb{C}_0^{(r)}$ allows to provide the link between $(\boldsymbol{\varepsilon}^*, d^*)$ and the variables $(\boldsymbol{\varepsilon}, d)$, which are similar as in (2.41) and (2.42). Taking into account hardening in the formulation of the proposed analytical model does not modify the definition of $\mathcal{A}_0^{(r)}$ which is expressed as in (2.43) by means of the second-order moment of the strain.

Using the expression of $\mathcal{A}_0^{(r)}$, the following form is obtained for (4.14)

$$\left(1-d_{opt}^{(r)}\right)\left\langle \boldsymbol{\varepsilon} : \mathbb{C}_s^{(r)} : \boldsymbol{\varepsilon}\right\rangle^{(r)} \;-\; \mathcal{Y}_c(d_n) \;=\; 0 \tag{4.18}$$

which provides :

$$d_{opt}^{(r)} = 1 - \frac{\mathcal{Y}_c(d_n)}{\left\langle \boldsymbol{\varepsilon} : \mathbb{C}_s^{(r)} : \boldsymbol{\varepsilon}\right\rangle^{(r)}} \tag{4.19}$$

Finally, carrying (4.14) into (4.11a), we obtain the expression of $\mathbb{C}_0^{(r)}$

$$\mathbb{C}_0^{(r)} = \left(1 - d_{opt}^{(r)}\right)^2 \mathbb{C}_s^{(r)} = \left(\frac{\mathcal{Y}_c \left(\gamma + 2\,\eta\, d_n\right)}{\left\langle \boldsymbol{\varepsilon} : \mathbb{C}_s^{(r)} : \boldsymbol{\varepsilon} \right\rangle^{(r)}} \right)^2 \mathbb{C}_s^{(r)} \tag{4.20}$$

which represents the moduli tensor of the Linear Comparison Composite (LCC) described by $w_0(\boldsymbol{\varepsilon})$ (4.15).

We consider now the case of a two-phase composite (N=2 being the number of phases) composed of an elasto-damageable matrix reinforced by elastic spherical particles.

The nonlinear problem is reduced to the solution of a two-function system of unknowns $\mathcal{A}_0^{(r)}$ and $\mathbb{C}_0^{(2)}$:

$$\begin{cases} F_1\left(\mathcal{A}_0^{(2)}, \mathbb{C}_0^{(2)}\right) = \mathcal{A}_0^{(2)} - \left\langle \boldsymbol{\varepsilon} : \mathbb{C}_s^{(2)} : \boldsymbol{\varepsilon} \right\rangle^{(2)} = 0 \\ F_2\left(\mathcal{A}_0^{(2)}, \mathbb{C}_0^{(2)}\right) = \mathbb{C}_0^{(2)} - \left(\dfrac{\mathcal{Y}_c \left(\gamma + 2\,\eta\, d_n\right)}{\left\langle \boldsymbol{\varepsilon} : \mathbb{C}_s^{(2)} : \boldsymbol{\varepsilon} \right\rangle^{(2)}} \right)^2 \mathbb{C}_s^{(2)} = 0 \end{cases} \tag{4.21}$$

The resolution of the system then allows to determine the damage and then the mechanical quantities of interest, locally and globally.

4.2.3 A first illustration of the homogenization model with hardening

In order to take into account the hardening due to the variation of the resistance to damage with the degradation level, we will consider $\gamma = 1$ and different values of parameter η : $\eta \in [3, 5]$. Note that $\gamma = 1$ together with $\eta = 0$ corresponds to the AT1 model already analyzed in chapter 3, while for completeness we also displayed the case $\gamma = 0$ together with $\eta = 1$ which corresponds to the so-called AT2 model that we will analyze in detail in the next section.
The material properties considered here are the ones introduced in (2.55). The composite is subjected to an isochoric macroscopic deformation.

In Fig.4.4, is represented the macroscopic response of the composite, the stress averages over the constitutive phases, as well as damage evolution within the matrix phase.

As previously seen, the AT1 model, is characterized by an elastic regime followed by a damage regime which induces a relatively rough softening behavior.

The model AT2, corresponding to the case $[\gamma = 0,\ \ \eta = 1]$, shows a damaging process that starts in the composites from the beginning of the loading, since as it is well-known, there is no elastic threshold for this model which applies to the matrix phase. For the composite, a

hardening regime is followed for a softening one which is also accompanied by an unloading of the inclusion constituent.

The model corresponding to $[\gamma = 1,\ \eta = 3]$ presents first an elastic regime followed by a hardening one which delays the instant of occurrence of a stress softening. This tendency is amplified in the case $[\gamma = 1,\ \eta = 5]$.

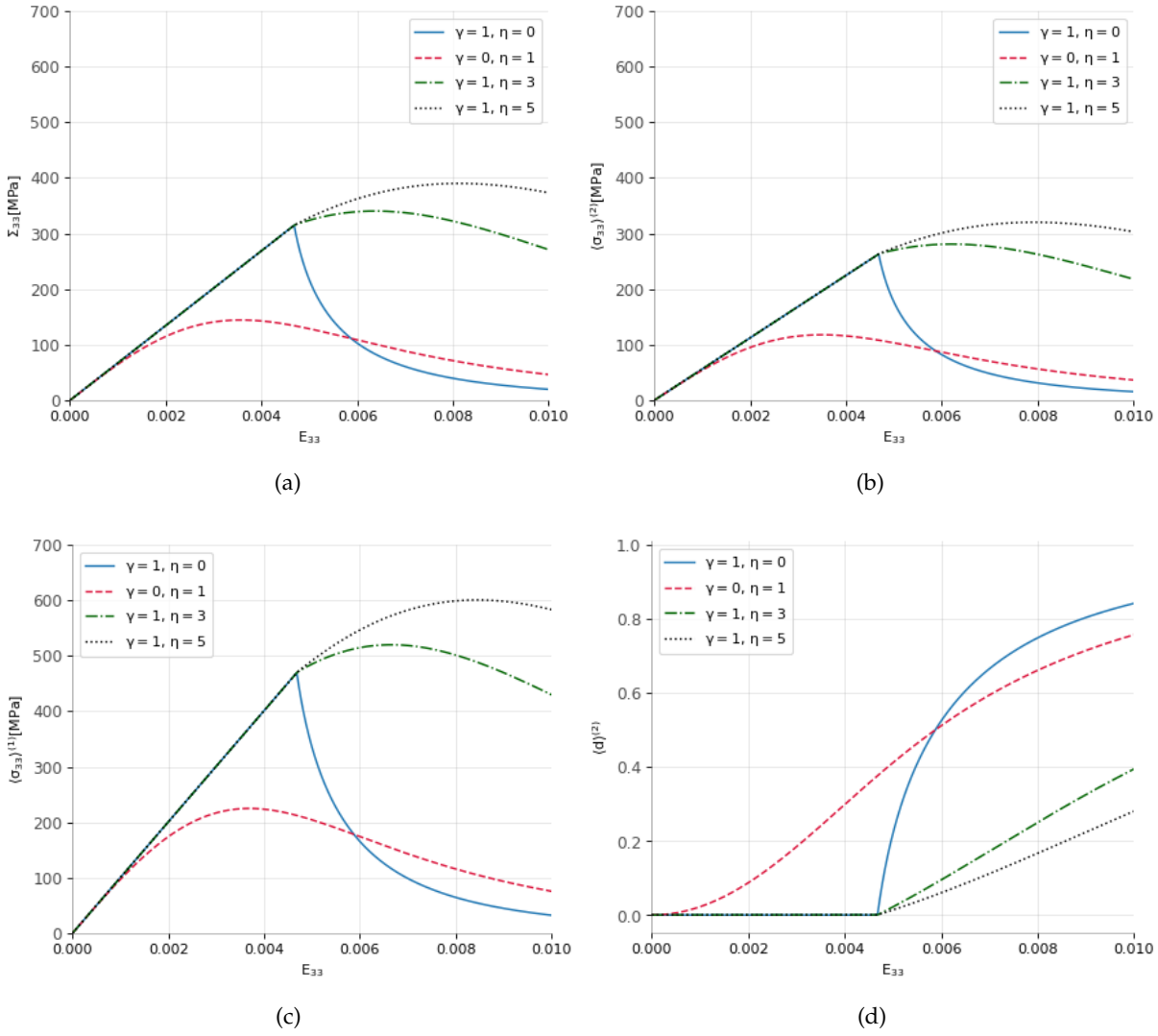

FIGURE 4.4: Elastically reinforced composite with an elasto-damageable matrix submitted to an isochoric macroscopic strain - illustration of the hardening effect, (a) Macroscopic axial stress, (b) Average axial stress in the matrix, (c) Average axial stress in the inclusion, (d) Damage evolution

To summarize, for the composite, the damage models with hardening of the matrix predict a macroscopic behavior that manifests the competition between a softening tendency due to damage growth and the hardening effect which takes its origin in the resistance to damage. In the next sections, we will assess these predictions by means of their comparison to full-field simulation results.

4.3 Gradient damage model accounting for hardening effects

Owing to the change introduced by the hardening term, the corresponding regularized energy functional has still the following form :

$$\mathcal{E}(u,d) = \int_\Omega \left(\frac{1}{2}(1-d)^2 \boldsymbol{\varepsilon}(u) : \mathbb{C}_s : \boldsymbol{\varepsilon}(u) \right) d\Omega + \frac{G_c}{l_0\, c_w} \int_\Omega \left(w(d) + l_0^2 \nabla d . \nabla d \right) d\Omega \tag{4.22}$$

The function w is continuously monotonic and is generally considered such that $w(0) = 0$; $w(1) = 1$ and $w(d \neq 0) > 0$. Finally, c_w is a normalization parameter defined by :

$$c_w \;=\; 4 \int_0^1 \sqrt{w(x)} dx \tag{4.23}$$

As previously introduced in the above-described framework, two specific models are generally considered: the so-called Ambrosio-Tortorelli models denoted by AT1 and AT2, and $w(d)$ amounts to d and d^2, respectively. Contrary to the AT1 model which exhibits a sudden fracture, the AT2 model predicts the occurrence of damage as soon as the loading takes place. Due to the limitations, these two models have shown, [65] proposed a more general expression of the local dissipation function as :

$$w(d) \;=\; \gamma d \,+\, \eta d^2 \tag{4.24}$$

which corresponds to a damage resistance

$$w'(d) \;=\; \gamma \,+\, 2\eta d \;;\; \begin{cases} \gamma = 1 \quad \text{and} \quad \eta = 0 \Longrightarrow \text{AT1} \\ \gamma = 0 \quad \text{and} \quad \eta = 1 \Longrightarrow \text{AT2} \end{cases} \tag{4.25}$$

In [135], the condition $w(d) = 1$ is considered and leads to the one-parameter function $w(d) = (1-\eta)d + \eta d^2$. In [65] that we followed here, such condition is not imposed, and it was established that the normalization parameter that corresponds to the AT-type model takes the following form :

$$\begin{aligned} c_w(\gamma,\eta) \;=\; \frac{1}{2\,\gamma^2\,\eta^{3/2}} \Bigg[& 2\,(\gamma+2\eta)\,\sqrt{\gamma+\eta}\,\left(-8\eta^{5/2} + \left(\gamma^2+8\eta^2\right)\sqrt{\eta}\right) \\ & - \gamma^4 \ln\left(\frac{\gamma + 2\left(\eta + \sqrt{\eta\,(\eta+\gamma)}\right)}{\gamma} \right) \Bigg] \end{aligned} \tag{4.26}$$

In the upcoming section, we will focus on two main models deriving from this approach. The first is commonly known as the AT2 model, its well-known particularity is the absence of a threshold since damage starts to evolve as soon as the material is loaded. The second one is more of a general AT-type model exhibiting a linear elastic regime up to a threshold, followed by an induced positive hardening preceding the softening behavior. For $\gamma = 1$, it can be seen as an AT1-like model with hardening.

4.4 Model evaluation without threshold : AT2

When it comes to the AT2 model, damage appears for any prescribed loading level as it has no damage threshold. For this model, the energy functional (4.22) takes classically the following form:

$$\mathcal{E}(u,d) = \int_\Omega \left(\frac{1}{2}(1-d)^2 \boldsymbol{\varepsilon} : \mathbb{C} : \boldsymbol{\varepsilon} + \underbrace{\frac{G_c}{c_w}}_{=2} l_0 \left(\underbrace{w(d)}_{=d^2} + l_0^2 \nabla d . \nabla d \right) \right) \tag{4.27}$$

With $\frac{Gc}{l_0\, c_w}$ being fixed by the damage threshold $\mathcal{Y}_c$ (see (2.55)), the internal length amounts to 1.03mm (with the inclusion's radius being roughly 2.2 times l_0).

4.4.1 Monotonous loadings

Isochoric macroscopic strain

For the evaluation of the nonlinear homogenization model predictions in the case of no threshold, the studied composite is submitted once again to a macroscopic isochoric strain introduced in (3.14). Fig. 4.5 represents the macroscopic response of the composite, the evolution of the stress averages in the matrix as well as in the inclusion, and finally the evolution of the average damage in the matrix (see eq.(2.37)). Again, though it might not be clear, damage appears from the very first stages of the loading, for this particular model.

Here as well, we observe a qualitative reproduction of the model with a notable difference in the start of the softening behavior and the remainder of it. Although the AT2 model is known to exhibit more diffuse damage in the matrix, we still observe a difference between the two approaches, but the qualitative tendency is similar.
From Fig. 4.5d, which concerns the damage calculated from the second-order moment, it can be seen that yet again the model underestimates the numerical simulations results.

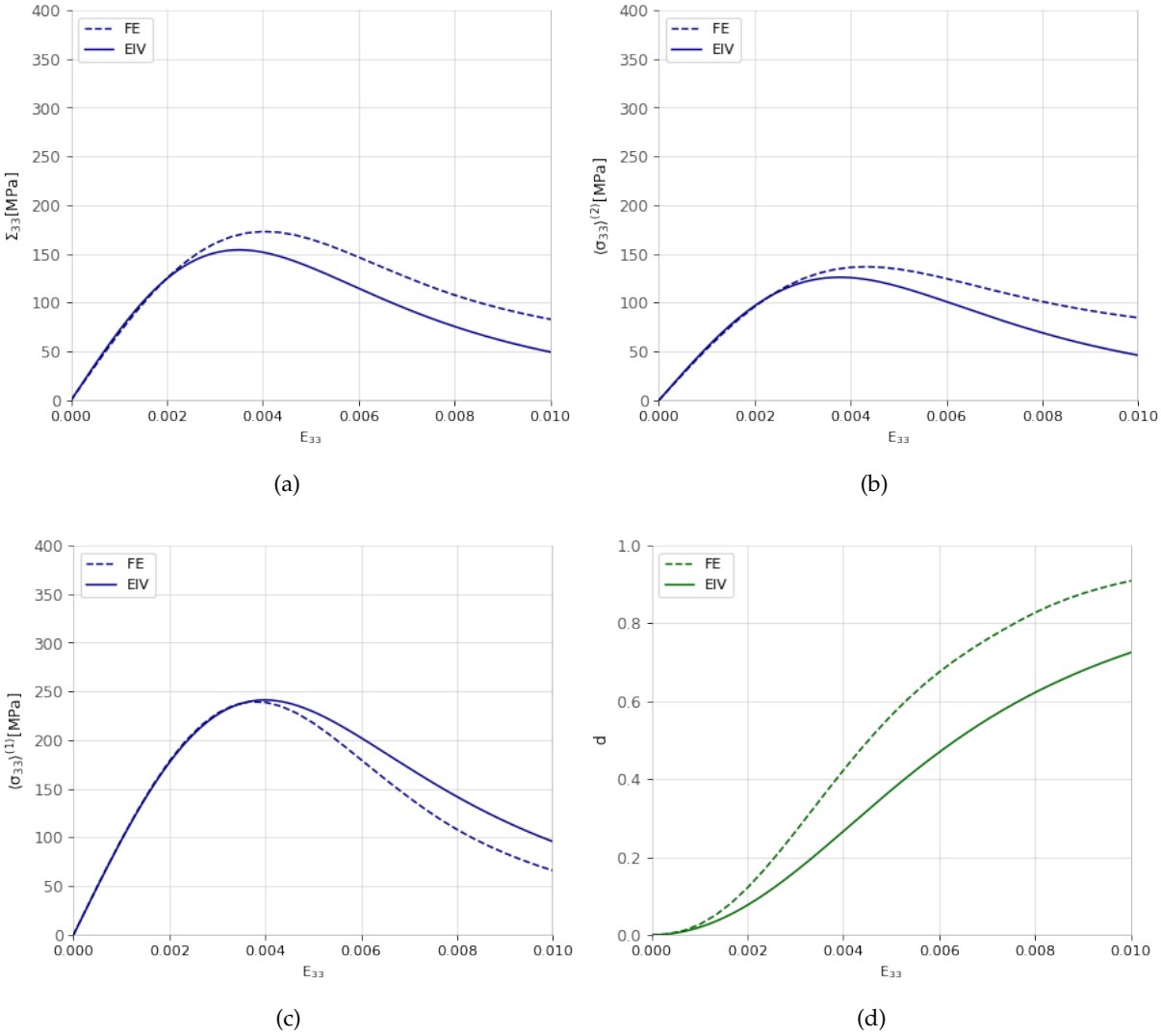

FIGURE 4.5: Elastically reinforced composite with an elasto-damageable matrix submitted to an isochoric macroscopic strain for the AT2 model. (a) Macroscopic axial stress, (b) Average axial stress in the matrix, (c) Average axial stress in the inclusion, (d) Damage evolution

Also, by examining Fig. 4.6, it can be seen that the actual damage pattern is set from the beginning of the loading. Compared to the AT1 model, d reaches here the value 1 for a higher level of macroscopic strain.

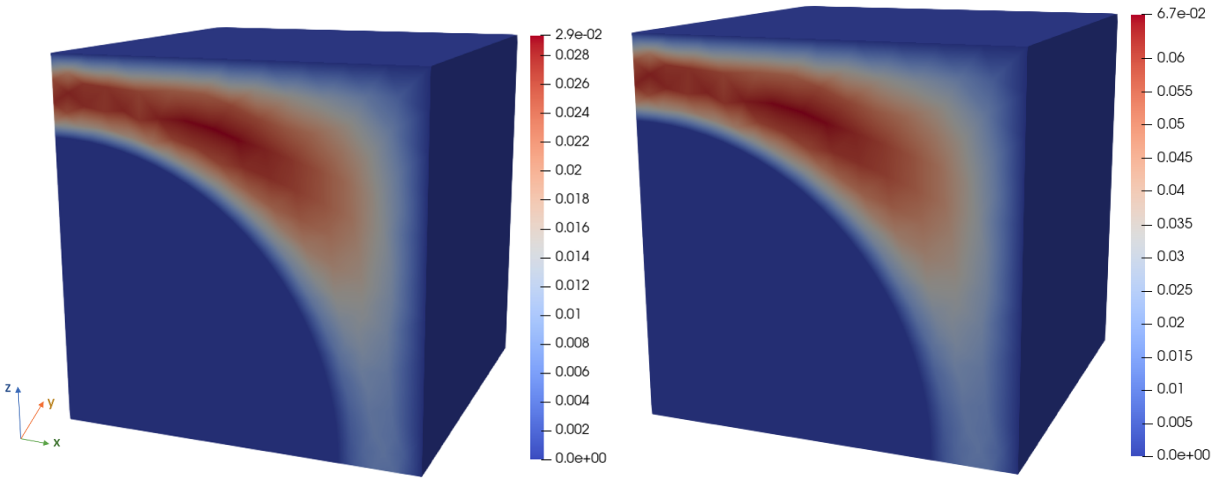

(a) $E_{33} = 0.0026$ (b) $E_{33} = 0.004$

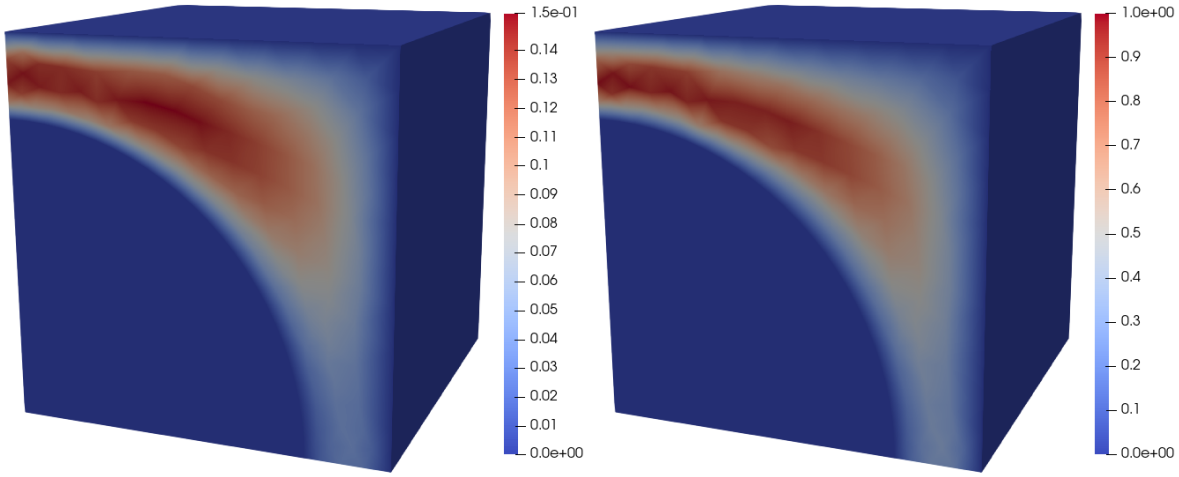

(c) $E_{33} = 0.006$ (d) $E_{33} = 0.01$

FIGURE 4.6: Damage evolution for the AT2 model at three different loading levels, each corresponding to (a) first regime, (b) maximum stress level, (c) softening regime, (d) $d(x) = 1$ locally attained

When it comes to the fluctuations represented in Fig. 4.7a, a rather good agreement is observed until $E_{33} = 0.004$, which marks the beginning of the softening regime. From this point on, the theoretical model predicts the drop of the fluctuations whereas, in the FEM simulations, the fluctuations keep on increasing.

As a way of gaining more clarification on the fluctuations' evolution, following what was previously illustrated, we put forth the evolution of the constitutive terms presented in (2.16). As it can be seen in Fig. 4.7a below, there is a rather good agreement between the homogenization model and the FEM simulations at the beginning of the loading. And although both terms decrease in the two approaches, the difference between the two terms is relatively steady in the theoretical approach beyond the peak stress whereas, in the numerical simulations, the difference actually increases with the loading. The fluctuations thus increase regardless of the development of damage within the matrix phase.

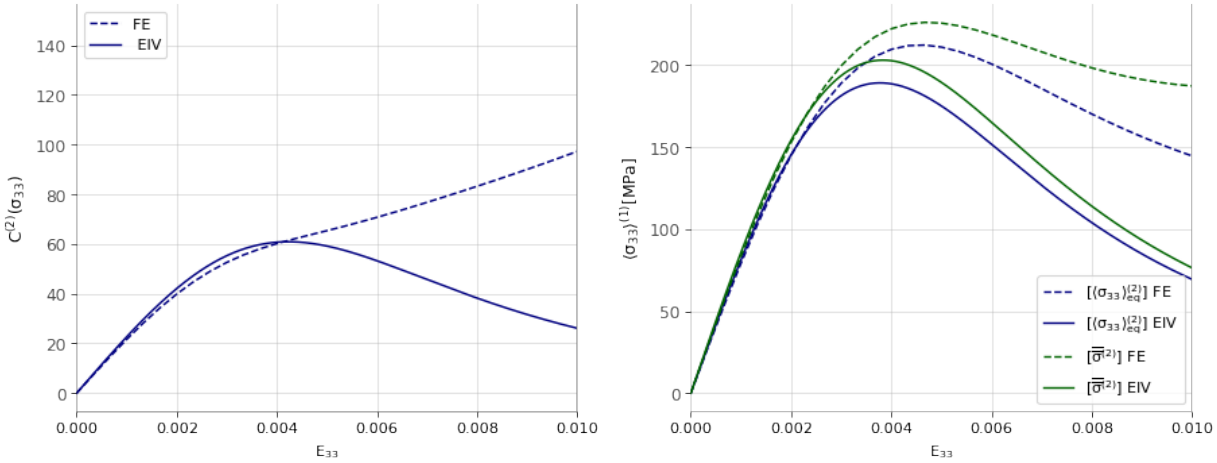

(a) (b)

FIGURE 4.7: Elastically reinforced composite with an elasto-damageable matrix submitted to an isochoric macroscopic strain for the AT2 model. (a) Stress fluctuations in the matrix, (b) Evolution of the fluctuations' constitutive terms

Finally, in Fig. 4.8 are represented the distributions of the dissipated energy and its different components (as depicted in (3.15)) at the end of the simulation. We observe that the distribution of the regularized term takes over as it reaches higher values that are concentrated in the interface between the inclusion and the matrix.
However, if we look at the evolution of these terms, it can be seen that this time around, the regularized term takes over here as well, it takes values much higher than the local part and is almost similar to the total dissipated energy. This constitutes a rather important difference from the model we have implemented where the dissipation potential is local.

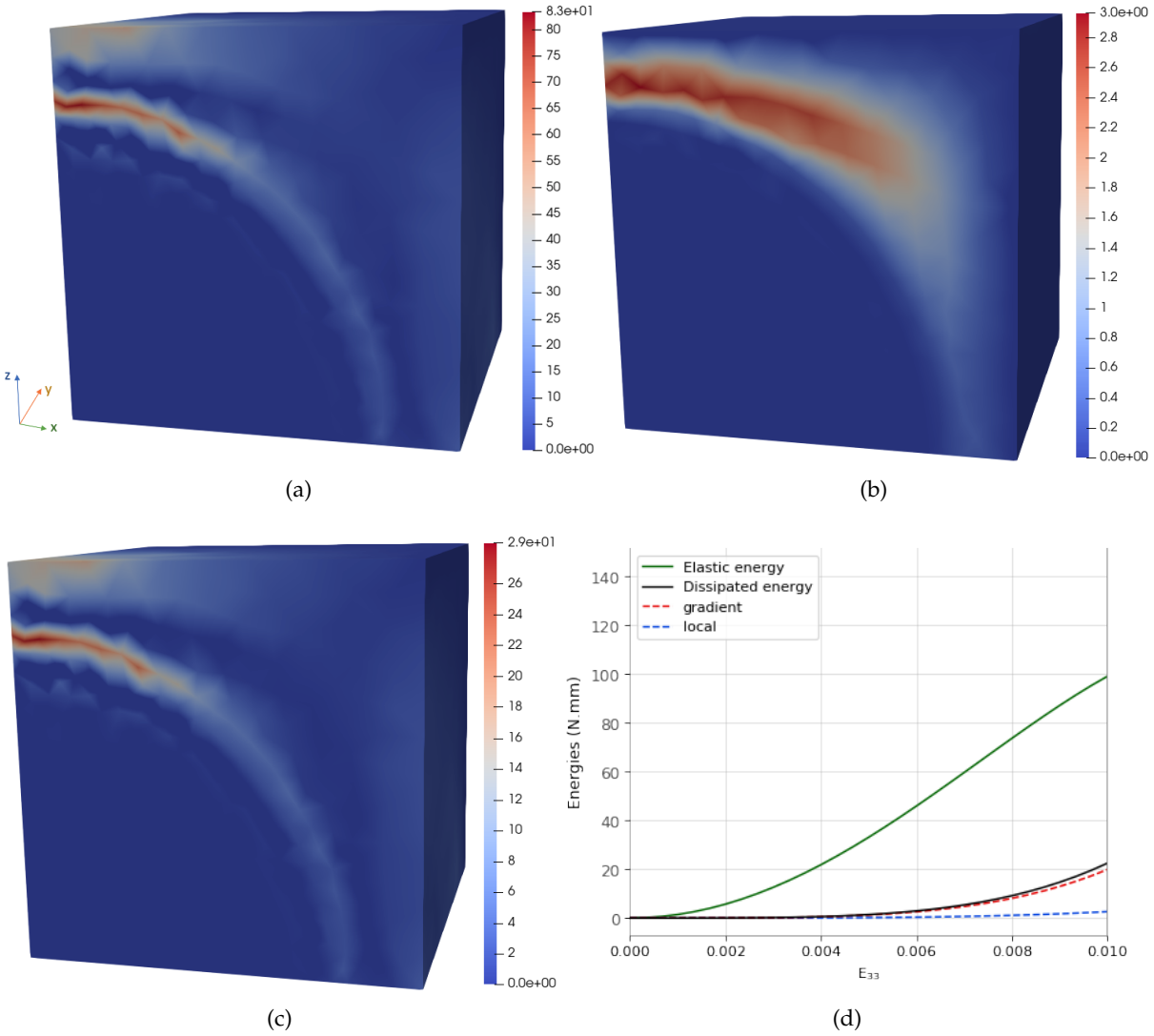

FIGURE 4.8: Elastically reinforced composite with an elasto-damageable matrix submitted to an isochoric macroscopic strain for the AT2 model. (a) Dissipated energy distribution, (b) Local term of the dissipated energy distribution, (c) Regularized term of the dissipated energy distribution, (d) Elastic energy, dissipated energy and its constitutive terms' evolution

4.4.2 Cyclic Loading

We will now explore the predictions of the AT2-based formulation when the composite is subjected to multi-cycle loading. The applied loading is the one already presented in Fig. 3.14a for the same material parameters (2.55).

Fig. 4.9 illustrates the variations of the macroscopic axial stress, phase-averaged stresses, and damage evolution[2]. The predictions of the proposed formulation are compared with FE data from the same cubic unit cell presented earlier. These evolutions are reproduced in a qualitative way by the developed homogenization model. Due to the difference observed in

[2]Reminder : we represent, exclusively for the cyclic loadings, the direct average of the damage field within the matrix

the softening behavior, the unloadings are not carried out according to the same slope in the two approaches.

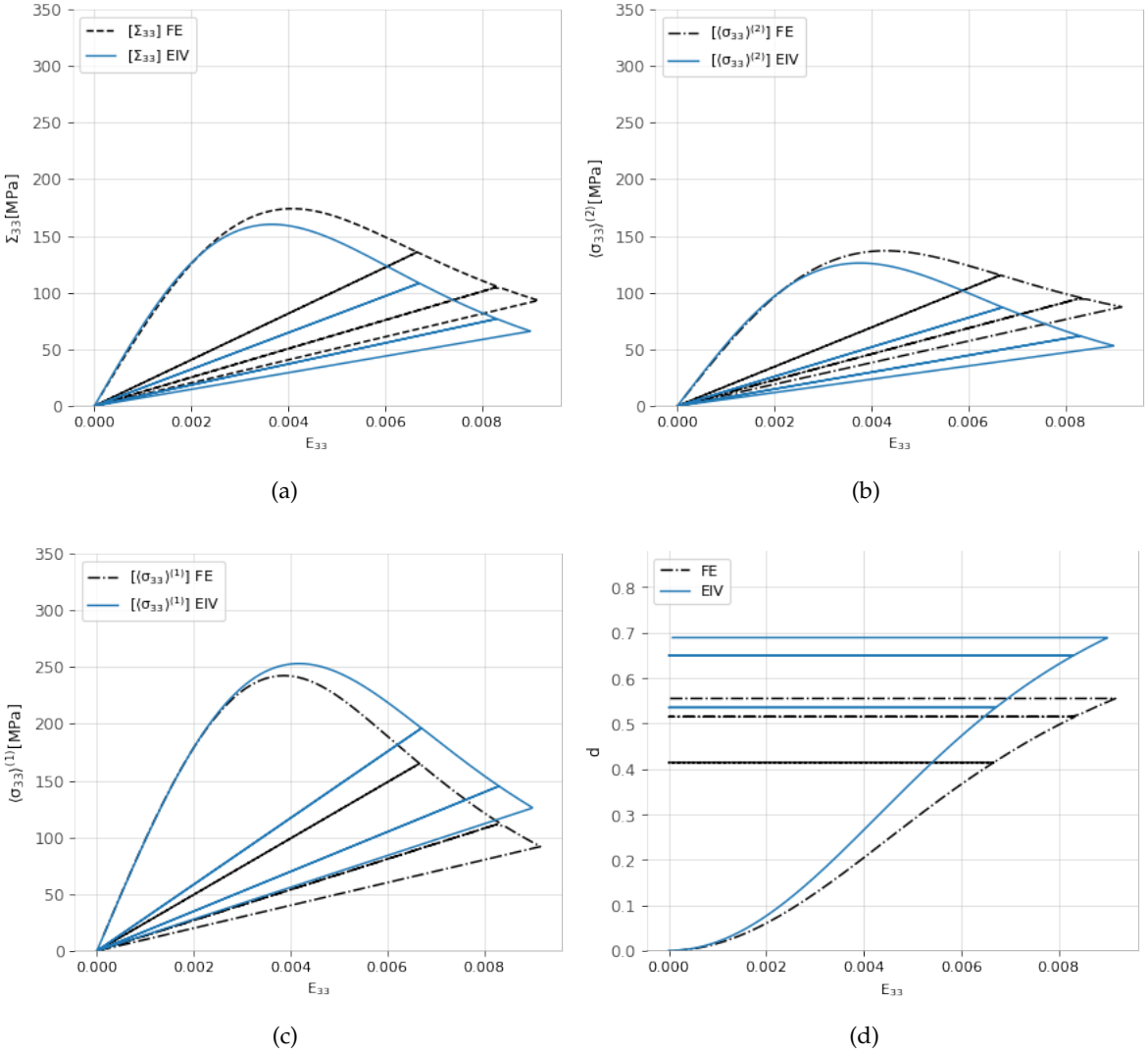

FIGURE 4.9: Elastically reinforced composite with an elasto-damageable matrix submitted to an isochoric macroscopic strain (3-cycle) for the AT2 model. (a) Macroscopic axial stress, (b) Average axial stress in the matrix, (c) Average axial stress in the inclusion, (d) Damage evolution

When applying a full loading cycle as shown in Fig. 3.14b, we note similar conclusions to those of the model with threshold presented in section 3.4.3. These results are not plotted here. Again, improvement of the modeling will require account for unilateral effect.

4.5 Evaluation of the extended AT1 model with hardening

In the models seen so far, although one is with damage threshold and the second without, softening behavior is still important. We propose here to consider $\gamma = 1$, allowing to preserve the elastic regime, and $\eta = 5$, this last one being the parameter driving the strain

hardening.
For this current model, the energy (4.22) is defined as : $w(d) = \left(\gamma\, d + 2\,\eta\, d^2\right)$ and c_w is defined using relation (4.26). With $\dfrac{Gc}{l_0\, c_w}$ being fixed by the elastic threshold, the internal length amounts to 0.39mm.

4.5.1 Monotonous loadings

Isochoric macroscopic strain

The composite is subjected to a macroscopic isochoric deformation, and we consider the same material properties as before (see 2.55). The predictions of the homogenization model with hardening are assessed by comparing them to the data from the FE calculations.

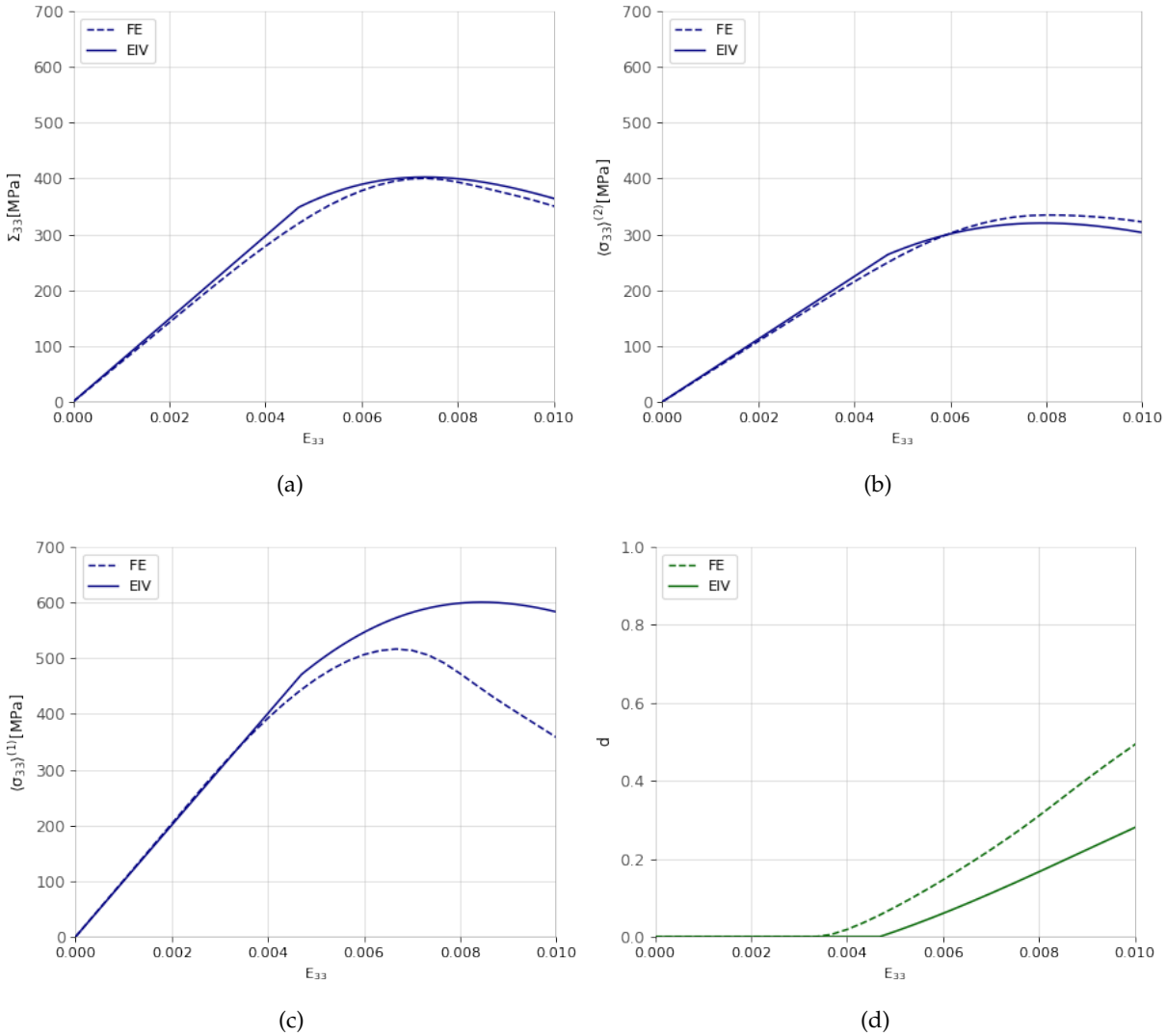

FIGURE 4.10: Elastically reinforced composite with an elasto-damageable matrix submitted to an isochoric macroscopic strain for the AT1-extended model. (a) Macroscopic axial stress, (b) Average axial stress in the matrix, (c) Average axial stress in the inclusion, (d) Damage evolution

We see on the macroscopic behavior and at the matrix level that the softening effects are very limited by the hardening contribution. The softening regime in the composite is indeed delayed to a higher level of stress with in addition a possible gain in ductility and a higher stress level.

This results in a better agreement between the homogenization model and the full-field simulations for the composite and in the matrix with a still notable difference in the inclusion. The evolution of damage is also relatively closer, remembering that for the damage, the same formula (4.14) involves the second-order moment of the strain field. It can be seen in Fig. 4.10d that the level of damage is significantly lower than the level attained in the AT1 model. This is a result of diffuse character of the damage field when taking into account the positive hardening.

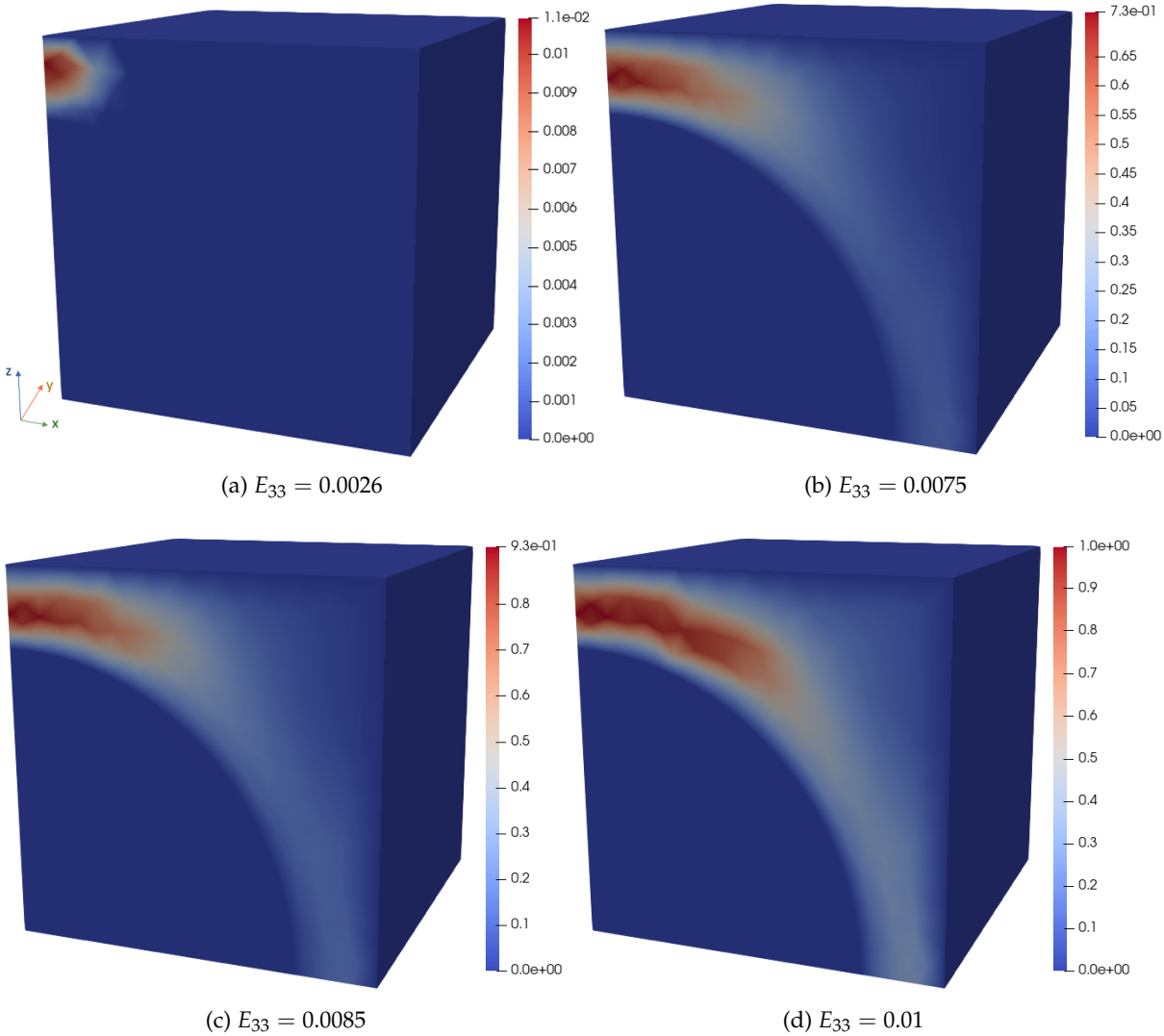

(a) $E_{33} = 0.0026$ (b) $E_{33} = 0.0075$

(c) $E_{33} = 0.0085$ (d) $E_{33} = 0.01$

FIGURE 4.11: Damage evolution for the AT1-extended model at four different loading levels, each corresponding to (a) damage appearance, (b) maximum stress level, (c) softening regime, (d) $d(x) = 1$ locally attained

If we look at the localization patterns, we see here that the damage evolves in a progressive and more diffuse way in the matrix, this can be more clearly seen when compared to damage evolution for the AT1 model as seen in Fig.3.7d. This makes the theoretical model more relevant.

Hereafter, Fig. 4.12 represents the fluctuations and the evolution of their two components. Regarding the fluctuations, we have a better agreement between the homogenization model and the numerical results than previously. The evolution of both terms in the two approaches seems to be more consistent. Moreover, the difference between $\left(\overline{\overline{\boldsymbol{\sigma}_d}}^{(2)}\right)$ and $\left(\overline{\boldsymbol{\sigma}_d}^{(2)}\right)_{eq}$ are relatively closer compared to the other models.

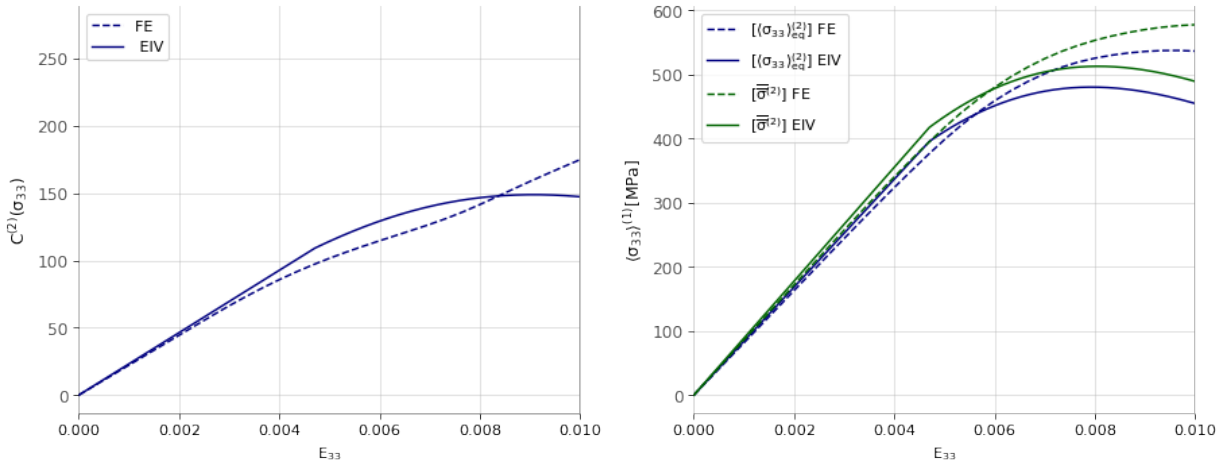

(a) (b)

FIGURE 4.12: Elastically reinforced composite with an elasto-damageable matrix submitted to an isochoric macroscopic strain for the AT1-extended model. (a) Stress fluctuations in the matrix, (b) Evolution of the fluctuations' constitutive terms

Moving forward with the distributions of the dissipated energy and the two terms composing it, it can be seen that the highest levels attained in both Fig. 4.13b and Fig. 4.13c are around the same magnitude. Also, in, Fig. 4.13d where we represent evolutions of the different energies, it is observed that $\mathcal{E}_{f-\text{local}}(d)$ and $\mathcal{E}_{f-\text{gradient}}(d)$ are not of the same order, the local term of the dissipated energy is higher than the regularized part, which aligns well with the homogenization model.

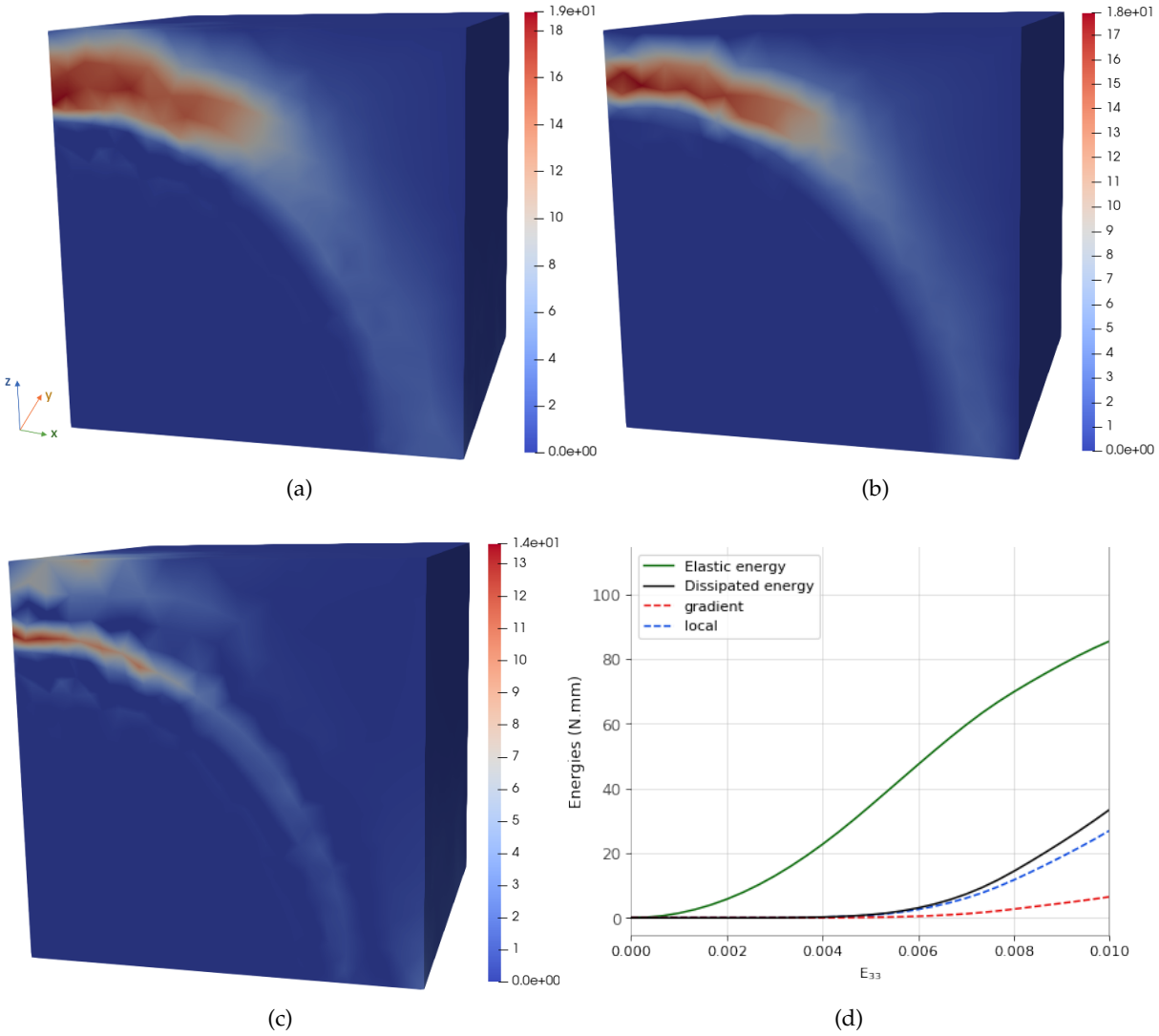

FIGURE 4.13: Elastically reinforced composite with an elasto-damageable matrix submitted to an isochoric macroscopic strain for the AT1-extended model. (a) Dissipated energy distribution, (b) Local term of the dissipated energy distribution, (c) Regularized term of the dissipated energy distribution, (d) Elastic energy, dissipated energy and its constitutive terms' evolution

4.5.2 Cyclic Loading

We will now investigate the response of the model with strain hardening when the composite is subjected to multi-cycle loading. The applied loading is the one presented in Fig.3.15a for the same material parameters (see 2.55).

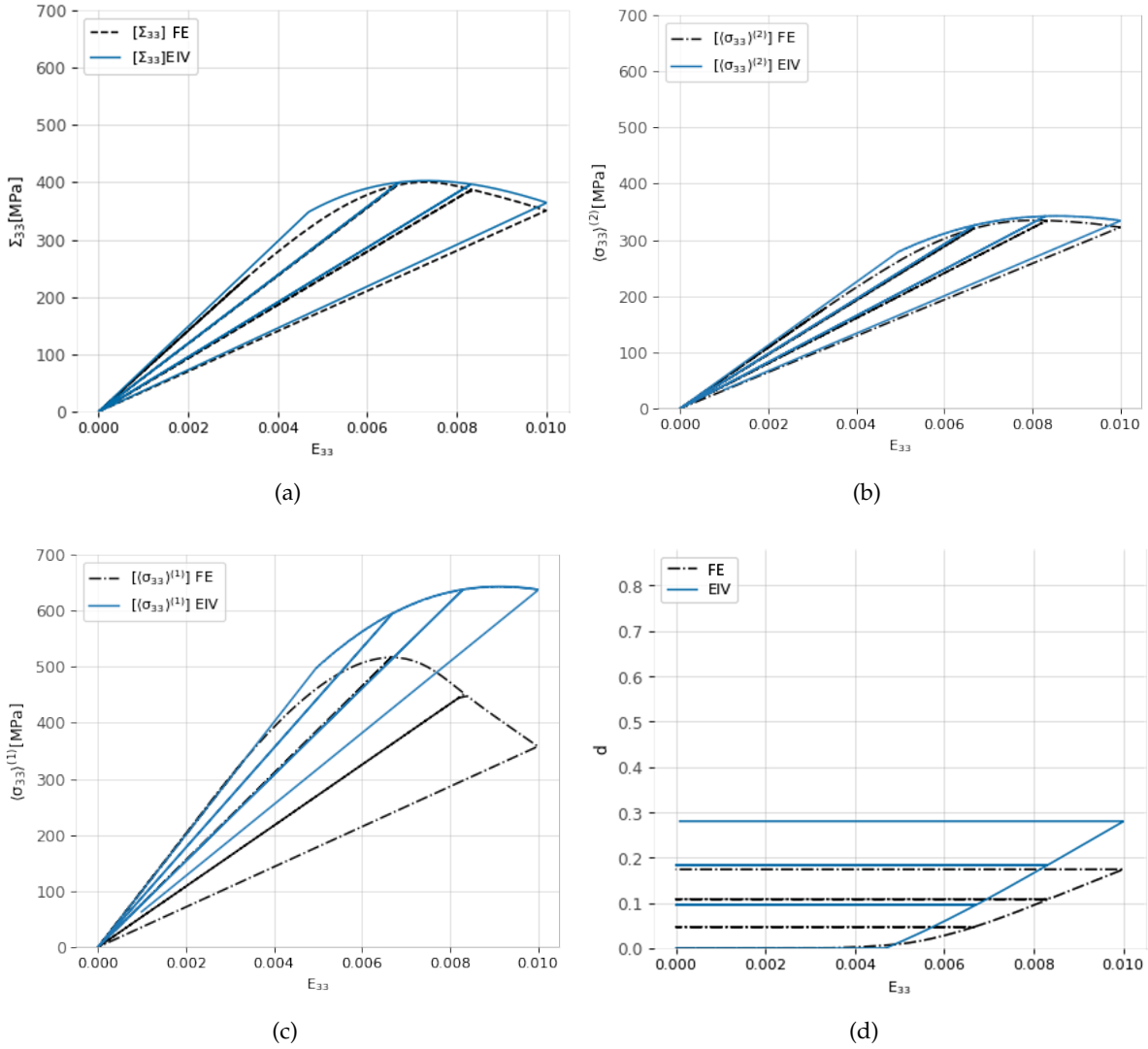

FIGURE 4.14: Elastically reinforced composite with an elasto-damageable matrix submitted to an isochoric macroscopic strain (3-cycle) for the AT1-extended model. (a) Macroscopic axial stress, (b) Average axial stress in the matrix, (c) Average axial stress in the inclusion, (d) Damage evolution

Fig. 4.14 illustrates the variations of the macroscopic axial stress, phase-averaged stresses, and damage evolution. The predictions of the proposed formulation are compared with FE data from the same cubic unit cell presented earlier. The evolutions obtained through the two approaches at the global composite level and at the local matrix level are in good agreement, with however a difference at the inclusion level.

And finally, we apply a full loading cycle as shown in Fig. 3.16a. We can see that for this model the slope of the second load obtained with the theoretical model, although different, is considerably closer to that obtained with the FE calculation. In fact, the level of damage and softening being limited by the introduction of the positive strain hardening, the lack of consideration of the unilateral effect in the formulation of the model does not lead to a

difference as important as previously.

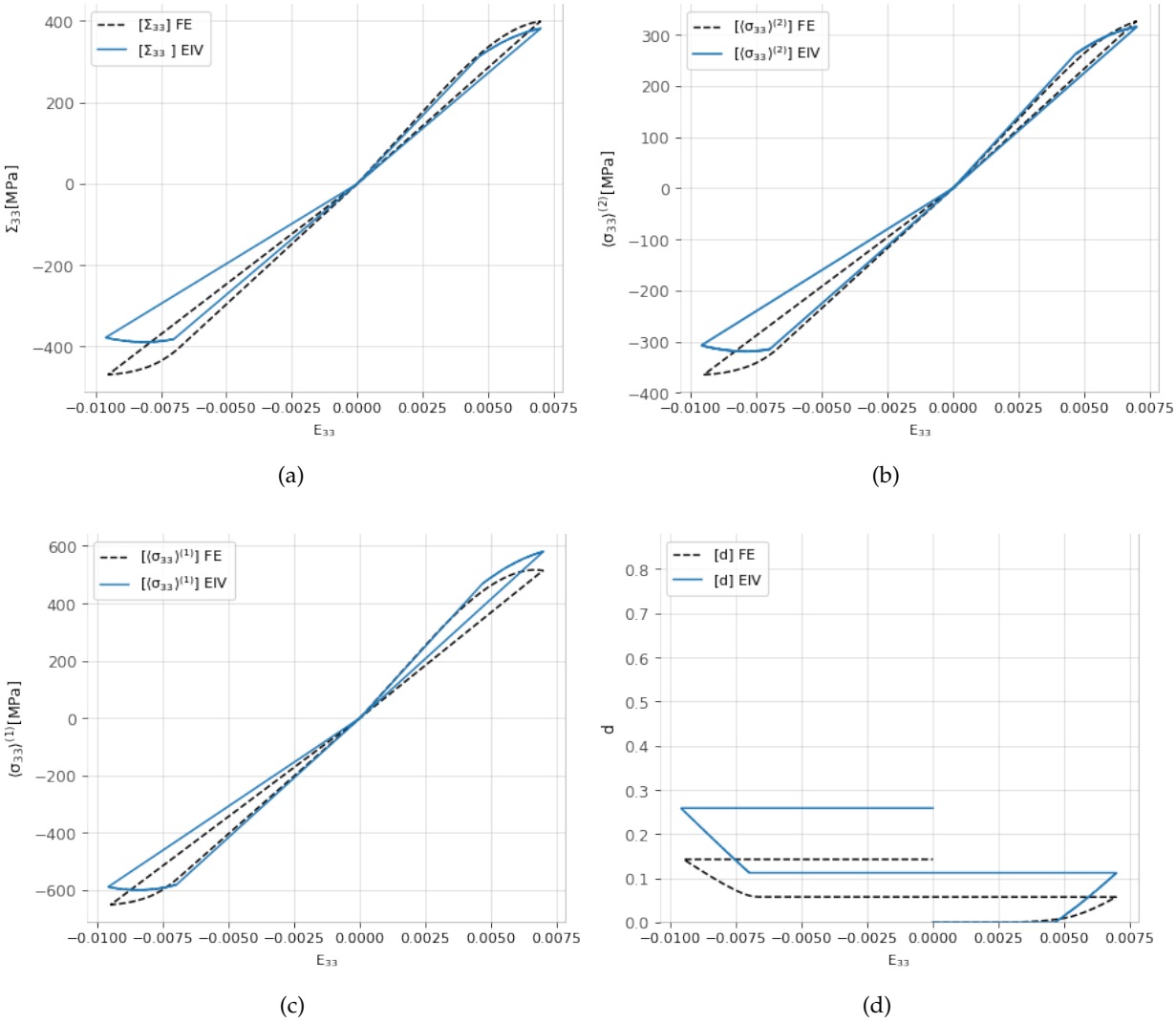

FIGURE 4.15: Elastically reinforced composite with an elasto-damageable matrix submitted to an isochoric macroscopic strain (full cycle) for the AT1-extended model. (a) Macroscopic axial stress, (b) Average axial stress in the matrix, (c) Average axial stress in the inclusion, (d) Damage evolution

4.6 Conclusion

This chapter was dedicated to an extension of the EIV model presented in chapter 2 by the incorporating a positive hardening accompanying the damage processes. We first recall some typical examples of the behavior of ceramics matrix reinforced by fibers and for which this kind of response is observed. And we proceed to a modification of the Effective Internal Variable formulation in order to include an affine variation of the yield energy with the damage variable. A first evaluation was made upon the no-threshold model, widely known

as the AT2 model, for a bi-phased composite made up of an elasto-damageable matrix reinforced by a linear elastic inclusion. This composite was submitted to monotonous and cyclic loadings. Although the AT2 exhibits relatively more diffuse damage when compared to the AT1 model, the damage gradient term of the dissipated energy remains significantly higher than its local counterpart, making the difference between the two formulations non-negligible. Despite this observed difference in the dissipated energy, the homogenization model was able to reproduce qualitatively the FE simulation results at both scales.
This was followed up with the evaluation of the developed model in a case extending the AT1 model for which we find a linear elastic regime preceding a hardening phase. This is followed by the occurrence of softening behavior. For this case, the theoretical model shows a good agreement with the full-field simulations at the global level of the composite and local level of the matrix, but it overestimates the response in the inclusion.

Conclusions and perspectives

As a general picture, the objective of this thesis consisted in developing for elasto-damageable composites a non-linear homogenization method through an extension of the Effective Internal Variable (EIV) method initially introduced by Lahellec and Suquet [75]. The latter allows to take into account the coupled effect of elasticity and dissipation induced by the damage process. In this framework, starting from the Generalized Standard description of the constitutive laws, an incremental potential J is first built thanks to the variational principle proposed by [109]. This allows taking advantage of the homogenization variational procedure of Ponte-Castañeda [116] for nonlinear material described by a single potential. Following the EIV method, it was possible to proceed simultaneously in the same step to the linearization of the local behavior as well as the uniformization of intraphase heterogeneity This has been done through the proposal of a simple linearized incremental potential J_0 as an approximation to J. This approximation has allowed the introduction of an LCC with per-phase uniform parameters. Finally, the macroscopic behavior has been established through the application of linear homogenization tools based on a Hashin-Shrikhman bound. The nonlinear homogenization elasto-damage model for composites, established in the framework of this thesis, has been assessed through a comparison of its predictions with a closed-form solution and more importantly with results obtained from appropriate full fields simulations. Finally, it has been extended by the incorporation of hardening effects related to the variation of the resistance to damage.

In detail, and following the different chapters :

- At the outset, this thesis started with a recall of some elements of classical continuum thermodynamics of irreversible processes and of the formulation of standard dissipative constitutive laws in the framework of Generalized Standard Materials (GSM). In this context, the nonlinear behavior of the constitutive phases is entirely determined by means of two potentials, namely the free energy and the dissipation potential. A standard local isotropic damage law has been presented using this classical procedure which couples elasticity and dissipation induced by the damage process.
  This preliminary step of the thesis was the occasion to present closed-form solutions of mechanical fields (including damage one) in a hollow sphere composed of an elastic damageable material subjected to radial loadings as in [30]. These simple solutions

constituted will serve as a basis for a first assessment of the theoretical model introduced further.

- The main objective being the development of a nonlinear homogenization method for an elasto-damageable composite, as recalled before, and consistently with the GSM framework and the associated incremental variational principle, we presented an extension of the EIV approach to the case of elasto-damageable constitutive behavior of the composite's phases. This was followed by a description of its numerical implementation. The procedure followed consisted in introducing a linearized incremental potential J_0 in order to approximate the local incremental potential J, the first being easily homogenized with the use of standard linear homogenization schemes and the difference between these two terms can be estimated via semi-analytical estimates, as shown in detail. We then proceed to the numerical implementation of the homogenization model, which was followed up with a first illustration for a composite composed of an elasto-damageable matrix reinforced by a linear elastic inclusion. It was observed that despite the elastic nature of the inclusion, it exhibited a decrease in the average stress with respect to the macroscopic strain which actually appears to be a consequence of the matrix softening. A first preliminary assessment of the homogenization model is found in the confrontation of its prediction to closed-form solutions presented for the hollow sphere subjected to radial macroscopic loading. The agreement between the two models was found to be reasonably satisfactory in both regimes. For completeness and in order to show the versatility of the proposed modeling approach, we also investigated the case of a damage law based on a different degradation function that does not exhibit softening.

- As also already mentioned, full-field simulations have been conducted, thanks to the FE method and phase-field approaches. Considering pathological limitations of the numerical use of local damage models (in particular mesh sensitivity shown through a first few series of simulations), we relied then throughout the whole study on gradient damage models for elasto-damageable constituents of the considered composites. These gradient damage models are now well recognized for their strong capability to describe damage growth and its transition to quasi-brittle failure (see for instance [19], [82], [93], etc..). The first step of validation by using full-field simulations concerned the closed-form solution presented for the damageable hollow sphere subjected to radial loading on its outer boundary. It has been noted that the damage yield stress takes place earlier in the full-field simulations, but the overall agreement is reasonably good in the non-negligible part of the softening behavior. This has been followed by the study of bi-phased composites consisting of an elasto-damageable matrix reinforced by a linear elastic inclusion. A classical first choice was the AT1 model which is known for its rough softening behavior. And despite the fundamental difference in the formulation of the gradient damage model and the considered model, the homogenization

model showed a remarkable qualitative agreement with the full-field computations predictions. However, we consider that there is still room for improvement. We also considered cyclic loadings where the full-cycle allows to show some limitations of the current stage of development of the homogenization model which does not account for unilateral effects which occur under "compressive-like" loading.

- Finally, an extension was made in order to take into account a positive hardening accompanying the damage process. To this end, we have adapted the above EIV formulation by slightly revisiting the incremental variational principle. Consideration of the hardening has allowed extending the predictive capability of the homogenization model and to limit or even delay the occurrence of softening in the composite. In this case, a more diffuse progressive evolution of the damage in the matrix has been observed in the full-field calculations. This resulted in a better agreement between the homogenization model and the FE calculations.

Work perspectives

Though some progresses have been made by establishing an appropriate framework for the nonlinear homogenization of the considered composites and have allowed to already achieve remarkably good results, the present thesis calls for future research efforts on several points among which the following ones.

- A short-term perspective consists of the consideration of bi-phased composites whose both phases are affected by the damage. This will only require a few modifications in the algorithm for the solution to the homogenization problem.
- An important aspect of the full-field simulations that can be also handled without difficulties lies in the consideration of a representative volume element with multiple inclusions, as it has been done by [43] in a context similar to that studied here. This will probably be more representative of the microstructures of some engineering composite materials.
- We have already started to explore the possibility to implement other linearization procedure which can allow to go beyond the simple one that was proposed in the thesis and to improve it. This could be an opportunity to test out if it is possible to obtain heterogeneous per-phase damage.
  In the same vein, another aspect on which we already started some developments for elasto-damageable composites concerns the derivation of a Double Incremental Variational method as proposed by [84] in the context of elasto(visco)plastic composites in the case of elasto-damageable composites. This has the advantage of separately proceeding with the linearization of the local behavior and the uniformization of the intraphase heterogeneities.

- Taking advantage of the framework established in this work and of previous studies on the EIV method (see for instance [75] or a previous thesis of [83] in our research team, it will be possible in a mid-term perspective to take into account coupling between elasto-damage phenomena and other dissipative behavior such as viscoelasticity or elasto(visco)plasticity.

- The present version of the homogenization model does not account for unilateral effects during the damage process. Owing to their importance for cyclic loadings of the composites, new developments in this direction will be required, probably by implementing some regularization/smoothing of the nonlinearity induced by the multimodular behavior in presence of unilateral effects (see for instance [99].)

- The important question of stability of the established homogenization models must deserve attention in future research works, surely by taking advantage of available studies in the field of quasi-brittle damage [114], [9, 7], etc...) and/or to explore mathematical properties of the condensed incremental potential which is of quasi-hyperelastic nature. This could be essential for the study of structures made up of the type of composites considered in this thesis.

- Owing to the difficulty to homogenize composites with nonlocal constituents[3], one can refer for local damage models to energy relaxation methods proposed as described in [50], [101] or [102].

[3]Mention has to be made of the interesting attempt by [43] to establish an upper bound of the composite by directly exploiting for the composite the two-field approach of [19].

Bibliography

[1] Farid Abed-Meraim and Quoc-Son Nguyen. "A quasi-static stability analysis for Biot's equation and standard dissipative systems". In: *European Journal of Mechanics-A/Solids* 26.3 (2007), pp. 383–393.

[2] M. Agoras, R. Avazmohammadi, and P. Ponte Castañeda. "Incremental variational procedure for elasto-viscoplastic composites and application to polymer- and metal-matrix composites reinforced by spheroidal elastic particles". In: *International Journal of Solids and Structures* (2016), 97-98:668–68.

[3] L. Ambrosio and V.M. Tortorelli. "Approximation of functional depending on jumps by elliptic functional via t-convergence". In: *Communications on Pure and Applied Mathematics* 43.8 (1990), pp. 999–1036.

[4] H. Amor, J.J. Marigo, and C. Maurini. "Regularized formulation of the variational brittle fracture with unilateral contact: Numerical experiments". In: *Journal of the Mechanics and Physics of Solids* 57.8 (2009), pp. 1209–1229.

[5] X. Aubard. "Modelisation et identification du comportement mecanique des materiaux composites 2D SiC-SiC". PhD thesis. Paris, 1992.

[6] S. Balay, S. Abhyankar, M.F. Adams, J. Brown, P. Brune, K. Buschelman, L. Dalcin, V. Eijkhout, W.D. Gropp, D. Kaushik, D. Karpeyev, M. Knepley, K. Rupp L. Curfman McInnes, B. Smith, H. Zhang, and S. Zampini. "PETSc users manual (Tech. Rep. ANL-95/11-Revision 3.7)". In: *Argonne National Laboratory* (2016).

[7] A.A.L. Baldelli and C. Maurini. "Numerical bifurcation and stability analysis of variational gradient-damage models for phase-field fracture". In: *Journal of the Mechanics and Physics of Solids* 152 (2021), p. 104424.

[8] S. Baste. "Inelastic behaviour of ceramic-matrix composites". In: *Composites Science and Technology* 61.15 (2001), pp. 2285–2297.

[9] A. Benallal and J.J. Marigo. "Bifurcation and stability issues in gradient theories with softening". In: *Modelling and Simulation in Materials Science and Engineering* 15.1 (2006), S283.

[10] M. Berveiller and A. Zaoui. "An extension of the self-consistent scheme to plastically flowing polycrystals". In: (1979).

[11] N. Bilger, F. Auslender, M. Bornert, and R. Masson. "New bounds and estimates for porous media with rigid perfectly plastic matrix". In: *Comptes Rendus Mécanique* 330.2 (2002), pp. 127–132.

[12] N. Bilger, F. Auslender, M. Bornert, H. Moulinec, and A. Zaoui. "Bounds and estimates for the effective yield surface of porous media with a uniform or a nonuniform

distribution of voids". In: *European Journal of Mechanics-A/Solids* 26.5 (2007), pp. 810–836.

[13] M.A. Biot. *Mechanics of incremental deformations*. 1965.

[14] M.A. Biot. *Variational principles in heat transfer: a unified Lagrangian analysis of dissipative phenomena*. Tech. rep. BIOT (MA) NEW YORK, 1970.

[15] J. Bleyer. "Applications of conic programming in non-smooth mechanics". In: *Journal of Optimization Theory and Applications* (2022), pp. 1–33.

[16] J. Bleyer and R. Alessi. "Phase-field modeling of anisotropic brittle fracture including several damage mechanisms". In: *Computer Methods in Applied Mechanics and Engineering* 336 (2018), pp. 213–236.

[17] M. Bornert. "Morphologie microstructurale et comportement mécanique; caractérisations expérimentales, approches par bornes et estimations autocohérentes généralisées." PhD thesis. École Nationale des Ponts et Chaussées, 1996.

[18] J. Boudet, F. Auslender, M. Bornert, and Y. Lapusta. "An incremental variational formulation for the prediction of the effective work-hardening behavior and field statistics of elasto-(visco) plastic composites". In: *International Journal of Solids and Structures* 83 (2016), pp. 90–113.

[19] B. Bourdin, G.A. Francfort, and J.J. Marigo. "Numerical experiments in revisited brittle fracture." In: *Journal of the Mechanics and Physics of Solids* 48 (2000), pp. 797–826.

[20] L. Brassart, L. Stainier, I. Doghri, and L. Delannay. "Homogenization of elasto-(visco) plastic composites based on an incremental variational principle". In: *International Journal of Plasticity* 36 (2012), pp. 86–112.

[21] L. Brassart, L. Stainier, I. Doghri, and L. Delannay. "A variational formulation for the incremental homogenization of elasto-plastic composites." In: *Journal of the Mechanics and Physics of Solids* 59 (2011), pp. 2455–2475.

[22] J.L. Chaboche. "Damage induced anisotropy: on the difficulties associated with the active/passive unilateral condition". In: *International Journal of Damage Mechanics* 1.2 (1992), pp. 148–171.

[23] J.L. Chaboche, S. Kruch, J.F. Maire, and T. Pottier. "Towards a micromechanics based inelastic and damage modeling of composites". In: *International Journal of Plasticity* 17.4 (2001), pp. 411–439.

[24] J.L. Chaboche, P.M. Lesne, and J.F. Maire. "Continuum damage mechanics, anisotropy and damage deactivation for brittle materials like concrete and ceramic composites". In: *International Journal of Damage Mechanics* 4.1 (1995), pp. 5–22.

[25] J.L. Chaboche and J.F. Maire. "A new micromechanics based CDM model and its application to CMC's". In: *Aerospace Science and Technology* 6 (2002), pp. 131–145.

[26] F. Chen, J. Sanahuja, B. Bary, and Y. Le Pape. "Effects of internal swelling on residual elasticity of a quasi-brittle material through a composite sphere model". In: *International Journal of Mechanical Sciences* 229 (2022), p. 107390.

[27] F. Cormery and H. Welemane. "A critical review of some damage models with unilateral effect". In: *Mechanics Research Communications* 29.5 (2002), pp. 391–395.

[28] F. Cormery and H. Welemane. "A stress-based macroscopic approach for microcracks unilateral effect". In: *Computational materials science* 47.3 (2010), pp. 727–738.

[29] A. Curnier, Q.C He, and P. Zysset. "Conewise linear elastic materials". In: *Journal of Elasticity* 37 (1994), pp. 1–38.

[30] L. Dormieux and D. Kondo. "Exact solutions for an elastic damageable hollow sphere subjected to isotropic mechanical loadings". In: *International Journal of Mechanical Sciences* 90 (2015), pp. 25–32.

[31] L. Dormieux and D. Kondo. *Micromechanics of fracture and damage*. John Wiley & Sons, 2016.

[32] A. Dragon and D. Halm. "Modélisation de l'endommagement par mésofissuration: comportement unilatéral et anisotropie induite". In: *Comptes rendus de l'Académie des sciences. Série II, Mécanique, physique, chimie, astronomie* 322.4 (1996), pp. 275–282.

[33] A. Ehrlacher and B. Fedelich. "Stability and bifurcation of simple dissipative systems; application to brutal damage". In: *Cracking and Damage: Strain localization and size effect* (1989), pp. 217–227.

[34] A. Ehrtacher. "Contribution à l'étude thermodynamique de la progression de fissure et à la mécanique de l'endommagement brutal". PhD thesis. Université de Paris VI, 1985.

[35] J. D. Eshelby. "The determination of the elastic field of an ellipsoidal inclusion, and related problems." In: *Proceedings of the Royal Society A* 437 (1957), pp. 311–327.

[36] F. Fantoni, A. Bacigalupo, M. Paggi, and J. Reinoso. "A phase field approach for damage propagation in periodic microstructured materials". In: *International Journal of Fracture* 223 (2020), pp. 53–76.

[37] P. Farrell and C. Maurini. "Linear and nonlinear solvers for variational phase-field models of brittle fracture". In: *International Journal for Numerical Methods in Engineering* 109.5 (2017), pp. 648–667.

[38] F. Feyel. "Multiscale FE2 elastoviscoplastic analysis of composite structures". In: *Computational Materials Science* 16.1 (1999), pp. 344–354.

[39] J. Florez-Lopez, A. Benallal, G. Geymonat, and R. Billardon. "A two-field finite element formulation for elasticity coupled to damage". In: *Computer methods in applied mechanics and engineering* 114.3-4 (1994), pp. 193–212.

[40] G.A. Francfort and J.J. Marigo. "Stable damage evolution in a brittle continuous medium". In: *European Journal of mechanics series a solids* 12 (1993), pp. 149–149.

[41] M. Frémond and B. Nedjar. "Damage, gradient of damage and principle of virtual power". In: *International journal of solids and structures* 33.8 (1996), pp. 1083–1103.

[42] A. Gasser, P. Ladevèze, and M. Poss. "Damage mechanisms of a woven sicsic composite: Modelling and identification". In: *Composites science and technology* 56.7 (1996), pp. 779–784.

[43] V. Gauthier. "Modélisation de l'endommagement dans les milieux hétérogènes élastiques fragiles". PhD thesis. Aix-Marseille, 2021.

[44] P. Germain, P. Suquet, and Q.S. Nguyen. "Continuum thermodynamics". In: *ASME Journal of Applied Mechanics* 50 (1983), pp. 1010–1020.

[45] C. Geuzaine and J.-F. Remacle. "Gmsh: a three-dimensional finite element mesh generator with built-in pre- and post-processing facilities." In: *International Journal for Numerical Methods in Engineering* 79(11) (2009), pp. 1309–1331.

[46] P. Gilormini. "Insuffisance de l'extension classique du modèle auto-cohérent au comportement non linéaire". In: *Comptes Rendus de l'Académie des Sciences. Paris (Série IIb)* 320 (1995), pp. 115–122.

[47] C. Goidescu, H. Welemane, C. Garnier, M. Fazzini, R. Brault, E. Péronnet, and S. Mistou. "Damage investigation in CFRP composites using full-field measurement techniques: Combination of digital image stereo-correlation, infrared thermography and X-ray tomography". In: *Composites Part B: Engineering* 48 (2013), pp. 95–105.

[48] C. Goidescu, H. Welemane, O. Pantalé, M. Karama, and D. Kondo. "Anisotropic unilateral damage with initial orthotropy: A micromechanics-based approach". In: *International Journal of Damage Mechanics* 24.3 (2015), pp. 313–337.

[49] L. Guillaumat. "Microfissuration des CMC : relation avec la microstructure et le comportement mecanique". PhD thesis. Bordeaux, 1994.

[50] E. Gürses and C. Miehe. "On evolving deformation microstructures in non-convex partially damaged solids". In: *Journal of the Mechanics and Physics of Solids* 59.6 (2011), pp. 1268–1290.

[51] C. Stolz H.D. Bui K. Van Dang. "Formulations variationnelles du problème en vitesses pour le solide élastique fragile avec zone endommagée". In: *C.R. Acad. Sci. Paris, Série II* 292.1981 (1981), pp. 251–254.

[52] D. Halm and A. Dragon. "A model of anisotropic damage by mesocrack growth; unilateral effect". In: *International Journal of Damage Mechanics* 5.4 (1996), pp. 384–402.

[53] B. Halphen and Q. Nguyen. "Sur les matériaux standard généralisés". In: *Journal de Mécanique* 14 (1975), pp. 39–63.

[54] Z. Hashin and S. Shtrikman. "A variational approach to the theory of the elastic behaviour of multiphase materials". In: *Journal of the Mechanics and Physics of Solids* 11 (1963), pp. 127–140.

[55] Z. Hashin and S. Shtrikman. "On some variational principles in anisotropic and nonhomogeneous elasticity". In: *Journal of the Mechanics and Physics of Solids* 10.4 (1962), pp. 335–342.

[56] Q.C. He and A. Curnier. "A more fundamental approach to damaged elastic stress-strain relations". In: *International Journal of Solids and Structures* 32.10 (1995), pp. 1433–1457.

[57] R. Hill. "Continuum micro-mechanics of elastoplastic polycrystals." In: *Journal of the Mechanics and Physics of Solids* 13 (1965), pp. 89–101.

[58] M. Idiart, H. Moulinec, P. Ponte-Castañeda, and P. Suquet. "Macroscopic behavior and field fluctuations in viscoplastic composites : second-order estimates versus full-field simulations". In: *Journal of the Mechanics and Physics of Solids* 54 (2006), pp. 1029–1063.

[59] M. Idiart and P. Ponte-Castañeda. "Field statistics in nonlinear composites I". In: *Proceeding of the Royal Society A* 348 (2007), pp. 101–127.

[60] M.I. Idiart, N. Lahellec, and P. Suquet. "Model reduction by mean-field homogenization in viscoelastic composites. I. Primal theory". In: *Proceedings of the Royal Society A* 476.2242 (2020), p. 20200407.

[61] M.I. Idiart, N. Lahellec, and P. Suquet. "Model reduction by mean-field homogenization in viscoelastic composites. II. Application to rigidly reinforced solids". In: *Proceedings of the Royal Society A* 476.2242 (2020), p. 20200408.

[62] M. Kachanov. "Elastic Solids with Many Cracks and Related Problems". In: ed. by J. W. Hutchinson and T. Y. Wu. Vol. 30. Advances in Applied Mechanics. Elsevier, 1993, pp. 259–445.

[63] P. Kanouté, D.P. Boso, J.L. Chaboche, and B.A. Schrefler. "Multiscale methods for composites: a review". In: *Archives of Computational Methods in Engineering* 16 (2009), pp. 31–75.

[64] D. Kondo, H. Welemane, and F. Cormery. "Basic concepts and models in continuum damage mechanics". In: *Revue européenne de génie civil* 11.7-8 (2007), pp. 927–943.

[65] K. Kpotufe. "Modèles d'endommagement à gradient : cadre thermodynamique, formulation variationnelle et Applications". In: *Ph.D. Thesis - Université de Lomé - Sorbonne Université* (2021).

[66] D. Krajcinovic. *Damage mechanics*. Elsevier, 1996.

[67] W. Kreher. "Residual stresses and stored elastic energy of composites and polycrystals". In: *Journal of the Mechanics and Physics of Solids* 38.1 (1990), pp. 115–128.

[68] W. Kreher and A. Molinari. "Residual stresses in polycrystals as influenced by grain shape and texture". In: *Journal of the Mechanics and Physics of Solids* 41.12 (1993), pp. 1955–1977.

[69] E. Kröner. "Berechnung der elastischen Konstanten des Vielkristalls aus den Konstanten des Einkristalls". In: *Zeitschrift für Physik* 151.4 (1958), pp. 504–518.

[70] Pierre Ladeveze, Alain Gasser, and Olivier Allix. "Damage mechanisms modeling for ceramic composites". In: *Journal of Engineering Materials and Technology;(United States)* 116.3 (1994).

[71] N. Lahellec, M.I. Idiart, and Pierre P. Suquet. "Model reduction by mean-field homogenization in viscoelastic composites. III. Dual theory". In: *Proceedings of the Royal Society A* 477.2249 (2021), p. 20200869.

[72] N. Lahellec, P. Ponte-Castañeda, and P. Suquet. "Variational estimates for the effective response and field statistics in thermoelastic composites with intra-phase property fluctuations." In: *Proceeding of the Royal Society A* 447 (2011), pp. 2224–2246.

[73] N. Lahellec and P. Suquet. "Effective behavior of linear viscoelastic composites : a time integration approach". In: *International Journal of Solids and Structures* 44 (2006), pp. 507–529.

[74] N. Lahellec and P. Suquet. "Effective response and field statistics in elasto-plastic and elasto-viscoplastic composites under radial and non radial loading." In: *International Journal of Plasticity* 42 (2013), pp. 1–30.

[75] N. Lahellec and P. Suquet. "On the effective behavior of nonlinear inelastic composites : I. Incremental variational principles". In: *Journal of the Mechanics and Physics of Solids* 55 (2007), pp. 1932–1963.

[76] N. Lahellec and P. Suquet. "On the effective behavior of nonlinear inelastic composites : II A second-order procedure". In: *Journal of the Mechanics and Physics of Solids* 55 (2007), pp. 1964–1992.

[77] G. Lancioni and G. Royer-Carfagni. "The variational approach to fracture mechanics. A practical application to the French Panthéon in Paris". In: *Journal of elasticity* 95 (2009), pp. 1–30.

[78] N. Laws. "On the thermostatics of composite materials". In: *Journal of the Mechanics and Physics of Solids* 21.1 (1973), pp. 9–17.

[79] J. Lemaître and J. Chaboche. "Mechanics des matériaux solides". In: *Dunod, Paris* (1985).

[80] E. Lorentz and S. Andrieux. "A variational formulation for nonlocal damage models". In: *International journal of plasticity* 15.2 (1999), pp. 119–138.

[81] E. Lorentz and A. Benallal. "Gradient constitutive relations: numerical aspects and application to gradient damage". In: *Computer methods in applied mechanics and engineering* 194.50-52 (2005), pp. 5191–5220.

[82] E. Lorentz and V. Godard. "Gradient damage models: Toward full-scale computations". In: *Computer Methods in Applied Mechanics and Engineering* 200.21-22 (2011), pp. 1927–1944.

[83] A. Lucchetta. "Homogénéisation des composites élasto-viscoplastiques écrouissables par une double procédure variationnelle incrémentale". PhD thesis. Sorbonne Université, 2019.

[84] A. Lucchetta, F. Auslender, M. Bornert, and D. Kondo. "A double incremental variational procedure for elastoplastic composites with combined isotropic and linear kinematic hardening". In: *International Journal of Solids and Structures* 158 (2019), pp. 243–267.

[85] J.F. Maire and P.-M. P.M. Lesne. "An explicit damage model for the design of composites structures". In: *Composites Science and Technology* 58.5 (1998), pp. 773–778.

[86] H. Maitournam. "Mécanique des structures anélastiques : Comportement, chargement, chargements cycliques et fatigue". In: (2012).

[87] J.-J. Marigo. "Formulation de l'endommagement d'un matériau élastique". In: *C. R. Acad. Sci. Paris Sér. II* 292.19 (1981), pp. 1309–1312.

[88] J.J. Marigo, C. Maurini, and K. Pham. "An overview of the modeling of fracture by gradient damage models". In: *Meccanica* 51(12) (2016), pp. 3107–3128.

[89] R. Masson, M. Bornert, P. Suquet, and A. Zaoui. "An affine formulation for the prediction of the effective properties of nonlinear composites and polycrystals". In: *Journal of the Mechanics and Physics of Solids* 48 (2000), pp. 1203–1227.

[90] R. Masson, R. Brenner, and O. Castelnau. "Incremental homogenization approach for ageing viscoelastic polycrystals". In: *Comptes Rendus Mécanique* 340.4-5 (2012), pp. 378–386.

[91] R. Masson and A. Zaoui. "Self-consistent estimates for the rate-dependentelastoplastic behaviour of polycrystalline materials". In: *Journal of the Mechanics and Physics of Solids* 47 (1999), pp. 1543–1568.

[92] G.A. Maugin. *The thermomechanics of nonlinear irreversible behaviours*. Vol. 27. World scientific, 1999.

[93] A. Mesgarnejad, B. Bourdin, and M.M. Khonsari. "Validation simulations for the variational approach to fracture". In: *Computer Methods in Applied Mechanics and Engineering* 290 (2015), pp. 420–437.

[94] P. Mialon. "Eléments d'analyse et de résolution numérique des relations de l'élasto-plasticité". In: *EDF : Bulletin de la Direction des études et recherches. Série C, Mathématiques, informatique* 3 (1986), pp. 57–89.

[95] J. C. Michel and P. Suquet. "Nonuniform transformation field analysis". In: *International Journal of Solids and Structures* 40 (2003), pp. 6937–6955.

[96] C. Miehe, F. Welschinger, and M. Hofacker. "Thermodynamically consistent phase-field models of fracture: Variational principles and multi-field FE implementations". In: *International journal for numerical methods in engineering* 83.10 (2010), pp. 1273–1311.

[97] A. Mielke. "Evolution of rate-independent systems". In: *Evolutionary equations* 2 (2005), pp. 461–559.

[98] A. Mielke and T. Roubıček. "Rate-independent systems". In: *Theory and Application (in preparation)* (2015).

[99] E. Monaldo, S. Brach, D. Kondo, and G. Vairo. "Effective mechanical response of non-linear heterogeneous materials comprising bimodular phases". In: *European Journal of Mechanics-A/Solids* 81 (2020), p. 103962.

[100] T. Mori and K. Tanaka. "Average stress in matrix and average elastic energy of materials withmisfitting inclusions". In: *Acta Metallurgica* 21 (1973), pp. 571–574.

[101] J. Mosler. "Variationally consistent modeling of finite strain plasticity theory with non-linear kinematic hardening". In: *Computer Methods in Applied Mechanics and Engineering* 199.45-48 (2010), pp. 2753–2764.

[102] J. Mosler and OT O.T. Bruhns. "On the implementation of rate-independent standard dissipative solids at finite strain–Variational constitutive updates". In: *Computer Methods in Applied Mechanics and Engineering* 199.9-12 (2010), pp. 417–429.

[103] H. Moulinec and P. Suquet. "A numerical method for computing the overall response of nonlinear composites with complex microstructure". In: *ArXiv* abs/2012.08962 (1998).

[104] Q.S. Nguyen. *Stability and nonlinear solid mechanics*. Wiley, 2000.

[105] Quoc-Son Nguyen. "Quasi-static response, implicit scheme and incremental problem in gradient plasticity". In: *J. Mech. Phys. Solids* 97 (2016), pp. 156–167.

[106] T.T. Nguyen, J. Yvonnet, Michel M. Bornert, and C. Chateau. "Initiation and propagation of complex 3D networks of cracks in heterogeneous quasi-brittle materials: Direct comparison between in situ testing-microCT experiments and phase field simulations". In: *Journal of the Mechanics and Physics of Solids* 95 (2016), pp. 320–350.

[107] T.T. Nguyen, J. Yvonnet, D. Waldmann, and Q.C. He. "Implementation of a new strain split to model unilateral contact within the phase field method". In: *International Journal for Numerical Methods in Engineering* 121.21 (2020), pp. 4717–4733.

[108] M. Ortiz and A. Molinari. "Microstructural thermal stresses in ceramic materials". In: *Journal of the Mechanics and Physics of Solids* 36 (1988), pp. 385–400.

[109] M. Ortiz and L. Stainier. "The variational formulation of viscoplastic constitutive updates". In: *Computer Methods in Applied Mechanics and Engineering* 171 (1999), pp. 419–444.

[110] C. Ouyang, B. Mobasher, and S.P. Shah. "An R-curve approach for fracture of quasi-brittle materials". In: *Engineering fracture mechanics* 37.4 (1990), pp. 901–913.

[111] V. Pensée, D. Kondo, and L. Dormieux. "Micromechanical analysis of anisotropic damage in brittle materials". In: *Journal of Engineering Mechanics* 128.8 (2002), pp. 889–897.

[112] K. Pham, H. Amor, J.J. Marigo, and C. Maurini. "Gradient damage models and their use to approximate brittle fracture". In: *International Journal of Damage Mechanics* 20.4 (2011), pp. 618–652.

[113] K. Pham and J.J. Marigo. "Approche variationnelle de l'endommagement: II. Les modèles à gradient". In: *Comptes Rendus Mécanique* 338.4 (2010), pp. 199–206.

[114] K. Pham, J.J. Marigo, and C. Maurini. "The issues of the uniqueness and the stability of the homogeneous response in uniaxial tests with gradient damage models". In: *Journal of the Mechanics and Physics of Solids* 59.6 (2011), pp. 1163–1190.

[115] P. Ponte-Castañeda. "Exact second-order estimates for the effective mechanical properties of nonlinear composite materials". In: *Journal of the Mechanics and Physics of Solids* 44 (1996), pp. 827–862.

[116] P. Ponte-Castañeda. "New variational principles in plasticity and their application to composite materials". In: *Journal of the Mechanics and Physics of Solids* 40 (1992), pp. 1757–1788.

[117] P. Ponte-Castañeda. "Second-order homogenization estimates for nonlinear composites incorporating field fluctuations : I-theory". In: *Journal of the Mechanics and Physics of Solids* 50 (2002), pp. 737–757.

[118] P. Ponte-Castañeda. "The effective mechanical properties of nonlinear isotropic composites". In: *Journal of the Mechanics and Physics of Solids* 39 (1991), pp. 45–71.

[119] P. Ponte-Castañeda and P. Suquet. "Nonlinear composites." In: *Advances in Applied Mechanics* 34 (1998), pp. 171–302.

[120] P. Ponte-Castañeda and J. R. Willis. "Variational second-order estimates for nonlinear composites". In: *Proceeding of the Royal Society A* 445 (1999), pp. 1799–1811.

[121] P. Ponte-Castañeda and J.R. Willis. "The effect of spatial distribution on the effective behavior of composite materials and cracked media". In: *Journal of the Mechanics and Physics of Solids* 43.12 (1995), pp. 1919–1951.

[122] K. Rajesh Reddy, S. Srinivasa Murthy, and G. Venkatarathnam. "Relationship between the cooldown characteristics of J–T refrigerators and mixture composition". In: *Cryogenics* 50.6 (2010), pp. 421–425.

[123] B.D. Reddy. "The role of dissipation and defect energy in variational formulations of problems in strain-gradient plasticity. Part 1: polycrystalline plasticity". In: *Continuum Mechanics and Thermodynamics* 23 (2011), pp. 527–549.

[124] M.E.B Seck, M. Gărăjeu, and R. Masson. "Exact solutions for the effective nonlinear viscoelastic (or elasto-viscoplastic) behaviour of particulate composites under isotropic loading". In: *European Journal of Mechanics-A/Solids* 72 (2018), pp. 223–234.

[125] Claude Stolz. *Energy Methods in Non-Linear Mechanics*. Ed. by WARSAW. 2004. Chap. Introduction.

[126] P. Suquet. "Overall properties of nonlinear composites: remarks on secant and incremental formulations". In: *IUTAM Symposium on Micromechanics of Plasticity and Damage of Multiphase Materials: Proceedings of the IUTAM Symposium held in Sèvres, Paris, France, 29 August–1 September 1995*. Springer. 1996, pp. 149–156.

[127] E. Tanné, T. Li, B. Bourdin, J.J. Marigo, and C. Maurini. "Crack nucleation in variational phase-field models of brittle fracture". In: *Journal of the Mechanics and Physics of Solids* 110 (2018), pp. 80–99.

[128] B. Tressou, M. Gueguen, and C. Nadot-Martin. "Application of the variational EIV approach to linear viscoelastic phases governed by several internal variables - Examples with the generalized Maxwell law". In: *European Journal of Mechanics - A/Solids* 97 (2023), p. 104778.

[129] H. Welemane. "Une modélisation des matériaux microfissurés: application aux roches et aux bétons". PhD thesis. Lille 1, 2002.

[130] H. Welemane and F. Cormery. "An alternative 3D model for damage induced anisotropy and unilateral effect in microcracked materials". In: *Journal de Physique IV (Proceedings)*. Vol. 105. EDP sciences. 2003, pp. 329–336.

[131] H. Welemane and F. Cormery. "Some remarks on the damage unilateral effect modelling for microcracked materials". In: *International Journal of Damage Mechanics* 11.1 (2002), pp. 65–86.

[132] H. Welemane and C. Goidescu. "Isotropic brittle damage and unilateral effect". In: *Comptes Rendus Mécanique* 338.5 (2010), pp. 271–276.

[133] Z. Wesolowski. "Elastic material with different elastic constants in two regions of variability of deformation(Energy balance relations for elastic material with different elastic moduli in two regions of deformation space)". In: *ARCHIWUM MECHANIKI STOSOWANEJ* 21.4 (1969), pp. 449–468.

[134] J.R. Willis. "Bounds and self-consistent estimates for the overall properties of anisotropic composites". In: *Journal of the Mechanics and Physics of Solids* 25.3 (1977), pp. 185–202.

[135] J.Y. Wu. "A unified phase-field theory for the mechanics of damage and quasi-brittle failure". In: *Journal of the Mechanics and Physics of Solids* 103 (2017), pp. 72–99.

[136] J. Yvonnet. "Computational Homogenization of Heterogeneous Materials with Finite Elements". In: *Solid Mechanics and Its Applications* (2019).

[137] A. Zaoui. "Continuum micromechanics : survey". In: *Journal of Engineering Mechanics, American Society of Civil Engineers* 128 (2002), pp. 808–816.

Appendix A

On unilateral effects in the context of isotropic damage models

It is well known that the mechanical response of microcracked media is highly dependent on the open/closed state of defects present in the material. In particular, it has generally been observed that compression in the same direction after the application of a tensile load results in full or partial recovery of the modulus in the compression region. From a modeling perspective, describing the unilateral effects in Continuum Damage Mechanics (CDM) remains a challenging task. The main difficulty lies in the need to predict both the continuity of the material response and the partial or total recovery of the elastic constant during microcracks closure process.

We propose to follow here a constructive method of writing the energy in the presence of one-sided effects based on the work of [29]. For the purpose of taking into account the unilateral effects, a differentiation is made for when the microcracks are opened or closed. The two response domains are bounded by a hyperplane $g(\varepsilon)$, the microcracks are opened if $g(\varepsilon) > 0$ and closed if $g(\varepsilon) \geq 0$. The strain energy takes the following form :

$$w(\varepsilon, d) = \begin{cases} \frac{1}{2}\,\varepsilon : \mathbb{C}^{+}(d) \; : \varepsilon & \text{si} \quad g(\varepsilon) \geq 0 \\ \frac{1}{2}\,\varepsilon : \mathbb{C}^{-}(d) \; : \varepsilon & \text{si} \quad g(\varepsilon) \leq 0 \end{cases} \tag{A.1}$$

where $\mathbb{C}^{+}$ and $\mathbb{C}^{+}$ represent the elasticity tensor in "tension" and "compression", respectively. The problem to be solved is to determine not only the function $g(\varepsilon)$ defining the hypersurface separating the two domains, but also the expressions for $\mathbb{C}^{+}(d)$ and $\mathbb{C}^{-}(d)$.

Since the thermodynamic potential has to be continuously differentiable, a few conditions must be applied to the elastic moduli. For this purpose, we will rely on the theorem of [29]. For the $\sigma - \varepsilon$ response to be continuous in the presence of the elasticity jump, that is :

$$\begin{cases} w(\varepsilon,d) \;=\; w(\varepsilon,d)^{+} \;=\; w(\varepsilon,d)^{-} \quad , \quad \forall \varepsilon \;/\; g(\varepsilon)=0 \\ \sigma(\varepsilon,d) \;=\; \sigma(\varepsilon,d)^{+} \;=\; \sigma(\varepsilon,d)^{-} \quad , \quad \forall \varepsilon \;/\; g(\varepsilon)=0 \end{cases} \tag{A.2}$$

it is necessary that this jump $[\mathbb{C}(d)]$ is expressed in the form :

$$[\mathbb{C}(d)] \;=\; \mathbb{C}^{+} - \mathbb{C}^{-} \;=\; s(d)\frac{\partial g}{\partial \varepsilon} \otimes \frac{\partial g}{\partial \varepsilon}\,, \quad \forall \varepsilon \;/\; g(\varepsilon) \neq 0 \tag{A.3}$$

where s is a continuous scalar-valued function depending on d. This general result is valid whatever the material symmetry of the medium considered.
Under the assumption of isotropy of the elasto-damageable behavior in the presence of the unilateral effect, we can write without loss of generality :

$$\begin{cases} \mathbb{C}^{+}(d) \;=\; 3k^{+}(d)\mathbb{J} + 2\mu^{+}\mathbb{K} \quad \text{si} \quad g(\varepsilon) \geq 0 \\ \mathbb{C}^{-}(d) \;=\; 3k^{-}(d)\mathbb{J} + 2\mu^{-}\mathbb{K} \quad \text{si} \quad g(\varepsilon) \leq 0 \end{cases} \tag{A.4}$$

the application of the theorem in this framework of isotropy gives :

$$[\mathbb{C}] \;=\; 3\left(k^{+}-k^{-}\right)\mathbb{J} + 2\left(\mu^{+}-\mu^{-}\right)\mathbb{K} \;=\; s(\varepsilon)\frac{\partial g}{\partial \varepsilon} \otimes \frac{\partial g}{\partial \varepsilon} \tag{A.5}$$

which, due to the structure of $\mathbb{J} = \dfrac{1}{3}\mathbb{1}\otimes\mathbb{1}$ and $\mathbb{K} = \mathbb{I} - \mathbb{J}$, leads to :

$$\mu^{+}(d) = \mu^{-}(d)\,, \quad \forall d \tag{A.6}$$

the continuity of W is then obtained if the shear moduli does not depend on the microcracks state.

A first simple choice is to consider the bulk modulus as that of the sound material, k_0. This corresponds to the case where all microcracks are closed and only affect the shear modulus of the damaged material. Therefore :

$$k^{-}(d) \;=\; k_0\,, \quad \forall d \tag{A.7}$$

and $k^{+}(d)$ will be denoted $k(d)$.
In view of (A.5) and (A.6), the tensor $[\mathbb{C}]$ is written in the form :

$$[\mathbb{C}] \;=\; 3\left(k^{+}-k^{-}\right)\mathbb{J} = \left(k^{+}-k^{-}\right)\mathbb{1}\otimes\mathbb{1} = s(\varepsilon)\frac{\partial g}{\partial \varepsilon} \otimes \frac{\partial g}{\partial \varepsilon} \tag{A.8}$$

Therefore :

$$\frac{\partial g}{\partial \varepsilon} \text{ colinear to } \mathbb{1} \tag{A.9}$$

that is $\frac{\partial g}{\partial \varepsilon} = \mathbb{1}$. Hence :

$$g(\varepsilon) = \mathbb{1} : \varepsilon = \text{tr}\,(\varepsilon) \tag{A.10}$$

The equation (A.1) takes the form :

$$w(\varepsilon, d) = \begin{cases} \frac{1}{2}k(d)\left(\text{tr}\,(\varepsilon)\right)^2 + \mu(d)\varepsilon^d : \varepsilon^d & \text{si} \quad \text{tr}\,(\varepsilon) \geq 0 \\ \\ \frac{1}{2}k_0\left(\text{tr}\,(\varepsilon)\right)^2 + \mu(d)\varepsilon^d : \varepsilon^d & \text{si} \quad \text{tr}\,(\varepsilon) \leq 0 \end{cases} \tag{A.11}$$

and

$$\sigma(\varepsilon, d) = \begin{cases} \sigma(\varepsilon, d)^+ = k(d)\text{tr}\,(\varepsilon)\ \mathbb{1} + \mu(d)\varepsilon^d & \text{si} \quad \text{tr}\,(\varepsilon) \geq 0 \\ \\ \sigma(\varepsilon, d)^- = k_0\text{tr}\,(\varepsilon)\,\mathbb{1} + \mu(d)\varepsilon^d & \text{si} \quad \text{tr}\,(\varepsilon) \leq 0 \end{cases} \tag{A.12}$$

In the same way, the irreversible thermodynamic force $\mathcal{Y}$ and thus the damage criterion are continuous.

Appendix B

Model extensions

B.1 Incremental variational approach for elasto-damageable composites : alternative linearization procedure

An extension of the proposed theoretical model can be considered by slightly altering the linearization procedure.
Indeed, the linearization procedure consisted of the decoupling of strain and the damage variable as can be seen in the chosen form of J_0 in (2.23). However, a term can be added to the definition of the linearized incremental potential, this term would bring back together ε and d without altering the constitutive laws, as J_0 would take the following form :

$$\begin{cases} J_0(x,\varepsilon,d) \;=\; \displaystyle\sum_{r=1}^{N} J_0^{(r)}(\varepsilon,d)\chi^{(r)}(x) \\ J_0^{(r)} = \dfrac{1}{2}(1-d)^2\mathcal{A}_0^{(r)} + \dfrac{1}{2}\varepsilon : \mathbb{C}_0^{(r)} : \varepsilon + (1-d)^2\,\mathcal{B}_0^{(r)} : \varepsilon + \mathcal{Y}_c\,(d-d_n) + \Delta t \Psi_c\left(\dfrac{d-d_n}{\Delta t}\right) \end{cases} \tag{B.1}$$

$\mathcal{B}_0^{(r)}$ being a uniform per phase second-order tensor. Also, as a simplification, we'll consider here the threshold model with no hardening.

From here on, we can proceed following the same steps introduced in (3). The difference $\Delta J = J - J_0$ of the potentials is then written :

$$\begin{cases} \Delta J(x,\varepsilon,d) \;=\; \displaystyle\sum_{r=1}^{N} \Delta J^{(r)}(\varepsilon,d)\chi^{(r)}(x) \\ \Delta J^{(r)} = \dfrac{1}{2}\,(1-d)^2\left[\varepsilon : \mathbb{C}_s^{(r)} : \varepsilon - \mathcal{A}_0^{(r)} - 2\mathcal{B}_0^{(r)} : \varepsilon\right] - \dfrac{1}{2}\varepsilon : \mathbb{C}_0^{(r)} : \varepsilon \end{cases} \tag{B.2}$$

We then optimize with respect to the parameters introduced in J_0, which gives the final estimate of $\tilde{w}_\Delta$

$$\tilde{w}_\Delta(E) \approx \underset{\mathcal{A}_0^{(r)},\mathbb{C}_0^{(r)},\mathcal{B}_0^{(r)}}{\text{stat}} \left[\inf_{\varepsilon/\langle\varepsilon\rangle=E} \left(\inf_{d/\Psi_c(\dot{d})} \langle J_0(\varepsilon,d)\rangle + \underset{\varepsilon^*,d^*}{\text{stat}} \langle \Delta J(\varepsilon,d)\rangle \right) \right] \tag{B.3}$$

1. Stationarity of ΔJ

The stationarity of ΔJ (2.24) with respect to ε^* can be written as :

$$\frac{\partial}{\partial \varepsilon^*} \left\{ \frac{1}{2}(1-d^*)^2 \left[\varepsilon^* : \mathbb{C}_s^{(r)} : \varepsilon^* - \mathcal{A}_0^{(r)} - 2\mathcal{B}_0^{(r)} : \varepsilon^* \right] - \frac{1}{2}\varepsilon^* : \mathbb{C}_0^{(r)} : \varepsilon^* \right\} = 0 \tag{B.4}$$

which implies

$$\Longrightarrow \quad (1-d^*)^2 \left[\mathbb{C}_s^{(r)} : \varepsilon^* - 2\mathcal{B}_0^{(r)} \right] - \mathbb{C}_0^{(r)} : \varepsilon^* = 0 \tag{B.5}$$

Similarly, the stationarity condition of ΔJ over d^* reads :

$$\frac{\partial}{\partial d^*} \left\{ \frac{1}{2}(1-d^*)^2 \left[\varepsilon^* : \mathbb{C}_s^{(r)} : \varepsilon^* - \mathcal{A}_0^{(r)} - 2\mathcal{B}_0^{(r)} : \varepsilon^* \right] - \frac{1}{2}\varepsilon^* : \mathbb{C}_0^{(r)} : \varepsilon^* \right\} = 0 \tag{B.6}$$

This leads to an expression for the first parameter introduced in J_0 :

$$\Longrightarrow \quad \varepsilon^* : \mathbb{C}_s^{(r)} : \varepsilon^* - \mathcal{A}_0^{(r)} - 2\mathcal{B}_0^{(r)} : \varepsilon^* = 0 \tag{B.7}$$

2. Minimization of $J_0^{(r)}$

The energy associated with the resulting LCC is defined as :

$$w_0(\varepsilon) = \inf_{d/\Psi_c(\dot{d})} J_0(\varepsilon,d) \tag{B.8}$$

The infimum of $J_0(\varepsilon,d)$ with respect to d is given with accountability to the irreversibility condition, which is written using the Karush-Kuhn-Tucker (KKT) optimality conditions:

$$\begin{cases} \dfrac{\partial}{\partial d}\left(J_0(\varepsilon,d) + \lambda\,\Psi(\dot{d})\right) = 0 \\ \lambda\,\dot{d} = 0 \\ \lambda \le 0\,, \quad \dot{d} \ge 0 \end{cases} \tag{B.9}$$

which can be rewritten over each phase as :

$$\begin{cases} \dfrac{\partial}{\partial d}\left\{\dfrac{1}{2}(1-d)^2\,\mathcal{A}_0^{(r)} + \dfrac{1}{2}\varepsilon : \mathbb{C}_0^{(r)} : \varepsilon + (1-d)^2\,\mathcal{B}_0^{(r)} : \varepsilon + \mathcal{Y}_c\,(d-d_n)\right\} + \lambda = 0 \\ \lambda\left(\dfrac{d-d_n}{\Delta t}\right) = 0 \\ \lambda \leq 0 \quad ; \dfrac{d-d_n}{\Delta t} \geq 0 \end{cases} \tag{B.10}$$

Case 1. $\lambda < 0$. According to (B.10)$_2$, this assumption leads to $d = d_n$ which is the same as the elastic case without the presence or evolution of damage. This case will therefore not be retained.
Case 2. $\lambda = 0$. From (2.35)$_1$, this assumption leads to:

$$\frac{\partial}{\partial d}\left\{\frac{1}{2}(1-d)^2\,\mathcal{A}_0^{(r)} + \frac{1}{2}\varepsilon : \mathbb{C}_0^{(r)} : \varepsilon + (1-d)^2\,\mathcal{B}_0^{(r)} : \varepsilon + \mathcal{Y}_c\,(d-d_n)\right\} = 0 \tag{B.11}$$

It is this case that we retain.
the resulting expression of the damage variable is as follows :

$$d_{opt} = 1 - \frac{\mathcal{Y}_c}{\mathcal{A}_0^{(r)} + 2\,\mathcal{B}_0^{(r)} : \varepsilon} \tag{B.12}$$

However, if we rewrite (B.12) as :

$$\left(\mathcal{A}_0^{(r)} + 2\,\mathcal{B}_0^{(r)} : \varepsilon\right)(1 - d_{opt}) = \mathcal{Y}_c \tag{B.13}$$

considering the uniformity of $\mathcal{Y}_c$, the left-hand term must be uniform as well. Therefore, (B.12) will be approximated by :

$$d_{opt}^{(r)} = 1 - \frac{\mathcal{Y}_c}{\mathcal{A}_0^{(r)} + 2\,\mathcal{B}_0^{(r)} : \langle\varepsilon\rangle^{(r)}} \tag{B.14}$$

which leads here as well to uniform per-phase damage.

3. Stationarity of $\left\langle J_0^{(r)} + \Delta J^{(r)}\right\rangle^{(r)}$

Optimality with respect to $\mathcal{A}_0^{(r)}$, $\mathbb{C}_0^{(r)}$ and $\mathcal{B}_0^{(r)}$ allows to link between (ε^*, d^*) and the variables (ε, d) :

$$\underset{\mathcal{A}_0^{(r)}}{\text{stat}}\left\langle J_0^{(r)} + \Delta J^{(r)}\right\rangle^{(r)} \Longrightarrow \left\langle (1-d)^2\right\rangle^{(r)} = \left\langle (1-d^*)^2\right\rangle^{(r)} \tag{B.15}$$

$$\underset{\mathbb{C}_0^{(r)}}{\text{stat}} \left\langle J_0^{(r)} + \Delta J^{(r)} \right\rangle^{(r)} \Longrightarrow \begin{cases} \langle \varepsilon : \mathbb{K} : \varepsilon \rangle^{(r)} = \langle \varepsilon^* : \mathbb{K} : \varepsilon^* \rangle^{(r)} \\ \langle \varepsilon : \mathbb{J} : \varepsilon \rangle^{(r)} = \langle \varepsilon^* : \mathbb{J} : \varepsilon^* \rangle^{(r)} \end{cases} \tag{B.16}$$

$$\underset{\mathcal{B}_0^{(r)}}{\text{stat}} \left\langle J_0^{(r)} + \Delta J^{(r)} \right\rangle^{(r)} \Longrightarrow \left\langle (1-d)^2 \, \mathbb{1} : \varepsilon \right\rangle^{(r)} = \left\langle (1-d^*)^2 \, \mathbb{1} : \varepsilon^* \right\rangle^{(r)} \tag{B.17}$$

4. Summary of the resulted equations

Using the optimality conditions above, we can gather them into the following :

$$\begin{cases} (B.15) \Rightarrow (1-d)^2 \left[\mathbb{C}_s^{(r)} : \varepsilon^* - 2\mathcal{B}_0^{(r)} \right] - \mathbb{C}_0^{(r)} : \varepsilon^* = 0 \\ (B.16) \Rightarrow \langle \varepsilon : \mathbb{C}_s^{(r)} : \varepsilon \rangle^{(r)} - \mathcal{A}_0^{(r)} - 2\mathcal{B}_0^{(r)} : \varepsilon^* = 0 \\ d_{opt}^{(r)} = 1 - \dfrac{\mathcal{Y}_c}{\mathcal{A}_0^{(r)} + 2\,\mathcal{B}_0^{(r)} : \langle \varepsilon \rangle^{(r)}} \\ (B.15) \Rightarrow \langle \mathbb{1} : \varepsilon \rangle^{(r)} = \langle \mathbb{1} : \varepsilon^* \rangle^{(r)} \end{cases} \tag{B.18}$$

Assumption 1. in order to move forward and to put to use ($B.18_4$), we consider $\mathcal{B}_0^{(r)} = b_0^{(r)} \mathbb{1}$, with $b_0^{(r)}$ a constant value (uniform per-phase) which can be discussed further.

Using this assumption, ($B.18_2$) can be rewritten as :

$$\langle \varepsilon : \mathbb{C}_s^{(r)} : \varepsilon \rangle^{(r)} - \mathcal{A}_0^{(r)} - 2\, b_0^{(r)} \text{tr}\,(\varepsilon^*) = 0 \tag{B.19}$$

Considering the uniformity of the first 2 terms constituting (B.19), it is therefore expected of $\text{tr}\,(\varepsilon^*)$ to be uniform as well. ($B.18_4$) would then take the following form :

$$\langle \text{tr}\,(\varepsilon) \rangle^{(r)} = \text{tr}\,(\varepsilon^*) \tag{B.20}$$

(B.19) can now be rewritten as :

$$\langle \varepsilon : \mathbb{C}_s^{(r)} : \varepsilon \rangle^{(r)} - \mathcal{A}_0^{(r)} - 2\, b_0^{(r)} \langle \text{tr}\,(\varepsilon) \rangle^{(r)} = 0 \tag{B.21}$$

Now from (B.21), $\mathcal{A}_0^{(r)}$ can be defined and replaced in ($B.18_3$), which would then take the following form :

$$d_{opt}^{(r)} = 1 - \frac{\mathcal{Y}_c}{\langle \varepsilon : \mathbb{C}_s^{(r)} : \varepsilon \rangle^{(r)}} \tag{B.22}$$

And finally, by multiplying (B.18$_1$) by ε^* and again using the optimality conditions results, the following can be obtained :

$$\mathbb{C}_0^{(r)} \;=\; (1-d)^2 \left[\langle \varepsilon : \mathbb{C}_s^{(r)} : \varepsilon \rangle^{(r)} \;-\; 2\, b_0^{(r)} \langle \mathrm{tr}\,(\varepsilon) \rangle^{(r)}\right] \left(\langle \varepsilon \otimes \varepsilon \rangle^{(r)}\right)^{-1} \tag{B.23}$$

Effective response of the elasto-damageable composite

Once all the parameters are known, the effective behavior of the composite can be specified. In order to do so, we proceed to the minimization of (2.39) with respect to ε. This functional is stationary with respect to $\mathcal{A}_0^{(r)}$, $\mathbb{C}_0^{(r)}$ and d and the term ΔJ of this functional is stationary with respect to ε^* and d^*. Given this, we can define the local problem that corresponds to the Euler-Lagrange equations providing the solution to the variational problem:

$$\begin{cases} \mathrm{div}\,\sigma(x) \;=\; 0 & \forall x \in \Omega \\ \sigma(x) = \mathbb{C}_0^{(r)} \;:\; \varepsilon(x) \;+\; \tau_0^{(r)} & \forall x \in \Omega, \quad \tau_0^{(r)} = (1-d)^2\, b_0^{(r)} \mathbb{1} \\ \langle \varepsilon(x) \rangle \;=\; E \qquad + & \text{Conditions aux limites sur } \partial\Omega \end{cases} \tag{B.24}$$

The behavior of the nonlinear composite can then be approximated from the estimate :

$$\Sigma \;=\; \langle \sigma(x) \rangle \;= \tilde{\mathbb{C}}_0 \;:\; \varepsilon(x) \;+\; \tilde{\tau}_0 \tag{B.25}$$

The nonlinear problem is reduced to the solution of a two-function system of unknowns $\mathcal{A}_0^{(r)}$ and $\mathbb{C}_0^{(r)}$:

$$\begin{cases} F_1\left(\mathcal{A}_0^{(r)}, \mathbb{C}_0^{(r)}\right) \;=\; \mathcal{A}_0^{(r)} \;-\; \left(\left\langle \varepsilon : \mathbb{C}_s^{(r)} : \varepsilon \right\rangle^{(r)} \;-\; 2\, b_0^{(r)} \langle \mathrm{tr}\,(\varepsilon) \rangle^{(r)}\right) \;=\; 0 \\ F_2\left(\mathcal{A}_0^{(r)}, \mathbb{C}_0^{(r)}\right) \;=\; \mathbb{C}_0^{(r)} \;-\; \left((1-d)^2 \left[\langle \varepsilon : \mathbb{C}_s^{(r)} : \varepsilon \rangle^{(r)} \;-\; 2\, b_0^{(r)} \langle \mathrm{tr}\,(\varepsilon) \rangle^{(r)}\right] \left(\langle \varepsilon \otimes \varepsilon \rangle^{(r)}\right)^{-1}\right) \end{cases} \tag{B.26}$$

B.2 Double incremental variational procedure : attempted extension to elasto-damageable composites

In the development of the theoretical model within the scope of this thesis, a critical aspect of consideration is the coupling between elasticity and damage. To address this intricate coupling, the approach followed involved the simultaneous linearization of the local behavior and the uniformization of parameters. However, based on the incremental variational procedure introduced by Lahellec and Suquet [75] and making use of the procedure proposed by Agoras et al. [2], in 2019 Luchhetta et al. [83] developed a double incremental variational

approach (DIV) for nonlinear composites. This new formulation allows dealing sequentially with the linearization and the uniformity of the local behavior.

The first step in this two-step methodology involves the linearization of the local behavior. At this stage, the primary objective is to approximate the incremental potential J by a linearized incremental potential J_L. This linearized form, although analogous in structure to the initial potential (as represented by (2.23)), possesses a key distinction. Specifically, the parameters $\mathcal{A}_0$ and $\mathbb{C}_0$ here are not uniform per the constitutive phases. As a result, this initial linearization step leads to the definition of a LCC characterized by heterogeneous material properties.

Building upon the heterogeneous LCC established in the first step, the second phase of this methodology involves a process referred to as uniformization. In this stage, the objective is to approximate the obtained LCC, with its heterogeneous properties, with an LCC with per-phase homogeneous properties. This approximation makes it amenable to classical linear homogenization schemes. By achieving per-phase homogeneity in the material properties, it becomes possible to apply well-established linear homogenization techniques to determine the effective behavior of the composite.

It is noteworthy that, within the scope of this current research, we have not embarked on this two-step approach. However, it is an intriguing avenue that could be explored in future research endeavors.

Appendix C

Comparative Analysis of Homogenization Model Results at 10% Volumetric Fraction and Effects of Boundary Condition Variations

C.1 Additional Results for 10% Volumetric Fraction

In this appendix, we present additional numerical results obtained using the incremental variational approach and computational homogenization model for composites with a reduced volumetric fraction of 10%. This section complements the main body of the thesis, where a volumetric fraction of 25% was primarily considered. The purpose of these results is to demonstrate the model's predictive capabilities and its sensitivity to changes in material configuration.

To maintain consistency with the primary analysis presented in the thesis, we have used the same material parameters for the composite material (see 2.55) with a 10% volumetric fraction. These parameters include the elastic constants, damage evolution laws, and failure criteria. In what follows, we present results for the AT1, AT2, and AT1-extended models and compare them to full-field calculations.

As shown in Figures C.1,C.2, C.3, we compare the predictions of our homogenization model with the results obtained from full-field calculations for the 10% volumetric fraction composite. The full-field calculations provide a detailed view of the composite's mechanical behavior at the microscale, while our model aims to capture the macroscopic response of the material.

We observe that, in general, the predictions of our homogenization model are closer to the full-field calculations when compared to the 25% volumetric fraction case studied in the main body of the thesis. This result suggests that the homogenization model is more accurate in capturing the mechanical behavior of composites with lower volumetric fractions.

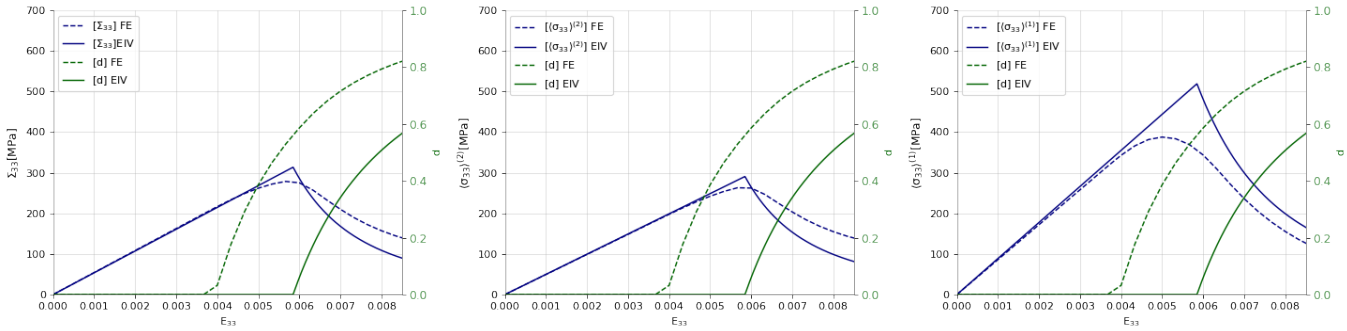

(a) (b) (c)

FIGURE C.1: Elastically reinforced composite with an elasto-damageable matrix submitted to an isochoric macroscopic strain for the AT1 model. (a) Macroscopic axial stress, (b) Average axial stress in the matrix, (c) Average axial stress in the inclusion

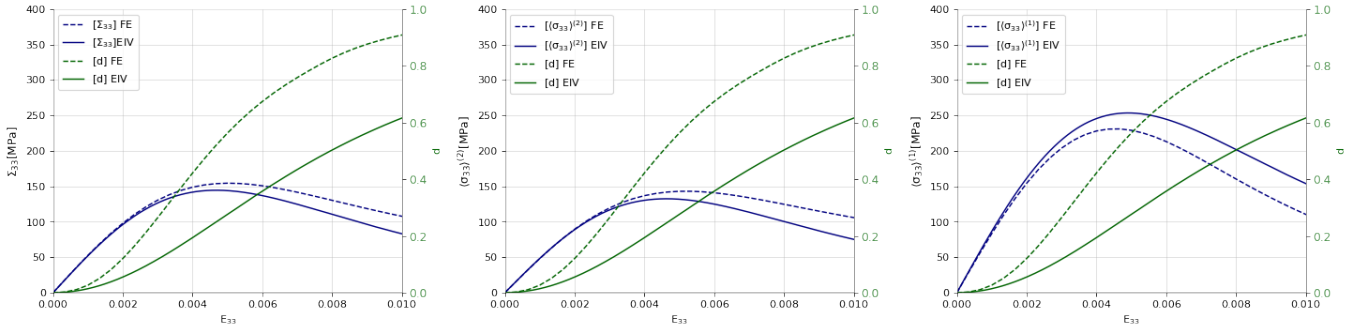

(a) (b) (c)

FIGURE C.2: Elastically reinforced composite with an elasto-damageable matrix submitted to an isochoric macroscopic strain for the AT2 model. (a) Macroscopic axial stress, (b) Average axial stress in the matrix, (c) Average axial stress in the inclusion

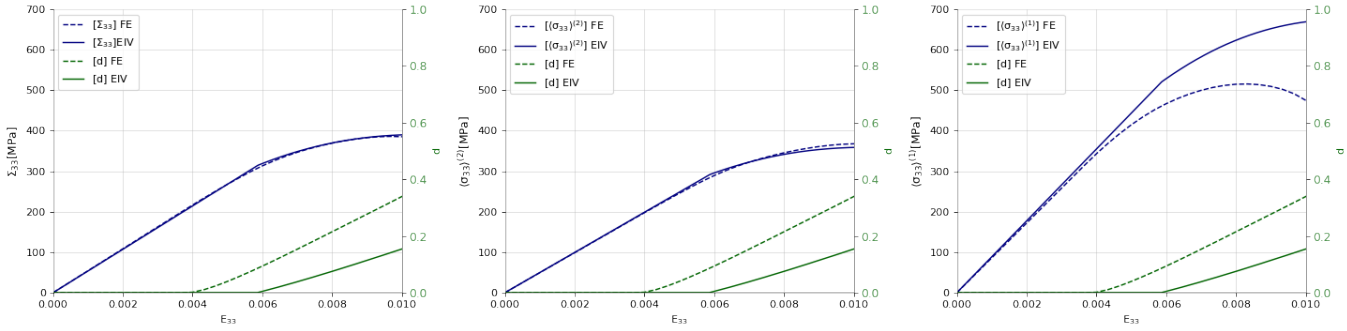

(a) (b) (c)

FIGURE C.3: Elastically reinforced composite with an elasto-damageable matrix submitted to an isochoric macroscopic strain for the AT1 extended model. (a) Macroscopic axial stress, (b) Average axial stress in the matrix, (c) Average axial stress in the inclusion

C.2 Alternative Boundary Conditions and Their Impact on Results

In this appendix, we explore an alternative boundary condition scenario that deviates from the primary methodology employed throughout this study. Specifically, we investigate the case where we do not enforce damage to be null on the edges where loading is applied in full-field simulations. This departure from our standard approach is undertaken to evaluate the effects on the predictions of the full-field calculations in regard to our homogenization model when natural boundary conditions are altered.

It is to be noted that this configuration is the initial one that had been considered -and then put aside-, and the following results are part of the first batch of results obtained. For these, we had considered a threshold of $\mathcal{Y}_c = 4.8MPa$, concerning the rest of the elastic properties of the composite, they can be found in (2.55), and the applied load is an isochoric macroscopic strain.

Throughout the study presented in the main body of this thesis, one of our key practices in full-field simulations has been to enforce damage to be null on the edges where loading is applied. This measure is implemented to mitigate the artificial localization of damage on the surface where the load is applied, ensuring a more representative simulation of the material behavior under mechanical loading.

In this alternative scenario, where we relax the constraint of enforcing null damage on the loaded edges, we observe notable differences in the predictions of full-field calculations compared to our homogenization model. One significant observation is that the overall agreement between the homogenization model's predictions and full-field calculations notably improves in this alternative boundary condition setting.

In the absence of enforcing null damage on the loaded edges, we observe a reduction in stress fluctuations within the matrix material. This effect is particularly pronounced when the stress reaches a certain threshold, as illustrated in Fig. C.4d and C.6d, which follows the same tendencies as in the theoretical model.

However, a notable drawback of not enforcing null damage on the loaded edges is the localization of damage in the upper corner of the cell, as shown in Fig. C.5. This localized damage behavior is a direct consequence of the altered boundary conditions and underscores the importance of our standard practice.

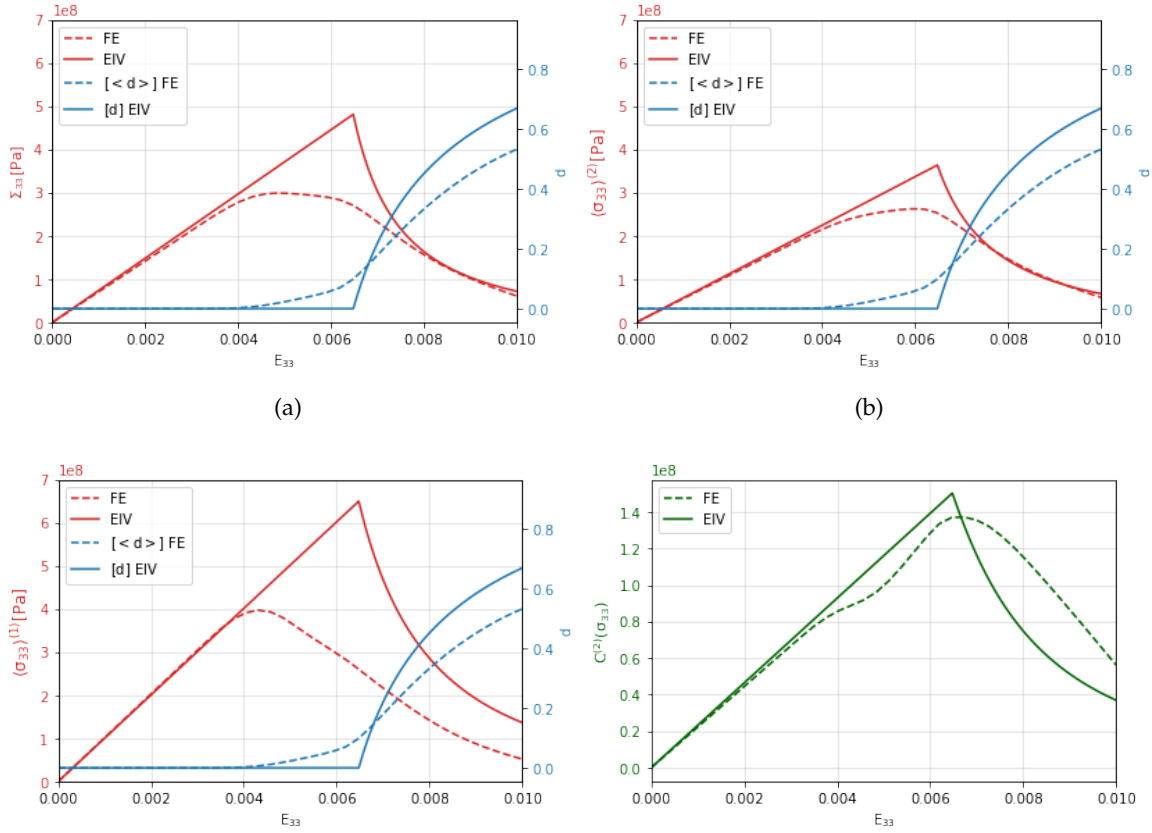

FIGURE C.4: Elastically reinforced composite with an elasto-damageable matrix submitted to an isochoric macroscopic strain for the AT1 model. (a) Macroscopic axial stress, (b) Average axial stress in the matrix, (c) Average axial stress in the inclusion, (d) Stress fluctuations

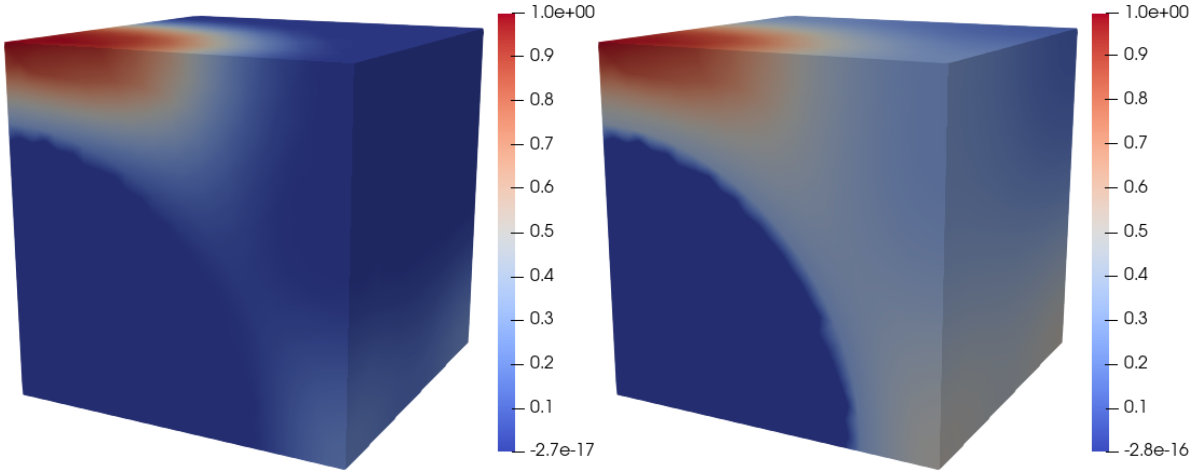

FIGURE C.5: Damage localization (a) AT1 model, (b) AT2 model

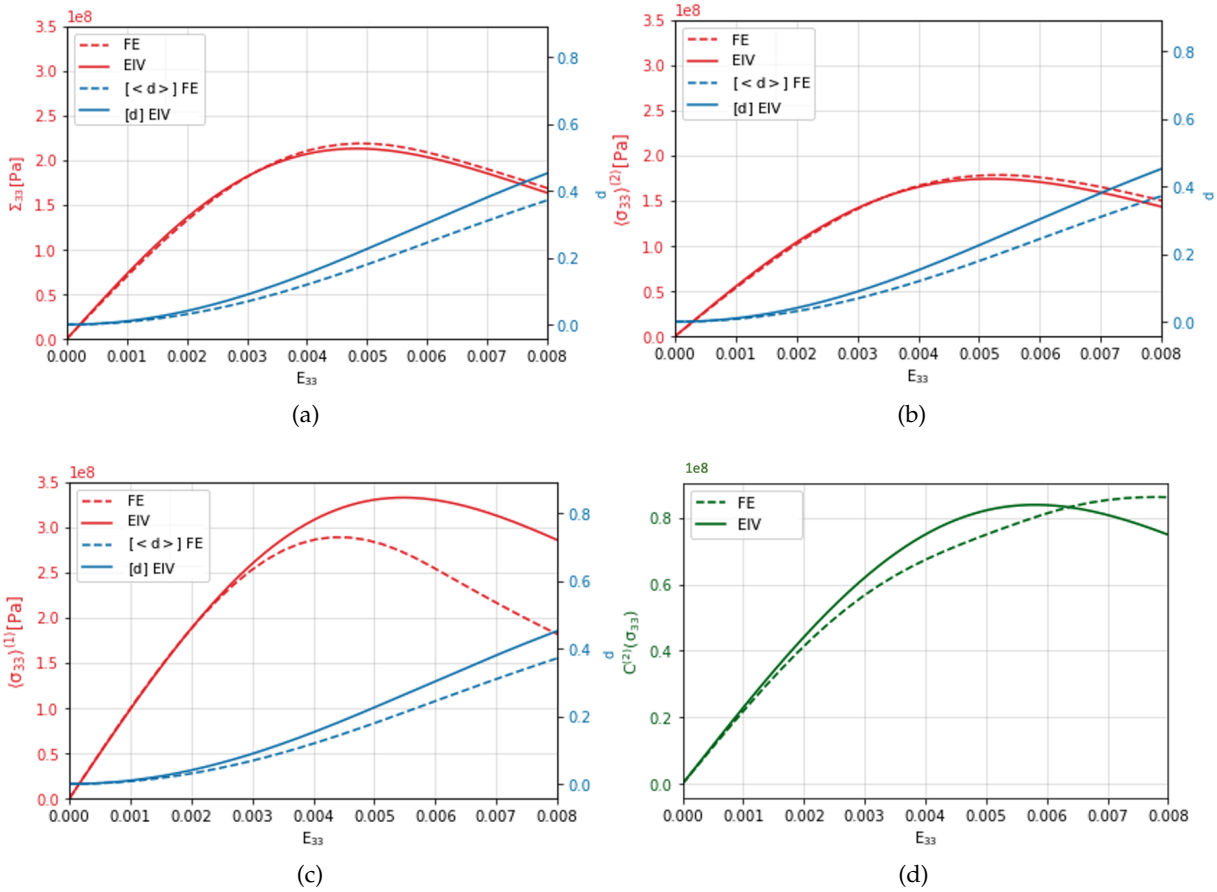

FIGURE C.6: Elastically reinforced composite with an elasto-damageable matrix submitted to an isochoric macroscopic strain for the AT2 model. (a) Macroscopic axial stress, (b) Average axial stress in the matrix, (c) Average axial stress in the inclusion, (d) Stress fluctuations

C.3 Conclusion

In this appendix, we have presented additional numerical results for a 10% volumetric fraction, expanding our investigation of the incremental variational approach and computational homogenization model. Notably, the delayed onset of damage and the closer agreement between the maximum stress values in the model's predictions and full-field calculations have been observed.

We have also examined the impact of an alternative boundary condition scenario where damage is not enforced to be null on the edges where loading is applied. While this approach yields improved agreement between the homogenization model and full-field calculations and reduced stress fluctuations, it also leads to undesirable damage localization. The rationale for enforcing null damage on these edges remains valid, as it prevents artificial damage behavior that could compromise the accuracy of our simulations. This alternative scenario serves as an illustrative example of the trade-offs and considerations involved in selecting appropriate boundary conditions for the study of composites with evolving damage.